

**CHARACTERISTICS OF CONCRETE  
INCORPORATING WASTE MARBLE POWDER**

*A Thesis*

*Submitted in fulfillment of the requirement*

*For the award of degree of*

**DOCTOR OF PHILOSOPHY  
IN  
CIVIL ENGINEERING**

**KIRTI VARDHAN**

**Registration No. 901502003**



**DEPARTMENT OF CIVIL ENGINEERING  
THAPAR INSTITUTE OF ENGINEERING AND TECHNOLOGY  
PATIALA – 147004  
2021**

## DECLARATION

---

I, Kirti Vardhan, hereby declare that the thesis titled, "**Characteristics of Concrete Incorporating Waste Marble Powder**" submitted to **Thapar Institute of Engineering and Technology (Deemed University), Patiala**, in fulfillment of the requirements for the award of degree of "**Doctor of Philosophy**" in Civil Engineering is a record of an original and independent research work done by me during the period 2015-2020, under the combined supervision and guidance of Dr. Rafat Siddique, Senior Professor, Department of Civil Engineering, Thapar Institute of Engineering and Technology, Patiala and Dr. Shweta Goyal, Professor, Department of Civil Engineering, Thapar Institute of Engineering and Technology, Patiala. The work contained in this thesis has not been previously submitted to meet the requirements for a degree or diploma at this or any other higher education institution.

  
(Kirti Vardhan)

Registration No. 901502003

## CERTIFICATE

---

Certified that the work presented in this thesis titled “**Characteristics of Concrete Incorporating Waste Marble Powder**” which is being submitted by **Mr. Kirti Vardhan (Regd. No. 901502003)** in fulfillment of the requirements for the award of degree of “**Doctor of Philosophy**” in the **Department of Civil Engineering, Thapar Institute of Engineering and Technology, Patiala, India**, is an authentic record of the research work carried out by him under our supervision and guidance. The contents of this thesis, in full or in part, have not been submitted to any other Institute or University for the award of any degree or diploma.



(Dr. Rafat Siddique)

Senior Professor

Department of Civil Engineering  
Thapar Institute of Engineering and  
Technology  
Patiala, India



(Dr. Shweta Goyal)

Professor

Department of Civil Engineering  
Thapar Institute of Engineering and  
Technology  
Patiala, India

## ACKNOWLEDGEMENT

Almighty has provided me the cherished opportunity to express my heartfelt gratitude to my guides for their priceless guidance and constant encouragement throughout the period of entire research programme. I am cherished to express my thankfulness to my mentors Dr. Rafat Siddique, Senior Professor and Dr. Shweta Goyal, Professor, Department of Civil Engineering, Thapar Institute of Engineering and Technology, Patiala. I will always remain obliged to them for their meticulous guidance, constructive criticism and constant encouragement till the completion of the work. Their systematic approach and unconditional cooperation made me work hard. Without their tireless efforts and outstanding knowledge of the subject, it would not have been possible for the investigations leading to this thesis.

I am thankful to Dr. Prem Pal Bansal, HCED for providing excellent academic environment and lab facilities. I am also thankful to doctoral committee members Dr. Kulvir Singh, Dr. Gurbir Kaur, Dr. AB Danie Roy for constantly encouraging and providing support for smooth completion of the experimental work. I would also like to thank all the supporting staff, especially Sh. Ram Sumiran, for the help rendered during the preparation of the experimental set up. I also acknowledge the support of SAI labs for SEM and EDX analysis.

As they say “It’s all about the Journey, not the destination”, this journey was tough but most satisfying. I would be honoured to take this opportunity to express my utmost gratitude to my pillar of strength, my loving wife, Mrs. Sunita Singla for bearing with me throughout this period. It will be incomplete without the mention of my late parents, Sh N.R. Singal and Smt Bimla Devi, for always showering their blessings and my brothers and sisters Pawan Singla, Timer Haran, Sunita Mittal & Geeta Didi, a parent figure, for supporting me with the best of their abilities. One’s life is filled with joy by his/her children. Special thanks to my daughter, Sunandini for enhancing my awareness in upcoming technologies and latest gadgets and my son, Karan Singla and his wife Dr. Raminder Gupta for having constant faith in me and most important to my four-month old loving granddaughter Rhythm who without speaking a word gave me the much needed confidence and vibes of becoming a Doctor.

  
(Kirti Vardhan)

## ABSTRACT

---

In the present study, the influence of using marble waste as fine aggregates in concrete is investigated. Seven mixes were prepared by varying the replacement levels of marble waste from 10 to 60%. The w/c ratio of the mixes was kept constant at 0.5. The effect of using marble waste aggregates is investigated in terms of workability, mechanical strength of concrete, permeation properties and durability properties of concrete. The various durability properties investigated in the study included abrasion resistance of concrete, drying shrinkage, resistance of concrete when subjected to external exposure to severe sulphuric acid and sodium sulphate exposure. All the studies are supported by micro-structural analysis of concrete.

Test results indicate that marble waste can be incorporated into concrete to improve its strength and permeation properties, with the maximum improvement obtained at 40% replacement level. The improvement in properties of concrete with the incorporation of marble waste can be attributed to better filler effect provided by marble waste, due to presence of more fines in the particle size range of 1.18mm - 300 $\mu$ m, which led to refinement of pore structure. Along with this, the angular sizes of marble waste aggregates helped in better bonding and improvement in interstitial transition zone of the resultant mix. At the chemical level, marble waste improves the binding ability of the mix. The reaction between calcite present in marble with C<sub>3</sub>A of cement provides a compact structure and helps in improving binding capability of the concrete matrix.

Micro-structural analysis also revealed densification of concrete matrix, which is attributed to refinement of pores because of both physical and chemical changes in the concrete matrix. The fact that marble is largely an inert material and has filler effect on the properties of the resultant mix, is confirmed from the SEM and XRD analysis which shows major phases formed in all mixes remained same, irrespective of the replacement levels of marble waste. Incorporation of marble waste as fine aggregates led to reduction in drying shrinkage strain of concrete mixes. During 270 days of drying duration, the ultimate shrinkage strain reduced gradually from  $478 \times 10^{-6}$  mm/mm to  $332 \times 10^{-6}$  mm/mm as the percentage of marble waste is increased from 10 to 60% of fine aggregates. A shrinkage prediction model incorporating 28-day compressive strength, drying duration and proportion of marble waste used, is proposed. The proposed model had high correlation coefficient ( $R^2$ ) which indicates its effectiveness in predicting drying shrinkage accurately.

The mixes were subjected to 3% sulphuric acid solution for a period of 180 days. The mixes were continuously monitored in terms of visual appearance, weight loss and compressive strength loss. SEM images and XRD patterns were also analysed to understand the performance of various mixes in severe sulphuric acid exposure. The mixes with marble waste were observed to have better performance towards severe sulphuric acid exposure. It is due to the high acid solubility of marble waste, due to which it had greater acid neutralizing capacity locally. It helped in reducing the local acid concentration and hence the rate of acid attack on compounds of concrete. In mixes containing marble waste, calcium carbonate present in marble waste reacts with sulphuric acid to form gypsum. Since marble waste is available for reaction with acid, reaction of cement hydration products with sulphuric acid is delayed; thereby delaying the conversion of cement hydration products into gypsum and ettringite.

The exposure to 5% sodium sulphate solution for 18 months indicated that the incorporation of marble waste helped in arresting the sodium sulphate attack. The mixes incorporating marble waste registered lower weight loss, lower compressive strength loss and expansion of the mixes reduced drastically. Lower expansion demonstrated that lesser amount of gypsum and ettringite were formed, which are mainly responsible for expansion and ultimate degradation of concrete under sodium sulphate exposure. Also, at the physical level, permeability of the mixes with marble powder decreased to the extent of exposure.

Overall, the results confirm that marble waste has the potential to be used as an alternate fine aggregate to improve overall performance of concrete for sustainable development.

## *LIST OF PUBLICATIONS*

---

### **Publication in SCI index journals:**

1. Kirti Vardhan, Rafat Siddique, Shweta Goyal, Influence of marble waste as partial replacement of fine aggregates on strength and drying shrinkage of concrete, *Construction and Building Materials*, 228 (2019), Impact Factor: 4.419. <https://doi.org/10.1016/j.conbuildmat.2019.116730>
2. Kirti Vardhan, Rafat Siddique, Shweta Goyal; Strength, permeation and micro-structural characteristics of concrete incorporating waste marble, *Construction and Building Materials* 203 (2019) 45–55. Impact Factor: 4.419 <https://doi.org/10.1016/j.conbuildmat.2019.01.079>

## *ABBREVIATIONS*

| <b>Abbreviation</b>                     | <b>Word(s)</b>                                    |
|---|---|
| <b>CaO</b>                              | <b>Calcium oxide</b>                              |
| <b>OPC</b>                              | <b>Ordinary Portland cement</b>                   |
| <b>MgO</b>                              | <b>Magnesium oxide</b>                            |
| <b>CaCO<sub>3</sub></b>                 | <b>Calcite</b>                                    |
| <b>C-S-H</b>                            | <b>Calcium silicate hydrate</b>                   |
| <b>Ca(OH)<sub>2</sub></b>               | <b>Calcium hydroxide</b>                          |
| <b>ITZ</b>                              | <b>Interfacial transition zone</b>                |
| <b>SEM</b>                              | <b>Scanning electron microscopy</b>               |
| <b>EDS</b>                              | <b>Energy dispersive spectroscopy</b>             |
| <b>CaMg(CO<sub>3</sub>)<sub>2</sub></b> | <b>Dolomite</b>                                   |
| <b>ANOVA</b>                            | <b>Analysis of variance</b>                       |
| <b>LOI</b>                              | <b>Loss of ignition</b>                           |
| <b>CO<sub>2</sub></b>                   | <b>Carbon dioxide</b>                             |
| <b>SCC</b>                              | <b>Self-compacting concrete</b>                   |
| <b>HPC</b>                              | <b>High performance concrete</b>                  |
| <b>BIS</b>                              | <b>Bureau of Indian Standards</b>                 |
| <b>TGA</b>                              | <b>Thermo gravimetric analysis</b>                |
| <b>C<sub>3</sub>A</b>                   | <b>Tri Calcium aluminate</b>                      |
| <b>ASTM</b>                             | <b>American Society for Testing and Materials</b> |
| <b>SiO<sub>2</sub></b>                  | <b>Silicon oxide</b>                              |
| <b>Al<sub>2</sub>O<sub>3</sub></b>      | <b>Aluminum oxide</b>                             |
| <b>Fe<sub>2</sub>O<sub>3</sub></b>      | <b>Ferric oxide</b>                               |
| <b>SO<sub>3</sub></b>                   | <b>Sulfur trioxide</b>                            |
| <b>Na<sub>2</sub>O</b>                  | <b>Sodium Oxide</b>                               |
| <b>K<sub>2</sub>O</b>                   | <b>Potassium oxide</b>                            |
| <b>LSF</b>                              | <b>Lime saturation factor</b>                     |

|                    |   |
|--------------------|---|
| <b>F.M.</b>        | <b>Fineness modulus</b>                 |
| <b>RCPT</b>        | <b>Rapid chloride permeability test</b> |
| $f_{st}$           | <b>Splitting tensile strength</b>       |
| <b>CRD</b>         | <b>Comparator reading</b>               |
| <b>SE</b>          | <b>Secondary electron</b>               |
| <b>CSL</b>         | <b>Compressive strength loss</b>        |
| <b>WL</b>          | <b>Weight loss</b>                      |
| $f_{ct}$           | <b>Compressive strength</b>             |
| <b>E</b>           | <b>Ettringite</b>                       |
| <b>V</b>           | <b>Voids</b>                            |
| $p_m$              | <b>proportion of marble waste</b>       |
| $d_w$              | <b>Depth of wear</b>                    |
| $\varepsilon_{sh}$ | <b>Shrinkage strain</b>                 |

## CONTENTS

|  |             |
|--|-------------|
| Declaration                                      | i           |
| Certificate                                      | ii          |
| Acknowledgement                                  | iii         |
| Abstract   | iv          |
| List of Publications                             | vi          |
| Abbreviations                                    | vii         |
| Tables of Content                                | ix          |
| List of Tables                                   | xv          |
| List of Figures                                  | xvii        |
| <br>   |             |
| <b>CHAPTER – 1 INTRODUCTION</b>                  | <b>1-11</b> |
| 1.1. GENERAL                                     | 1           |
| 1.2. MARBLE POWDER                               | 2           |
| 1.3. PROPERTIES OF WASTE MARBLE POWDER           | 4           |
| 1.3.1 Chemical Composition                       | 4           |
| 1.3.2 Physical Properties of waste marble powder | 5           |
| 1.3.3 Morphology of marble waste                 | 6           |
| 1.3.4 Minerology of marble waste                 | 7           |
| 1.4 USE OF MARBLE WASTE AS CONSTRUCTION MATERIAL | 9           |
| 1.5 SIGNIFICANCE OF RESEARCH                     | 9           |
| 1.6 GAPS IN THE PROPOSED RESEARCH AREA           | 10          |
| 1.7 OBJECTIVES OF THE PROPOSED WORK              | 10          |
| 1.8 ORIENTATION OF THESIS                        | 10          |

**CHAPTER – 2 LITERATURE REVIEW** **12-32**

|       |  |    |
|-------|--|----|
| 2.1   | GENERAL  | 12 |
| 2.2   | RE-USE OF MARBLE WASTE   | 14 |
| 2.3   | USE OF MARBLE WASTE AS REPLACEMENT OF CEMENT                           | 16 |
| 2.3.1 | Fresh Properties   | 17 |
| 2.3.2 | Mechanical Properties  | 18 |
| 2.3.3 | Durability Properties  | 21 |
| 2.4   | USE OF MARBLE WASTE AS REPLACEMENT OF FINE AGGREGATES                  | 23 |
| 2.4.1 | Use of Marble Waste as Replacement of Very Fine Aggregates in Concrete | 24 |
| 2.4.2 | Use of Marble Waste as Replacement of Fine Aggregates in Concrete      | 24 |
| 2.4.3 | Use of Marble Waste as Fine Aggregates in Mortar                       | 26 |
| 2.4.4 | Use of Marble Waste as Coarse Aggregates                               | 27 |
| 2.5.  | USE OF MARBLE WASTE IN SELF COMPACTING CONCRETE                        | 28 |
| 2.6.  | USE OF MARBLE WASTE FOR MAKING CELLULAR CONCRETE                       | 31 |
| 2.7.  | USE OF MARBLE WASTE IN BRICKS  | 32 |
| 2.8.  | CONCLUDING REMARKS   | 32 |

**CHAPTER – 3 EXPERIMENTAL PROGRAMME** **33-64**

|        |                 |    |
|--------|-----------------|----|
| 3.1.   | GENERAL         | 33 |
| 3.2.   | MATERIALS       | 33 |
| 3.2.1. | Cement          | 33 |
| 3.2.2. | Fine Aggregates | 35 |

|          |  |    |
|----------|--|----|
| 3.2.2.1. | River Sand   | 36 |
| 3.2.2.2. | Marble Waste   | 37 |
| 3.2.3.   | Coarse Aggregates  | 40 |
| 3.2.4.   | Water  | 42 |
| 3.3.     | MIX PROPORTIONS  | 42 |
| 3.4.     | CASTING AND CURING OF SPECIMENS  | 43 |
| 3.5.     | TESTING PROCEDURE  | 45 |
| 3.5.1.   | Workability  | 45 |
| 3.5.2.   | Compressive Strength   | 45 |
| 3.5.3.   | Split Tensile Strength   | 47 |
| 3.5.4.   | Permeation Characteristics of the Mixes  | 49 |
| 3.5.4.1. | Rapid Chloride Permeability Test (RCPT)  | 49 |
| 3.5.4.2. | Sorptivity Test  | 50 |
| 3.5.4.3. | Water Absorption Test  | 51 |
| 3.5.5.   | Abrasion Resistance  | 52 |
| 3.5.6.   | Drying Shrinkage   | 53 |
| 3.5.7.   | Mineralogical and Microstructural Analysis                                     | 54 |
| 3.5.7.1. | Scanning Electron Microscopy (SEM) and<br>Energy Dispersive Spectroscopy (EDS) | 55 |
| 3.5.7.2. | X- Ray diffraction (XRD)   | 56 |
| 3.5.8.   | Acid Exposure  | 56 |
| 3.5.8.1. | Acid Solubility Index of Basic Ingredients                                     | 57 |
| 3.5.8.2. | Exposure Details   | 59 |
| 3.5.8.3. | Test Method  | 60 |
| 3.5.9.   | Sulphate Attack  | 61 |
| 3.5.9.1. | Length Change of Specimens   | 64 |
| 3.5.9.2. | Mineralogical and Microstructural Analysis                                     | 64 |

|  |               |
|--|---------------|
| <b>CHAPTER – 4 STRENGTH ASPECTS OF TESTED CONCRETE</b>                           | <b>65-135</b> |
| 4.1 GENERAL  | 65            |
| 4.2 CHARACTERIZATION OF MARBLE WASTE   | 65            |
| 4.3 WORKABILITY OF FRESH CONCRETE  | 69            |
| 4.4 COMPRESSIVE STRENGTH   | 70            |
| 4.5 SPLIT TENSILE STRENGTH   | 73            |
| 4.6 PERMEATION PROPERTIES OF THE MIXES   | 75            |
| 4.6.1. Rapid Chloride Permeability Test (RCPT)                                   | 76            |
| 4.6.2. Sorptivity  | 77            |
| 4.6.3 Water Absorption Test  | 81            |
| 4.7 MICROSTRUCTURE ANALYSIS  | 82            |
| 4.7.1 XRD Analysis   | 82            |
| 4.7.2 Scanning Electron Micrographs  | 84            |
| 4.8 STATISTICAL ANALYSIS OF MECHANICAL STRENGTH AND PERMEATION PARAMETER RESULTS | 88            |
| 4.8.1 Relationship between Compressive Strength and Split Tensile Strength       | 88            |
| 4.8.2 Relationship between Compressive Strength and Chloride Ion Permeability    | 90            |
| 4.9 ABRASION RESISTANCE OF CONCRETE  | 92            |
| 4.9.1 Effect of Addition of marble waste on Abrasion Resistance of Concrete      | 92            |
| 4.9.2 Statistical Analysis of Abrasion Resistance Results                        | 96            |
| 4.10. DRYING SHRINKAGE OF CONCRETE   | 100           |
| 4.10.1. Effect of marble waste on Drying Shrinkage                               | 101           |
| 4.10.2. Shrinkage Strain Prediction Model  | 104           |

|                                    |  |                    |
|------------------------------------|--|--------------------|
| 4.11.                              | ACID ATTACK  | 110                |
| 4.11.1.                            | Visual Observations  | 110                |
| 4.11.2.                            | Weight Loss  | 112                |
| 4.11.3.                            | Compressive Strength Loss  | 113                |
| 4.11.4.                            | Microstructural Investigations                                       | 115                |
| 4.12.                              | SODIUM SULFATE EXPOSURE  | 119                |
| 4.12.1.                            | Visual Observations  | 119                |
| 4.12.2.                            | Weight Loss/Gain   | 120                |
| 4.12.3.                            | Compressive Strength Loss/Gain                                       | 121                |
| 4.12.4.                            | Linear Expansion   | 123                |
| 4.12.5.                            | Mechanism of Sodium Sulphate Attack                                  | 124                |
| 4.12.6.                            | Microstructure Analysis  | 126                |
| <br><b>CHAPTER – 5 CONCLUSIONS</b> |  | <br><b>136-142</b> |
| 5.1.                               | GENERAL  | 136                |
| 5.2.                               | FRESH PROPERTIES OF CONCRETE   | 136                |
| 5.3.                               | STRENGTH PROPERTIES OF HARDENED CONCRETE:                            | 136                |
| 5.3.1.                             | Compressive Strength   | 137                |
| 5.3.2.                             | Split Tensile Strength   | 137                |
| 5.3.3.                             | Relationship between Compressive Strength and Split Tensile Strength | 138                |
| 5.4.                               | PERMEATION PROPERTIES  | 138                |
| 5.4.1.                             | Rapid Chloride Permeability Test (RCPT)                              | 138                |
| 5.4.2.                             | Sorptivity   | 138                |
| 5.4.3.                             | Water Absorption   | 138                |
| 5.5.                               | MICROSTRUCTURE ANALYSIS  | 139                |
| 5.5.1.                             | XRD Analysis   | 139                |

|        |   |                |
|--------|---|----------------|
| 5.5.2. | Scanning Electron Micrographs                                     | 139            |
| 5.6.   | ABRASION RESISTANCE OF CONCRETE                                   | 140            |
| 5.6.1. | Effect of Addition of Marble Waste                                | 140            |
| 5.6.2. | Relationship between Abrasion resistance and Compressive Strength | 140            |
| 5.7.   | DRYING SHRINKAGE  | 140            |
| 5.7.1. | Effect of Marble Waste Addition                                   | 140            |
| 5.7.2. | Drying Shrinkage Strain Prediction Model                          | 141            |
| 5.8.   | RESISTANCE TO ACID ATTACK   | 141            |
| 5.9.   | RESISTANCE TO SODIUM SULPHATE EXPOSURE                            | 141            |
| 5.10.  | SCOPE FOR FUTURE WORK   | 142            |
|        | <b>REFERENCES</b>   | <b>143-157</b> |

## LIST OF TABLES

| <b>Table No.</b> | <b>TITLE</b>  | <b>Page No.</b> |
|------------------|---|-----------------|
| <b>CHAPTER 1</b> |   |                 |
| Table 1.1        | Statistics related to marble production and waste generation                  | 3               |
| Table 1.2        | Chemical composition of marble waste used by researchers                      | 5               |
| Table 1.3        | Physical properties of marble waste used by researchers                       | 6               |
| <b>CHAPTER 2</b> |   |                 |
| Table 2.1        | Summary of research related to use of marble waste as a construction material | 15              |
| <b>CHAPTER 3</b> |   |                 |
| Table 3.1        | Chemical composition of cement  | 35              |
| Table 3.2        | Physical properties of cement   | 35              |
| Table 3.3        | Physical properties of river sand   | 36              |
| Table 3.4        | Chemical composition of river sand  | 36              |
| Table 3.5        | Sieve analysis results for river sand aggregates                              | 37              |
| Table 3.6        | Physical properties of marble waste   | 38              |
| Table 3.7        | Chemical composition of marble waste  | 38              |
| Table 3.8        | Sieve analysis results for marble waste                                       | 39              |
| Table 3.9        | Physical properties of coarse aggregates                                      | 40              |
| Table 3.10       | Chemical composition of coarse aggregates                                     | 41              |
| Table 3.11       | Sieve analysis of 20 mm crushed gravel coarse aggregates                      | 41              |
| Table 3.12       | Sieve analysis of 10 mm crushed gravel coarse aggregates                      | 42              |
| Table 3.13       | Properties of laboratory tap water  | 42              |
| Table 3.14       | Mix proportions and nomenclature of mixes                                     | 43              |
| Table 3.15       | Chloride ion penetration based on charge passed                               | 50              |
| Table 3.16       | Sources of sulphuric acid exposure to reinforced concrete structures          | 58              |

|            |   |     |
|------------|---|-----|
| Table 3.17 | Acid solubility fraction of materials used in the study   | 59  |
| Table 3.18 | Deterioration scale used for evaluating visual distress in concrete   | 63  |
| CHAPTER 4  |   |     |
| Table 4.1  | Physical properties of natural river sand and marble waste  | 66  |
| Table 4.2  | Chemical composition of natural river sand and marble waste   | 66  |
| Table 4.3  | Ratio of split tensile strength and compressive strength  | 75  |
| Table 4.4  | Charge passed through different concrete mixes in rapid chloride ion penetration test                           | 76  |
| Table 4.5  | Values of sorptivity coefficient of concrete mixes  | 81  |
| Table 4.6  | Water absorption of mixes at 28 days and 365 days of curing   | 81  |
| Table 4.7  | Description of data points used for checking the developed model for split tensile strength                     | 91  |
| Table 4.8  | Details of existing relationship between compressive strength and abrasion resistance for conventional concrete | 98  |
| Table 4.9  | Ultimate shrinkage strain, shrinkage half-time and shrinkage rate of concrete mixes                             | 103 |
| Table 4.10 | Details of shrinkage prediction models used for conventional concrete   | 105 |
| Table 4.11 | Residual error for mixes containing marble waste as fine aggregates   | 109 |
| Table 4.12 | Acid solubility fraction of materials used in the study   | 115 |
| Table 4.13 | Deterioration rating observed from visual appearance of specimens under 5% sodium sulfate exposure              | 119 |

## LIST OF FIGURES

| <b>Figure No.</b> | <b>TITLE</b>  | <b>Page No.</b> |
|-------------------|---|-----------------|
| <b>CHAPTER 1</b>  |   |                 |
| Fig. 1.1          | Steps in marble processing units leading to formation of marble waste   | 3               |
| Fig. 1.2          | SEM micrographs of marble waste   | 7               |
| Fig. 1.3          | XRD patterns of marble waste  | 7               |
| <b>CHAPTER 2</b>  |   |                 |
| Fig. 2.1          | Proportion of marble and associated waste produced during various processing operations                                 | 13              |
| <b>CHAPTER 3</b>  |   |                 |
| Fig. 3.1          | Relative material proportions in a conventional concrete  | 34              |
| Fig. 3.2          | (a) Scanning electron microscopy (SEM) image and (b) Energy dispersive spectroscopy (EDS) of OPC cement                 | 34              |
| Fig. 3.3          | Scanning electron microscopy (SEM) image of river sand aggregates   | 37              |
| Fig. 3.4          | XRD spectra of marble waste   | 39              |
| Fig. 3.5          | SEM image of marble waste   | 40              |
| Fig. 3.6          | (a) Scanning electron microscopy (SEM) image and (b) Energy dispersive spectroscopy (EDS) for crushed gravel aggregates | 41              |
| Fig. 3.7          | (a) Greasing and oiling of moulds, (b) Casting of concrete mix  | 44              |
| Fig. 3.8          | Curing of concrete specimens in the temperature-controlled curing tank  | 44              |
| Fig. 3.9          | Slump test apparatus  | 46              |
| Fig. 3.10         | (a) Test set-up of compression testing machine, (b) Compression test in progress  | 46              |
| Fig. 3.11         | Test set up and crack development in split tensile strength   | 47              |

|                  |  |    |
|------------------|--|----|
| Fig. 3.12        | (a) Test arrangement for split tensile strength (b) Tested split tensile strength test specimen            | 48 |
| Fig. 3.13        | (a) Rapid chloride ion penetration test apparatus; (b) Display sheet of the charge passed through concrete | 49 |
| Fig. 3.14        | Specimens kept for sorptivity test   | 51 |
| Fig. 3.15        | Experimental setup for measurement of abrasion resistance of concrete                                      | 53 |
| Fig. 3.16        | Unrestrained drying shrinkage test set-up  | 54 |
| Fig. 3.17        | Experimental set up for SEM and EDS spectroscopy   | 55 |
| Fig. 3.18        | Experimental set up for X-Ray diffraction (XRD) instrument   | 56 |
| <b>CHAPTER 4</b> |  |    |
| Fig. 4.1         | Particle size distribution of natural river sand and marble waste used as fine aggregates                  | 67 |
| Fig. 4.2         | XRD spectra of marble waste  | 68 |
| Fig. 4.3         | SEM image of (a) natural river sand; (b) marble waste  | 69 |
| Fig. 4.4         | Slump of the mixes incorporating various percentages of marble waste                                       | 70 |
| Fig. 4.5         | Compressive strength of mixes with varying percentage of marble waste                                      | 72 |
| Fig. 4.6         | Compressive strength development of the mixes at various replacement levels of marble waste                | 73 |
| Fig. 4.7         | Split tensile strength of concrete with varying percentages of marble waste as fine aggregates             | 74 |
| Fig. 4.8         | Split tensile strength development of the mixes at various replacement levels of marble waste              | 75 |
| Fig. 4.9         | RCPT test results for concrete specimens at different testing ages   | 77 |
| Fig. 4.10        | Absorption of different mixes at 28 days of curing during sorptivity test                                  | 79 |
| Fig. 4.11        | Primary absorption data upto 6 hours for mixes at 28 days of curing  | 79 |

|           |   |     |
|-----------|---|-----|
| Fig. 4.12 | Absorption of different mixes at 365 days of curing during sorptivity test  | 80  |
| Fig. 4.13 | Primary absorption data up to 6-hours for mixes at 365 days of curing   | 80  |
| Fig. 4.14 | XRD spectrum of various mixes at 28 days of casting   | 83  |
| Fig. 4.15 | XRD spectrum of various mixes at 365-days of casting  | 83  |
| Fig. 4.16 | SEM images of concrete mixes containing varying percentage of marble waste as replacement of fine aggregates at the age of 28 days  | 85  |
| Fig. 4.17 | SEM images of concrete mixes containing varying percentage of marble waste as replacement of fine aggregates at the age of 365 days | 86  |
| Fig. 4.18 | Relation between observed and predicted split tensile strength  | 90  |
| Fig. 4.19 | Relation between compressive strength and RCPT values   | 91  |
| Fig. 4.20 | Final depth of wear of all mixes incorporating marble waste   | 93  |
| Fig. 4.21 | Progressive depth of wear versus number of revolutions for all mixes at 7 days of curing  | 94  |
| Fig. 4.22 | Progressive depth of wear versus number of revolutions for all mixes at 28 days of curing   | 95  |
| Fig. 4.23 | Progressive depth of wear versus number of revolutions for all mixes at 90 days of curing   | 95  |
| Fig. 4.24 | Progressive depth of wear versus number of revolutions for all mixes at 365 days of curing  | 96  |
| Fig. 4.25 | Relationship between depth of wear and compressive strength   | 99  |
| Fig. 4.26 | Relationship between depth of wear and split tensile strength   | 99  |
| Fig. 4.27 | Comparison between observed and predicted depth of year using developed relationship at 95% prediction band                         | 100 |
| Fig. 4.28 | Unrestrained drying shrinkage test set-up   | 101 |
| Fig. 4.29 | Shrinkage strain evolution with drying time for concrete mixes  | 102 |
| Fig. 4.30 | Comparison between observed shrinkage data with established prediction model  | 107 |

|           |  |     |
|-----------|--|-----|
| Fig. 4.31 | Comparison of shrinkage strain prediction by proposed model with experimental data   | 108 |
| Fig. 4.32 | Visual appearance of concrete cubes after 180 days of sulphuric acid exposure  | 110 |
| Fig. 4.33 | Weight loss of all the mixes subjected to sulphuric acid exposure  | 112 |
| Fig. 4.34 | Compressive strength loss of all the mixes subjected to sulphuric acid exposure  | 114 |
| Fig. 4.35 | XRD patterns of mixes upon exposure to sulphuric acid solution for 180 days  | 116 |
| Fig. 4.36 | SEM images and EDS analysis of concrete mixes after exposure to sulphuric acid solution for 180 days                       | 116 |
| Fig. 4.37 | Progressive weight loss/gain of various concrete mixes under cyclic exposure to 5% sodium sulfate solution                 | 120 |
| Fig. 4.38 | Final weight loss of mixes at the end of 18 monthly cycles of sodium sulfate exposure                                      | 121 |
| Fig. 4.39 | Progressive compressive strength loss / gain of various concrete mixes under cyclic exposure to 5% sodium sulfate solution | 122 |
| Fig. 4.40 | Final compressive strength loss of mixes at the end of 18 monthly cycles of sodium sulfate exposure                        | 123 |
| Fig. 4.41 | Linear expansion registered in various concrete mixes under cyclic exposure to 5% sodium sulfate solution                  | 124 |
| Fig. 4.42 | XRD of the control mix (M0) at 4 month and 18 months of 5% sodium sulphate exposure  | 127 |
| Fig. 4.43 | SEM-EDS image for control mix (M0) when exposed to 5% sodium sulphate solution for 18 months                               | 128 |
| Fig. 4.44 | XRD for M10 mix at exposure duration of 18 months  | 129 |
| Fig. 4.45 | XRD for M20 mix at exposure duration of 18 months  | 130 |
| Fig. 4.46 | XRD for M30 mix at exposure duration of 18 months  | 130 |
| Fig. 4.47 | XRD for M40 mix at exposure duration of 18 months  | 131 |
| Fig. 4.48 | XRD for M50 mix at exposure duration of 18 months  | 131 |

|           |  |     |
|-----------|--|-----|
| Fig. 4.49 | XRD for M60 mix at exposure duration of 18 months  | 132 |
| Fig. 4.50 | SEM-EDS image for M10 mix at exposure duration of 18 months to 5% sodium sulphate solution | 133 |
| Fig. 4.51 | SEM-EDS image for M20 mix at exposure duration of 18 months to 5% sodium sulphate solution | 134 |
| Fig. 4.52 | SEM-EDS image for M30 mix at exposure duration of 18 months to 5% sodium sulphate solution | 134 |
| Fig. 4.53 | SEM-EDS image for M40 mix at exposure duration of 18 months to 5% sodium sulphate solution | 134 |
| Fig. 4.54 | SEM-EDS image for M50 mix at exposure duration of 18 months to 5% sodium sulphate solution | 135 |
| Fig. 4.55 | SEM-EDS image for M60 mix at exposure duration of 18 months to 5% sodium sulphate solution | 135 |

# CHAPTER 1

## INTRODUCTION

### 1.1. GENERAL

New developments in construction technologies and growing population give rise to more building constructions and hence lead to larger consumption of natural materials used during the manufacture of concrete. Sustainability in concrete production can be achieved by innovations in substitution of materials used.

Aggregates are the major constituents of concrete, contributing towards nearly 70% of concrete weight. Most of the aggregates are obtained from the natural quarries or river beds. With the rapid increase in construction activities, the demand for natural aggregates are on the rise, which is further contributing towards uncontrolled exploitation of the natural resources. For instance, natural river sand, which is considered to be the most suitable fine aggregate in concrete production, is extensively exploited to meet the ever-increasing demand in concrete production. It has led to serious environmental and economic concerns (Rashad, 2013; Sankh et al., 2014). Due to infrastructural growth, the demand of natural sand is very high particularly in developing countries. The sand deposits are being used up and hence causing serious threat to the environment. The use of sand in construction activities results in the excessive mining, increase in scour depth, loss of vegetation cover to banks of rivers, lowering of water table, disturbs the aquatic life etc. Thus, it is becoming inevitable to use alternative material for sand in concrete.

On the one hand, the natural resources are being over exploited for their use as fine aggregates; while, on the other hand, the materials generated from other industries in the same particle size range are treated as waste and are discarded. These industrial wastes have the potential to become sustainable alternatives to fine aggregates. Various researchers have explored the use of different inert waste materials as partial or complete substitution of river sand as fine aggregates. Foundry sand, discarded rubber, quarry dust, sand bottom ash etc. are some examples of alternative fine aggregates that have been investigated. Another material that can be used as an alternative to fine aggregates is waste marble powder.

## 1.2. MARBLE POWDER

Marble waste powder is an inert material obtained from the sawing and processing operations of marble stone (Belaidi et al., 2012). Marble stone is a metamorphic rock that results from the transformation of pure limestone.

The five leading countries in production of marble are China, India, Brazil, Turkey and Italy, in which India ranks second (Ashish, 2018; Marras et al., 2017a). The data related to the production of marble and waste generated by different countries is provided in Table 1.1. During the marble processing operations, enormous amount of waste is generated, which is estimated to be as high as 60% of total marble quarried (Ashish, 2018). Waste generation continues from mining process to finished product. The waste is generated by cutting of marble slabs into required shapes and sizes using diamond wires or gang saw which uses multiple diamond-tipped blades to slice a marble block.

The waste material so generated is of different sizes. Large marble pieces that are discarded as scraps of improperly cut marble can be used as directly as coarse aggregates (Silva et al., 2014) or is further crushed to size range of fine aggregates. The fine particles of marble are produced during cutting operation and forms large volume of marble slurry, which is a mix of fine marble particles and water. This marble slurry is channelized through a series of sedimentation tanks (generally three), so that the coarser stone pieces are separated from slurry by settlement. The slurry settled in the sedimentation tanks is of the size that can be used as fine aggregates in concrete. The remaining waste material consists of very fine particles impounded with water. The excess water from the slurry is extracted and is recycled, while the remaining mud like marble slurry, with 90% of the particles below 200 $\mu$ m, is disposed in the open land.

Fig. 1.1 shows the typical set up of the marble processing industry and the marble sludge produced as a waste material. The extremely fine grained marble sludge constitutes about 20-30 % of weight of marble worked (Silva et al., 2014). Due to its extremely fine particle size, it has been primarily utilized as a replacement of cement in concrete. The extremely fine grained marble sludge can further be processed into marble powder by combinations of drying and loading applications. This powder is

sometimes processed further for various industrial applications like plastic industry, glass industry, paper and dying industry (Alyamaç and Aydin, 2015). The marble waste generated in India does not get fully consumed in alternate industries.

**Table 1.1: Statistics related to marble production and waste generation  
(Marras et al., 2017a)**

| Country | Marble production ( $10^9$ kg) | Waste generation ( $10^9$ kg) |
|---------|--------------------------------|-------------------------------|
| China   | 45                             | 23                            |
| India   | 21                             | 7                             |
| Turkey  | 10.5                           | 2.5                           |
| Brazil  | 8.2                            | 3                             |
| Italy   | 6.5                            | 2.5                           |



(a) Marble extraction



(b) Marble cutting



(c) Sedimentation tanks used for settlement of coarser marble particles



(d) Disposal of marble slurry

**Fig. 1.1: Steps in processing units leading to formation of marble waste  
(Vardhan et al., 2019)**

The left-out waste, either in sludge form or in powder form, is left unattended; thus causing water and air pollution (Singh et al., 2017). The high chemical content of marble leads to ground water contamination (Rizzo et al., 2008). The fine particles of marble waste clog the agricultural land leading to loss of soil fertility (Vardhan et al., 2015). Construction industry can become the potential consumer of marble waste, wherein it can be used as a constituent of concrete production. However, the clear understanding of various aspects of the waste that can affect the performance of concrete is required before using them in actual practice.

### **1.3. PROPERTIES OF WASTE MARBLE POWDER**

The properties of marble powder that is available as waste after processing of marble slabs vary depending upon the origin of the parent rock. The following section describes the chemical composition, physical properties and mineralogical characteristics of marble waste used by various researchers:

#### **1.3.1. Chemical Composition**

Major component of chemical composition in waste marble powder is calcium oxide (CaO) as reported by various researchers. Chemical analysis of various parameters of waste marble powder varies from source to source. Some of the chemical composition as reported by researchers is presented in Table 1.2. From the chemical composition of marble waste provided by various researchers, it can be concluded that calcium oxide is the major constituent of the waste. Also, among the minor constituents, MgO is present in significant quantity. It is because, chemically, marble consists of calcium carbonate ( $\text{CaCO}_3$ ) and dolomite ( $\text{CaMg}(\text{CO}_3)_2$ ) or serpentine minerals (Bilgin et al., 2012).

The chemical composition of marble waste shows that loss on ignition (LOI) of marble waste is very high. It can be attributed to the loss of carbon dioxide due to dissolution of calcium carbonate and dolomite.

**Table 1.2: Chemical composition of marble waste used by researchers**

| Authors                  | Chemical Components (%) |                   |                                |                                |                  |       |                 |                   | LOI   |
|--------------------------|-------------------------|-------------------|--------------------------------|--------------------------------|------------------|-------|-----------------|-------------------|-------|
|                          | MAJOR                   |                   |                                |                                | MINOR            |       |                 |                   |       |
|                          | CaO                     | Si <sub>2</sub> O | Al <sub>2</sub> O <sub>3</sub> | Fe <sub>2</sub> O <sub>3</sub> | K <sub>2</sub> O | MgO   | SO <sub>3</sub> | Na <sub>2</sub> O |       |
| Saboya et al. (2007)     | 49.82                   | 4.30              | 0.30                           | 1.96                           | -                | 2.64  | -               | -                 | 4.080 |
| Binici et al. (2008)     | 50.13                   | 5.10              | 0.40                           | 1.98                           | -                | 2.72  | -               | -                 | 35.50 |
| Topçu et al. (2009)      | 51.80                   | 4.67              | -                              | 0.03                           | -                | 0.40  | -               | -                 | -     |
| Aruntaş et al. (2010)    | 54.43                   | 0.67              | 0.12                           | 0.08                           | -                | 0.59  | -               | 0.14              | 43.40 |
| Demirel (2010)           | 40.45                   | 38.35             | 0.42                           | 9.70                           | -                | 16.25 | -               | -                 | -     |
| Hebhoub et al. (2011)    | 54.86                   | 0.15              | 0.08                           | 0.04                           | -                | 1.03  | -               | -                 | -     |
| Ergün (2011)             | 51.70                   | 0.18              | 0.67                           | 0.44                           | 0.21             | 0.40  | 0.03            | -                 | 46.04 |
| Belaidi et al. (2012)    | 52.60                   | 1.00              | 0.20                           | 0.20                           | -                | 2.10  | 0.07            | 0.06              | 43.63 |
| Aliabdo et al. (2014)    | 83.22                   | -                 | 0.73                           | 0.05                           | 0.09             | 0.52  | 0.56            | 1.12              | 2.50  |
| Rana et al. (2015)       | 42.13                   | 44.10             | 2.20                           | 2.98                           | -                | 3.72  | -               | 0.08              | 3.50  |
| Tennich et al. (2017)    | 49.46                   | 7.36              | 0.46                           | 0.66                           | -                | 0.23  | 0.08            | -                 | -     |
| Rodrigues et al. (2015)  | 54.20                   | 1.39              | 0.32                           | 0.14                           | -                | 0.64  | -               | 0.04              | 42.60 |
| Kore and Vyas (2016)     | 33.12                   | 3.75              | Traces                         | 0.13                           | -                | 17.91 | -               | -                 | 5.07  |
| Alyamaç and Aydin (2015) | 40.45                   | 28.35             | 0.17                           | 9.70                           | -                | 16.25 | -               | 0.04              | 4.84  |
| Singh et al. (2017)      | 28.63                   | 3.86              | 4.62                           | 0.78                           | -                | 16.90 | -               | -                 | 43.30 |
| Khyaliya et al. (2017)   | 33.12                   | 3.75              | Traces                         | 0.13                           | -                | 17.91 | -               | -                 | 45.07 |
| Ashish (2018)            | 61.83                   | 8.38              | 30.87                          | 0.65                           | 0.07             | 14.36 | 0.33            | 0.60              | 36.87 |
| Munir et al. (2017)      | 51.02                   | 6.56              | 0.84                           | 0.24                           | 0.11             | 1.12  | 0.09            | 0.41              | 38.92 |
| Vardhan et al. (2019)    | 28.67                   | 4.66              | 0.21                           | 0.49                           | 0.05             | 22.30 | -               | 0.06              | 43.70 |
| Çınar et al. (2020)      | 54.40                   | 0.47              | 0.50                           | 0.08                           | -                | 1.23  | -               | -                 | 43.30 |

### 1.3.2. Physical Properties of Waste Marble Powder

The fineness of marble waste powder varies from source to source. Depending upon the fineness of the waste, it can either be used as replacement of cement or sand. The typical range as reported by various researchers are given in Table 1.3.

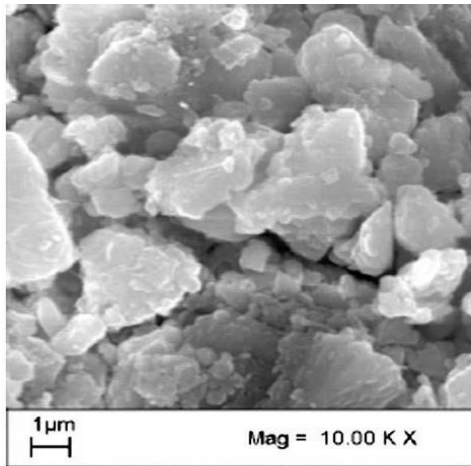
**Table 1.3: Physical properties of marble waste used by researchers**

| <b>Authors</b>           | <b>Specific gravity</b> | <b>Blaine (cm<sup>2</sup>/g)</b> | <b>Water Absorption</b> | <b>Bulk Density (g/cm<sup>3</sup>)</b> |
|--------------------------|-------------------------|----------------------------------|-------------------------|--|
| Binici et al. (2008)     | 2.72                    | -                                | 1.40                    | -                                      |
| Demirel (2010)           | 2.80                    | -                                | -                       | -                                      |
| Aruntaş et al. (2010)    | 2.60                    | 3097                             | -                       | -                                      |
| Hebhoub et al. (2011)    | 2.68                    | -                                | 0.39                    | -                                      |
| Ergün (2011)             | 2.68                    | 5960                             | -                       | -                                      |
| Belaidi et al. (2012)    | 2.70                    | 3500                             | -                       | -                                      |
| Gesoğlu et al. (2012)    | 3.13                    | 2870                             | -                       | -                                      |
| Aliabdo et al. (2014)    | 2.50                    | 3996                             | -                       | -                                      |
| Alyamaç and Ince (2009)  | 2.71                    | 4372                             | -                       | -                                      |
| Rodrigues et al. (2015)  | 2.73                    | 2150                             | -                       | 3.12                                   |
| Vardhan et al. (2015)    | 2.60                    | 3290                             | -                       | -                                      |
| Kore and Vyas (2016)     | 2.70                    | -                                | 0.5                     | -                                      |
| Sadek et al. (2017)      | 2.78                    | 2420                             | -                       | -                                      |
| Alyamaç and Aydın (2015) | 2.71                    | 3920                             | -                       | -                                      |
| Khyaliya et al. (2017)   | 2.56                    | -                                | -                       | 1.67                                   |
| Singh et al. (2017)      | 2.67                    | 3500                             | -                       | 2.78                                   |
| Ashish (2018)            | 2.21                    | 3320                             | -                       | -                                      |
| Vardhan et al. (2019)    | 2.88                    | -                                | 1.1                     | -                                      |
| Çınar et al. (2020)      | 2.70                    | 3090                             | -                       | -                                      |

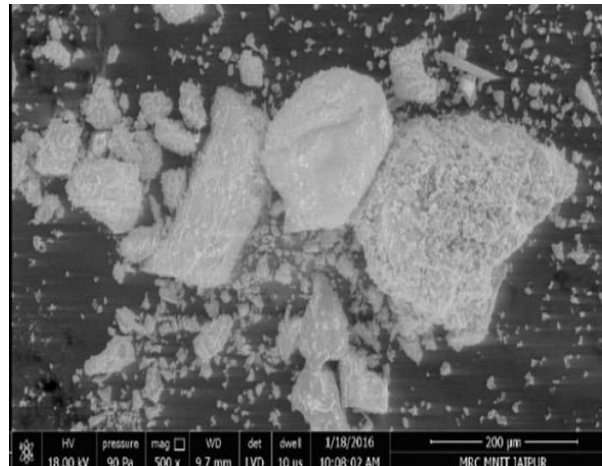
### **1.3.3. Morphology of Marble Waste**

The morphology of marble waste was studied through scanning electron micrographs (SEM) by the various researchers. They stated that the particles of marble waste were of angular in shape and had rough texture (Alyamaç and Ince, 2009).

Fig. 1.2 shows some of the scanning electron micrographs images of marble waste used by the researchers. The angular shape particles are clearly visible in the micrographs.



(a) Alyamac and Ince (2009)



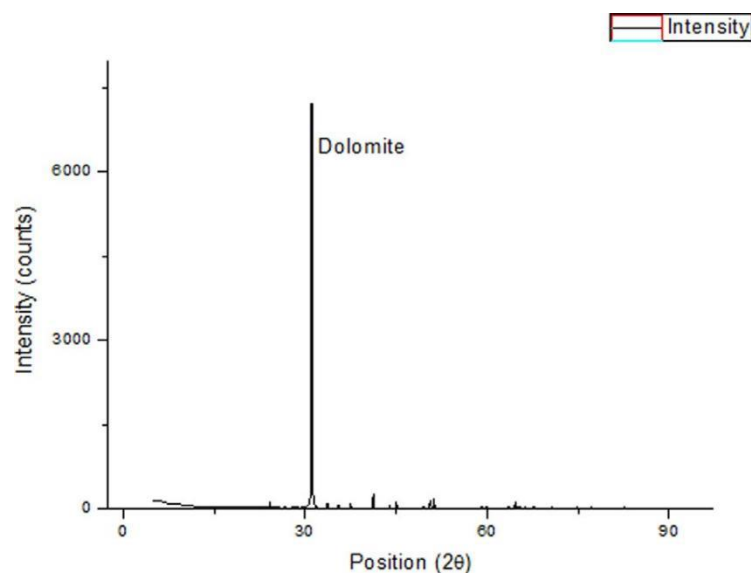
(b) Khaliya et al. (2007)

**Fig. 1.2: SEM micrographs of marble waste**

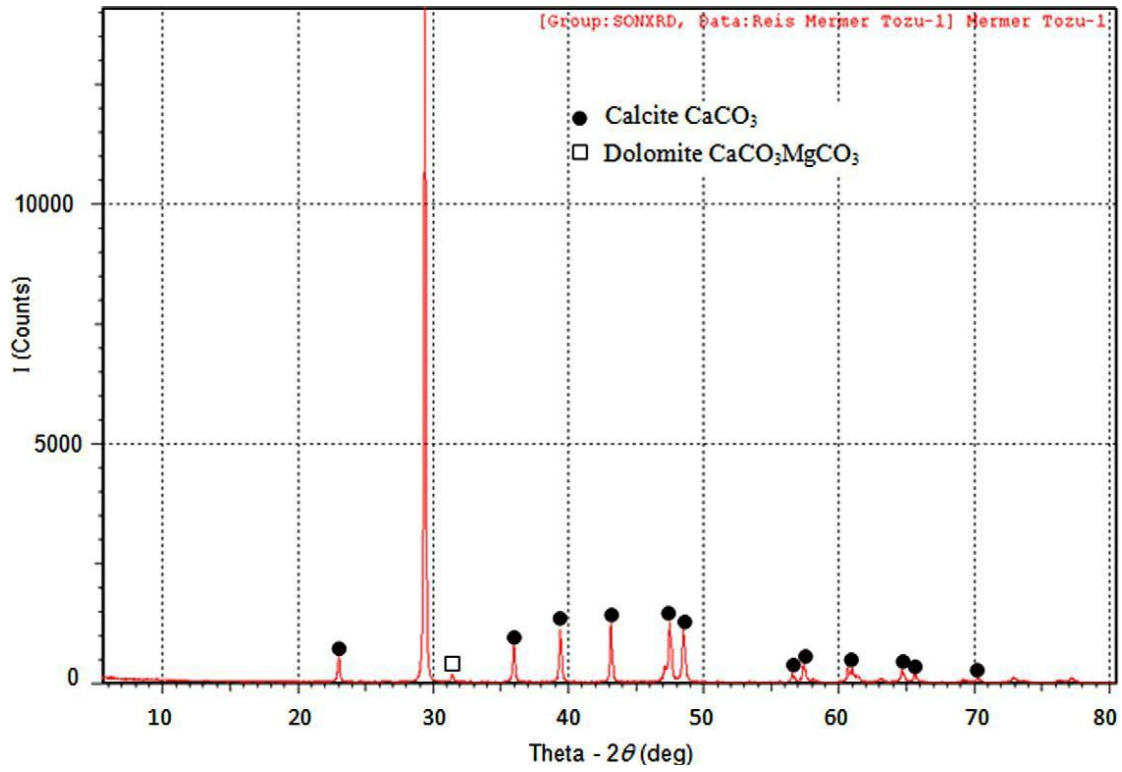
#### 1.3.4. Minerology of Marble Waste

The XRD pattern of marble waste used by (Kabeer and Vyas, 2018; Vardhan et al., 2015) clearly shows a major peak corresponding to dolomite (Fig. 1.3 a).

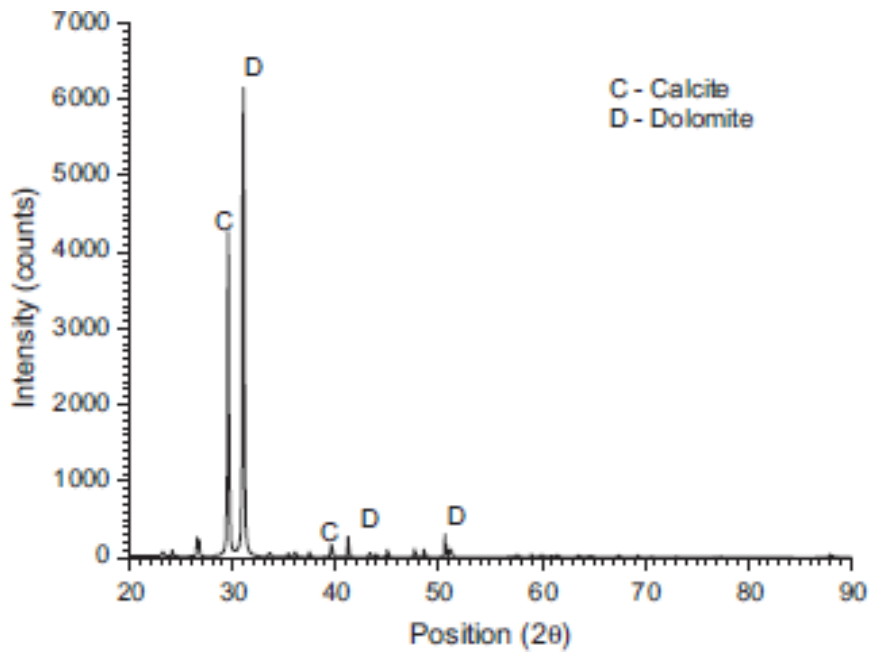
The XRD pattern of marble waste used by (Ergün, 2011) showed that calcite was the main mineral, while dolomite was present in low concentration (Fig. 1.3 b, c). Bilgin et al. (2012), Khyaliya et al. (2017) and Singh et al. (2017) also stated that the main crystalline phase was calcite and small amounts of dolomite.



(a) Reported by (Kabeer and Vyas 2019)



(b) Reported by (Ergün, 2011)



(c) Reported by (Khyaliya et al., 2017)

**Fig. 1.3: XRD patterns of marble waste**

#### **1.4. USE OF MARBLE WASTE AS CONSTRUCTION MATERIAL**

Depending upon the particle size of marble powder, it can be used either as replacement of cement (Aliabdo et al., 2014; Aruntaş et al., 2010; Corinaldesi et al., 2010; Ergün, 2011) or as aggregates (Gameiro et al., 2014; Rodrigues et al., 2015). It is also successfully used for production of self-compacting concrete (Gesoglu et al., 2012; Topçu et al., 2009).

While marble sludge has been utilized as a partial replacement of cement, marble waste collected in the sedimentation tanks can be explored for its potential as a replacement of fine aggregates. There is a dual advantage of using marble powder as fine aggregates. Firstly, since the fine aggregate fraction in concrete is much larger than the cement fraction, large amount of marble waste can be incorporated in concrete as replacement of fine aggregate. Secondly, marble being an inert material, will be more suitable as fine aggregate replacement than being used as a cement replacement. It has already been established that marble dust has a filler effect in concrete and it does not participate effectively in the hydration process (Aliabdo et al., 2014). Also, the mechanical properties of marble waste make it a material of choice that can be used as an aggregate in concrete.

#### **1.5. SIGNIFICANCE OF RESEARCH**

The economic benefit of utilizing waste materials usually attributes to the reduction of the amount of expensive and/or scarce ingredients with inexpensive materials. Environmentally, when industrial wastes are used, not only the CO<sub>2</sub> emissions are reduced, but also residual products from other industries are re-used, and resulting in lesser material being dumped in landfills. With the enormous increase in the quantity of wastes needing disposal, acute shortage of dumping sites, sharp increase in transportation and dumping costs necessitates the need for effective utilization of these wastes.

The present experimental study was conceived following the general purpose of testing sustainable building processes, aimed at saving natural resources and recycling industrial wastes. The primary purpose of the study is to evaluate the efficacy of using marble waste as an alternate to virgin fine aggregates as a measure for sustainable development. If the data of the engineering properties confirm that marble aggregates, which appear similar to sand, also has comparable engineering properties,

it will pave a way for using such materials in engineering design. The objective of present investigations is to replace the natural sand with marble waste from low levels of replacement to very high replacement levels and to provide practical information regarding strength, durability and micro-structure of the resultant mix.

## **1.6. GAPS IN THE PROPOSED RESEARCH AREA**

Marble waste powder is abundantly available by-product of marble industry. It is available in varied sizes, thus making it suitable for use in concrete either as replacement of sand or cement. Most of the research work on the use of marble waste powder in concrete has a focus on the mechanical properties of the mix. The durability aspect on the mix made by incorporating marble waste powder has not been addressed till date. Therefore, all these aspects have to be explored in order to use this material in concrete.

## **1.7. OBJECTIVES OF THE PROPOSED WORK**

The objectives of the proposed work are:

- To evaluate the strength properties of concrete made by incorporating waste marble powder as partial replacement of fine aggregates.
- To determine the durability properties of the concrete made by incorporating marble waste powder as partial replacement of fine aggregates.
- To investigate the microstructure of the resultant concrete.

## **1.8. ORIENTATION OF THESIS**

The thesis has been organized in five chapters. In the first chapter, introduction about the topic including background of waste generated by the marble industry has been presented. The objectives of the present study have also been laid out in this chapter. In the second chapter, literature review regarding the use of marble waste powder as a replacement to both cement and aggregates has been presented. The effect of using marble waste powder on the resulting properties of cement mortar or concrete has been thoroughly reviewed. The third chapter focuses on the details of experimental program that was adopted in this study to systematically study the effect of using marble waste for making concrete. The fourth chapter deals with the results obtained

from the experimental program. The test results are thoroughly discussed to find the effect of using marble waste on fresh properties, strength properties and durability aspects of concrete. Based on the test results, various mathematical models are developed and are presented in this chapter. Fifth chapter deals with the relevant conclusions drawn from the present study and suggestions for the future work. At the end, references cited in the entire work are presented.

## CHAPTER 2

### LITERATURE REVIEW

#### 2.1. GENERAL

Marble is one of the most commonly used natural stones in buildings. Its use is reported right from the ancient times. The major producers of marble are China, India, Turkey, Brazil and Italy in which India ranks second (Vardhan et al., 2019). India is recognized as a nation, well-endowed in natural mineral resources. The country produces about 87 minerals, which include metallic, non-metallic, atomic minerals and minerals used in construction industry. Among minerals used as building materials, India has large deposits of high-quality marble, with its various varieties available in different parts of the country. In India, Rajasthan is the richest state with regards to marble deposits (1100 million tons) both in quality and quantity (Central Pollution Control Board, 2010). Around 3600 marble mines, 1200 marble processing (gang-saws) units and 400 Automatic Tiling Plants (Block cutters) are spread over 16 districts of Rajasthan. These units generate five to six million tons of marble waste annually (Singh et al., 2017). Marble is a metamorphic rock that results from the transformation of pure limestone. Chemically, it consists predominantly of calcite, dolomite or serpentine minerals (Rashad, 2013; Sankh et al., 2014).

The quarrying of marble has to be done very carefully because the whole block of rock is required to be taken out from the parent rock without damaging the block. In order to get the undamaged block at one stretch, finest quarrying techniques have been developed over the years. Further, the extracted block is to be processed in order to cut it into slabs of required thickness by sawing. The prepared slabs are further polished and smoothed to get extremely fine end product. During the quarrying and processing of marble, large amount of waste is generated. It is reported that around 5 mm of marble is lost for every 20 mm quarried marble slab (Aliabdo et al., 2014). The amount of marble waste generated depends upon the processing and quarrying methods adopted. On an average, 20-25% waste sludge is generated from the processing operations, depending upon the kind of processing operations (Alyamaç and Ince, 2009; Ashish, 2018; Marras et al., 2017a) and the waste generation can be as high as 60% during quarrying of marble blocks (Singh et al., 2017). It is reported

that around 3 million tons of marble waste is produced per year in India (Vardhan et al., 2015). Fig. 2.1 shows the approximate percentage of waste generated during various processing operation of the quarried marble.

The waste generated in quarrying is mainly in the form of small blocks, powder or slurry (Kabeer and Vyas, 2018), while the waste generated during processing of marble is finer than the waste generated during quarrying. The waste generated during processing is mostly in powder or slurry form. The particle size of marble waste achieved during processing can be even smaller than the particle size of cement. Li et al. (2018) reported that the hardness of marble is about 3 on Moh's scale, indicating that it is not a hard rock and has a tendency to reduce to very small particle size level (Li et al., 2018b). Due to this, the waste generated can be of extremely fine particle size.

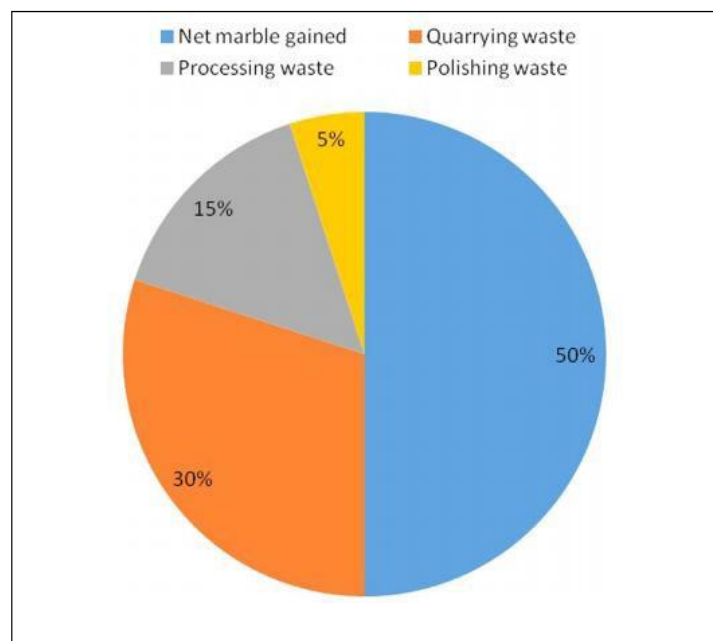


**Fig. 2.1: Proportion of marble and associated waste produced during various processing operations (Singh et al., 2017)**

The marble waste so generated, either in sludge form or in powder form, is generally disposed off in an open area. The waste of higher particle size ultimately gets converted into smaller size particles due to physical and chemical processes under the action of rain and sunlight (Alyamaç and Aydin, 2015). Ultimately, the marble waste gets converted into very small size particles and if left unattended, it can be a major

source of water and air pollution (Singh et al., 2017). The fine particles of marble waste clogs the agricultural land leading to loss of soil fertility (Vardhan et al., 2015). The big heaps of the waste that is dumped alters the natural landscape of the area and hinders the natural flow of storm water thereby leading to artificial flooding of the vicinity. The very fine particles also caused air pollution. The fine marble dust, if left in the environment, gets suspended in air and cause health related hazards. The high chemical content of marble leads to groundwater contamination (Rizzo et al., 2008).

## **2.2. RE-USE OF MARBLE WASTE**

The researchers have now started recommending the use of marble waste in various industries. For instance, Careddu and Marras (2015) and Careddu et al. (2014) suggested that the marble slurry can be used in production of tires, rubber, cement, paint, lime and cosmetic industries due to the high amount of calcium carbonate present in it (Careddu et al., 2014; Careddu and Marras, 2015). The use of marble slurry is also proposed as artificial soil for rehabilitation, as filler material and as water proofing material when mixed with bentonite clay (Dino et al. 2013). The bigger size waste particles can be directly used for land filling at some construction sites. Marras et al. (2017) recommended the use of marble waste for production of gypsum paste (Marras et al., 2017b). Ayber and Ulutas (2017) also suggested the use of marble waste in roads, plastics, chemicals and ceramic industries. Along with all these uses, the major advantage of reuse of marble waste can be achieved if it is reused as an alternative to the basic constituents of concrete. It will lead to sustainable development by reducing the over exploitation of natural resources and by increasing the utilization of industrial by-products. The wide range of sizes of marble waste allows it to be used as replacement of either cement or aggregates. Table 2.1 summarizes the research carried out on the reuse of marble waste in construction sector. Some researchers have utilized marble waste as partial to full replacement of fine aggregates, since it is considered to be an inert material. When used as replacement of fine aggregates, the replacement levels are as high as 100%. However, the very small particle size of the waste makes it an appropriate product to be utilized as cement replacement. When used as cement replacement, the replacement levels are generally kept small. Aydin and Arel (2019) attempted the replacement level of up to 60% for making various uses, such as manufacturing of tiles, controlled low strength materials and bricks.

**Table 2.1: Summary of research related to use of marble waste as a construction material**

| <b>Author</b>             | <b>Type</b>                 | <b>Substituted with</b>    | <b>Substitution level</b> |
|---------------------------|-----------------------------|----------------------------|---------------------------|
| Binici et al. (2007)      | Concrete                    | Fine sand                  | Up to 15%                 |
| Binici et al. (2008)      | Concrete                    | Coarse aggregates          | 100%                      |
| Topçu et al. (2009)       | SCC                         | Binder                     | 0-300 kg/m <sup>3</sup>   |
| Alyamaç and Ince (2009)   | SCC                         | Filler                     | -                         |
| Aruntaş et al. (2010)     | Mortar                      | Additive in cement clinker | Up to 10%                 |
| Demirel (2010)            | Concrete                    | Fine sand                  | Up to 100%                |
| Corinaldesi et al. (2010) | Mortar, concrete            | Fine aggregates            | Up to 20%                 |
| Hebhoub et al. (2011)     | Concrete                    | Fine and coarse aggregates | Up to 100%                |
| Rai et al. (2011)         | Mortar, concrete            | Fine aggregates            | 0-20%                     |
| Ergün (2011)              | Concrete                    | Cement                     | Up to 10%                 |
| Belaidi et al. (2012)     | SCC                         | Cement                     | Up to 40%                 |
| Gesoğlu et al. (2012)     | SCC                         | Filler                     | Up to 20%                 |
| Bilgin et al. (2012)      | Bricks                      | Brick mortar               | Up to 80%                 |
| Keleştemur et al. (2014)  | Mortar                      | Fine sand                  | 0 – 50%                   |
| Aliabdo et al. (2014)     | Blended cement and Concrete | Cement and sand            | Up to 15%                 |
| André et al. (2014)       | Concrete                    | Coarse aggregates          | Up to 100%                |
| Gameiro et al. (2014)     | Concrete                    | Fine aggregates            | Up to 100%                |
| Silva et al. (2014)       | Concrete                    | Fine aggregates            | Up to 100%                |
| Vardhan et al. (2015)     | Mortar                      | Cement                     | Up to 50%                 |
| Talah et al. (2015)       | HPC                         | Cement                     | Up to 15%                 |
| Rodrigues et al. (2015)   | Concrete                    | Very fine aggregates       | Up to 20%                 |
| Alyamaç and Aydin (2015)  | Concrete                    | Fine aggregates            | Up to 90%                 |
| Rana et al. (2015)        | Concrete                    | Cement                     | Up to 25%                 |
| Arel (2016)               | Concrete                    | Fine aggregates            | Up to 75%                 |

|                              |                   |                         |            |
|------------------------------|-------------------|-------------------------|------------|
| Molnar and Manea (2016)      | Mortar as plaster | Fine aggregates         | Up to 100% |
| Kore and Vyas (2016)         | Lean concrete     | Coarse aggregates       | Up to 100% |
| Sardinha et al. (2016)       | Concrete          | Cement                  | Up to 20%  |
| Sadek et al. (2016)          | SCC               | Cement                  | Up to 50%  |
| Khyaliya et al. (2017)       | Mortar            | Fine aggregates         | 0-100%     |
| Tennich et al. (2017)        | SCC               | Filler                  | -          |
| Singh et al. (2017)          | Concrete          | Cement                  | Up to 15%  |
| Buyuksagis et al. (2017)     | Mortar            | Additive                | Up to 100% |
| Munir et al. (2017)          | Mortar, Concrete  | Cement                  | Up to 40%  |
| Binici and Aksogan (2018)    | Concrete          | Fine aggregates         | Up to 100% |
| Khodabakhshian et al. (2018) | Concrete          | Cement                  | Up to 20%  |
| Li et al. (2018a)            | Mortar            | Paste                   | Up to 20%  |
| Ashish (2018)                | Concrete          | Cement, Fine aggregates | Up to 15%  |
| Kabeer and Vyas (2019)       | Mortar            | Fine aggregates         | 0-40%      |
| Aydin and Arel (2019)        | Mortar            | Cement                  | Upto 60%   |
| Varadharajan et al. (2020)   | Concrete          | Fine aggregate          | Upto 30%   |
| Vaidevi et al. (2020)        | SCC               | Fine aggregates         | Upto 100%  |
| Zhang et al. (2020)          | Cellular concrete | Cement                  | Upto 20%   |

\*SCC: Self-compacting concrete, HPC: High performance concrete

In concrete, the attempts are made to make conventional concrete, self-compacting concrete, high performance concrete and cellular concrete by using marble waste in place of cement, fine aggregates or coarse aggregates. The use of marble waste will be a step towards better sustainability.

### **2.3. USE OF MARBLE WASTE AS REPLACEMENT OF CEMENT**

Since cement is the major binding material for making mortar and is responsible for about 2.5% of total worldwide emission of carbon dioxide from industrial sources (Aldea et al., 2000), the researchers are looking for the alternative materials that can be used as a partial replacement of cement. The particle size of marble waste that is obtained in a marble slurry is extremely small and has the potential to be used as an

alternative to cement. The effect of using marble waste on various properties of the resultant system is discussed here under.

### **2.3.1. Fresh Properties**

Munir et al. (2017) prepared mortar mixes by replacing up to 40% of cement by marble waste powder. They observed increase in consistency of the mixes after addition of marble waste powder. It was attributed to higher specific surface area of the powder (3512 cm<sup>2</sup>/g as compared to 2961 cm<sup>2</sup>/g for cement). Also, both initial setting time and final setting time of the mixes increased by incorporating marble waste powder. At the same time, the authors reported decrease in soundness of the mixes from 1.6 mm to 1.2 mm, when the replacement of 40% of cement by marble waste powder was attempted. The change in soundness of the mix was correlated with magnesia present in cement which is considered to be responsible for expansion. Since the magnesia content was smaller in marble waste powder than in cement, it reduced the expansion and hence improved soundness of the resultant mixes.

Vardhan et al. (2015) also observed slight decrease in consistency of the binder mix in which marble waste was used as replacement of cement. Test results indicated that the water requirement of the binder paste mixes made with marble powder was lesser than that of the control cement paste. Also, there was a systematic increase in both initial and final setting times of the binder mixes. The increase in final setting time of mix containing marble powder indicated delay in hydration process. However, the initial setting time of all binder mixes complied with the limits prescribed by (BIS 4031: Part 5, 1988).

Similar observations on the setting behavior of cement pastes made with marble powder were made by (Aliabdo et al., 2014), although the properties of marble powder used in both the cases were very different. The decrease in viscosity (and hence decrease in flow time) by the addition of marble powder was also reported by (Belaidi et al., 2012).

The authors suggested that small increase in initial setting time would be helpful for blended mixes, so that the mixes remain workable for more time (Berra et al., 2012). The difference in final and initial setting time varied only in a narrow range for all the mixes. It indicated that once the initial setting has reached, the setting process takes similar time for all mixes. Also, the expansion values of the mixes were almost

similar; indicating that there was no effect of marble powder addition on expansion of binder pastes. Aydin and Arel (2019) made cement-paste system by replacing up to 40% of cement with marble waste powder. They observed reduction in slump flow upon addition of marble waste powder, due to higher specific surface area of the powder, which resulted in higher internal friction between the particles; thereby leading to reduction in slump.

Buyuksagis et al. (2017) made mortars meant to be used as an adhesive for binding of ceramic tiles on floors and walls. The marble waste powder was used as an additive in place of dolomite for making of the mortar. It was observed that a dense mortar could be obtained on addition of marble waste powder. The initial setting time of the mixes reduced due to fineness of the powder used. The authors further said that all mixes had the setting time of more than two hours, as desired by EN 196-3 + A1 (EN 196-3+ A1, 2010) for ease of application.

Li et al. (2018a) used marble dust as a paste replacement rather than the cement replacement. They also observed that the mixes having higher volume of marble dust were drier during mixing and required higher super plasticizer dosage. Ashish (2018) also observed decrease in workability of the concrete mixes having marble waste as a replacement to cement. Khodabakhshian et al. (2018) used both silica fume and marble waste as replacement of cement to prepare concrete mixes. They observed substantial decrease in workability due to higher fineness of both silica fume and marble powder.

### **2.3.2. Mechanical Properties**

Aliabdo et al. (2014) prepared marble waste dust blended cement by replacing up to 15% of cement with the dust. It was observed that compressive strength was higher than that of control mix up to 5% replacement level; whereas the decrease of 5% was reported at 15% marble dust replacement level. In terms of steel-concrete bond strength, 10% marble dust replacement level was found to be most appropriate. The TGA analysis of the mixes indicated that there was no change in the chemistry of the mixes modified with marble dust. SEM images also revealed similar morphology of mixes indicating no noticeable change in the hydration process due to incorporation of marble dust. The authors further used marble dust as replacement of cement and sand. They concluded that incorporation of marble dust as sand replacement had more

significant effect on the properties of concrete as compared to the mixes in which marble dust was used as cement replacement. The marble powder improved properties of mainly due to filler effect.

Aruntaş et al. (2010) studied the usability of marble waste powder as an additive material in blended cement clinker by inter-grinding marble powder with cement clinker at different blend ratios of 2.5%, 5%, 7.5% and 10%. The studies carried out on mortar prisms concluded that 10% marble powder can be used as an additive in cement production.

Rana et al. (2015) used up to 25% of marble dust as replacement of cement and observed that both compressive strength and flexural strength decreased at each replacement level; although the reduction in strength was very small up to 10% replacement level. On the other hand, better resistance to water penetration was observed up to 15% replacement level. The authors explained that the higher fineness of marble particles filled the capillary pores present in concrete, which led to lesser number of connected pores in concrete with marble powder. The authors observed that the porosity was higher in mix containing 15% marble dust, till the permeability value of the mix was low because of lower number of interconnected pores in mixes having marble waste dust.

Ashish (2018) used an amalgam of cement and sand for making concrete and observed that 10% sand and 10% cement substituted by marble powder had optimum performance in terms of both compressive strength and split tensile strength. Talah et al. (2015) further reported that the concrete with marble powder was less sensitive to aggressive curing practices than the control high performance mix.

Munir et al. (2017) prepared mortar specimens using up to 40% of marble powder as replacement of cement. They reported increase in strength with 10% use of marble waste powder. Similar observations of increase in strength up to 10% replacement was reported by Vardhan et al. (2015). The initial increase in strength was attributed to the filler effect due to use of more fine particles in the mix. The authors further concluded that the large replacement levels of cement by marble powder are detrimental to the mechanical properties of cement pastes. The large levels of replacement lead to delayed hydration of the mix, and porous microstructure, as is visible from the microstructure studies on the mixes.

Similar observations were made by Corinaldesi et al. (2010) wherein mechanical behaviors of mortars with 10 and 20% marble powder was reported at ages of 3, 7, 28 and 56 days. Singh et al. (2017) studied the effect of percentage replacement of marble powder on mixes made at three different water-binder ratios of 0.35, 0.40 and 0.45. The authors reported improvement in mechanical properties up to 15% replacement level for mixes made at water-binder ratios of 0.35 and 0.40. For water-binder ratio of 0.45, replacement level of 10% was found to be most efficient. The better performance of mixes with marble dust at lower water-binder ratios was attributed to better dispersion of particles due to use of super plasticizers. It resulted in homogeneous packing of particles, thereby providing better mechanical properties. The authors also gave compressive strength prediction model based on artificial neural network.

In order to further improve the mechanical performance of concrete having marble waste powder, some additives were used along with marble waste powder. For instance, Khodabakhshian et al. (2018) used up to 10% silica fume along with marble powder to make concrete mixes. The authors reported that silica fume was able to counteract the decrease in properties of concrete due to addition of marble waste powder. The mix having 20% marble waste powder and 10% silica fume as replacement of cement gave almost similar mechanical properties as the original mix. Ergün (2011) used marble powder along with diatomite as partial replacement of cement. Strength tests on concrete specimens concluded that either 5% marble powder separately or 5% marble powder along with 10% diatomite can be utilized to improve mechanical properties of concrete.

Buyuksagis et al. (2017) attempted using marble waste powder in making cement based adhesive mortar. The authors reported that 28 days compressive strength and bending strength increased by using up to 10% of marble powder. Gesoğlu et al. (2012) studied the effect of addition of marble powder as replacement of concrete binder in self-compacting concrete at substitution ratios of 5%, 10% and 20%. The authors concluded that high replacement ratios adversely affect the fresh properties of self-compacting concrete. (Aydin and Arel, 2019) recommended the use of up to 60% of marble waste powder as replacement of cement for building materials that could be used for bricks, tiles and controlled low strength materials.

Corinaldesi et al. (2010) evaluated various mix based upon cement or sand substitution and stated that 10% substitution of sand by marble powder provides maximum compressive strength at about same workability. Hebhouh et al. (2011) investigated effect of addition of marble aggregates either as substitution of gravel or sand and confirmed the use of marble waste aggregates up to 75% as an alternative to natural aggregates. Similar results were obtained by Gameiro et al. (2014).

### **2.3.3. Durability Properties**

Apart from mechanical strength, various durability properties were investigated by the authors because durability is a major concern that defines overall performance in the long term. Rana et al. (2015) tried up to 25% of marble powder as replacement of cement and investigated permeability, chloride migration, rebar corrosion and carbonation of the mixes. The results displayed that up to 15% use of marble powder provided better resistance to aggressive environments; while further addition of marble powder led to increase in permeability.

The authors suggested that the decrease in connectivity of pores due to addition of finer particles led to decrease in permeability at lower replacement levels. However, at higher replacement levels, reduced cement content decreased hydration leading to poor microstructure that could not be compensated by the filler effect provided by marble powder. Even the chloride ion migration reduced by using up to 10% of marble powder. The corrosion resistance was also enhanced for mixes having 10% of marble powder. However, carbonation depth was reported to be high for all mixes having marble powder. It was attributed to lower bicarbonate alkalinity of marble powder as compared to cement, which led to increase in carbonation depth of mixes.

Munir et al. (2017) studied the effect of using waste marble powder in controlling alkali-silica reactivity of concrete. They used up to 40% of marble waste powder as replacement of cement. The authors observed about 50% reduction in expansion of mortar bars with use of 40% of marble waste powder. No signs of cracking related to alkali-silica reactivity was observed in SEM images for the mixes having marble waste powder. EDS analysis also showed lower amount of alkalis in mixes made with marble waste powder. The amount of alkalis reduced due to presence of lower alkalis in marble powder (0.48%) as compared to the corresponding value in cement (0.84%).

Singh et al. (2017) investigated the effect of using marble waste powder of mixes made at different water-cement ratios. They used up to 20% of marble waste powder for making concrete mixes at three water-cement ratios of 0.35, 0.40 and 0.45. The durability performance of the mixes was analyzed by performing ultrasonic pulse velocity test, surface resistivity test and bond strength test.

The test results of ultrasonic pulse velocity test indicated better quality of mixes with marble waste powder. Surface resistivity and bond strength of the mixes also improved up to 15% replacement level for all water-binder ratios.

Li et al. (2018a) investigated the use of marble dust as paste replacement without changing the mix proportions. Marble dust was used to make mortar mixes and the performance was checked in terms of water absorption, drying shrinkage and carbonation depth. The results indicated that by this method, the cement content in the mixes could be reduced by 33% and improvement in durability performance was observed. The addition of marble dust could reduce the carbonation depth of the mixes by 43%. The water absorption rate was reduced by 45% and the ultimate drying shrinkage strain was reduced by 50%.

Some authors made binary mixes using one more additive along with marble powder for further improving durability performance of the mixes. For instance, Khodabakhshian et al. (2018) studied the durability performance of mixes made by using both silica fume and marble dust as partial replacement of cement.

The durability performance of the mixes was studied in terms of resistance under sodium sulphate attack, magnesium sulphate attack and acid attack, all taken separately. Apart from these, water absorption and electric resistivity of the mixes was measured. It was observed that a combination of 10% silica fume and 20% marble powder had better performance with sodium sulphate and magnesium sulphate exposures. The mixes with 20% of marble waste powder had best performance under the acid exposure. The authors stressed that up to 30 % of cement could be saved without comprising of any of the properties of the mixes by using a suitable combination of silica fume and marble waste powder.

#### **2.4. USE OF MARBLE WASTE AS REPLACEMENT OF FINE AGGREGATES**

The different sizes in which marble waste can be obtained helped in exploring its use as replacement to different components of concrete. While some researchers have studied the potential of using marble waste as cement replacement, some others have tried to explore its potential as replacement to aggregates.

The replacement of cement was earlier considered to be most appropriate because of the association of cement with production of green-house gases. Therefore, such substitutions will help in reducing the carbon footprints associated with the production of cement. The alternatives for natural aggregates are also required for sustainable development. Aggregates are the major constituents of concrete, contributing towards nearly 70% of concrete weight. Most of the aggregates are obtained from the natural quarries or river beds. With the rapid increase in construction activities, the demand for natural aggregates are on the rise, which is further contributing towards uncontrolled exploitation of the natural resources. For instance, natural river sand, which is considered to be the most suitable fine aggregate in concrete production, is extensively exploited to meet the ever-increasing demand in concrete production. It has led to serious environmental and economic concerns (Rashad, 2013; Sankh et al., 2014).

On one hand, the natural resources are over exploited for their use as fine aggregates; while, on the other hand, the materials generated from other industries in the same particle size range are treated as waste and are discarded. These industrial wastes have the potential to become sustainable alternatives to fine aggregates. Various researchers have explored the use of different inert waste materials as partial or complete substitution of river sand as fine aggregates. There is a dual advantage of using marble powder as fine aggregates. Firstly, since the fine aggregate fraction in concrete is much larger than the cement fraction, large amount of marble waste can be incorporated in concrete as replacement of fine aggregate. Secondly, marble being an inert material, will be more suitable as fine aggregate replacement than being used as a cement replacement.

Ulubeyli et al. (2016) summarized that the incorporation of marble powder as aggregates improved most of the strength and durability properties of concrete.

Among the studies related to the use of marble powder as aggregates, the review can be divided into three main categories: use as very fine aggregates (passing through 0.25 mm sieve), fine aggregates (passing through 4.36 mm sieve) and as coarse aggregates (passing through 20 mm sieve). Accordingly, the review is divided into three sections:

#### **2.4.1. Use of Marble Waste as Replacement of Very Fine Aggregates**

Demirel (2010) studied the effect of using marble waste dust as a replacement of very fine sand (passing through 0.25 mm sieve) in making conventional concrete. The percentage replacement of very fine sand portion was attempted at 25%, 50% and 100%. The performance of the prepared mixes was studied at 3, 7, 28 and 90 days in terms of change in compressive strength, porosity and sorptivity. It was observed that the compressive strength of the mixes kept on increasing with the increase in percentage replacement level with maximum compressive strength obtained at 100% replacement level. The porosity and sorptivity of the mixes also decreased. The authors claimed that marble dust particles played an important role in hydration process, apart from the reported filler effect.

#### **2.4.2. Use of Marble Waste as Replacement of Fine Aggregates in Concrete**

Gameiro et al. (2014) used up to 100% of waste generated from marble quarry industry as a replacement of fine aggregates. The authors tried to investigate the influence of addition of marble dust on fresh and hardened properties of concrete including water absorption both by immersion and by capillary action, chloride ion penetration, carbonation and drying shrinkage. Four types of natural aggregates were used as primary aggregates, viz. silicious river sand, basalt sand, granite sand and limestone gravel. It was observed that water absorption of the mixes improved with the incorporation of marble waste. The authors further established correlation between water absorption and chloride ion penetration and observed that chloride migration coefficient also decreased for mixes having marble waste as fine aggregates. The most important effect of the incorporation was observed on drying shrinkage of the mixes, in which drying shrinkage of marble waste mixes was found to be lower than the primary mixes. Silva et al. (2014) further reported the abrasion resistance of these mixes. It was observed that marble powder mixes were more sensitive to wear and hence reduced the abrasion resistance of concrete.

Binici and Aksogan (2018) concentrated more on the durability performance of mixes with marble dust. The size of marble dust particles was in the range of 0-5 mm. The major performance parameters were compressive strength, abrasion resistance, freeze-thaw and sulphate resistance of the mixes. For freeze thaw test, the temperature variation was kept from -20° to +20°C. The sulphate resistance was determined in 10% magnesium sulphate exposure for 90 days. The samples with marble powder were found to be more resistant to abrasion which was due to greater hardness of marble waste as compared to the reference aggregates. The compressive strength of the mixes after freeze-thaw cycles was reported to be 60% higher than the control mix. Even the sulphate resistance of the mixes with marble powder was higher. It was indicated that the increase in marble powder was effective in increasing durability of concrete.

The authors explained that it was due to better bonding of constituents that resulted in condensed matrix and hence improved the durability performance of the mixes. Alyamaç and Aydin (2015) also reported better abrasion resistance of mixes made with 40% of marble dust. The authors further commented that use of marble powder was more economical than sand because of higher production cost of sand that includes washing, sieving and transportation.

Varadharajan et al. (2020) used a combination of rice husk ash and marble powder for preparation of concrete mixes. Rice husk ash was used as a partial replacement of cement and marble powder was used a partial replacement of fine aggregates, along with the use of 1.5% of hooked steel fibers was made to further improve mechanical properties of concrete. The replacement level of cement was kept at 0% to 20%; while the fine aggregates were replaced from 0% to 30% with marble waste powder. The performance of the mixes was assessed through workability tests, mechanical properties like compressive strength, split tensile strength and flexural strength of the mixes. Apart from these, the durability parameters like sorptivity and porosity were also investigated.

The results indicated an increase in compressive strength with the addition of marble powder. The 28-day compressive strength increased by 9% for 10% addition of marble powder and increased by 28% for 30% addition level. The researchers attributed the enhancement in performance to the filler effect provided by marble particles, which were in particle size range of 300 µm to 1.18 mm. Also, the reaction

between dolomite and  $C_3A$  improved the binding ability of the mixes. In terms of overall performance of the mix, a mix with 20% rice husk ash, 30% marble powder along with 1.5% fibers proved to be most effective.

#### **2.4.3. Use of Marble Waste as Fine Aggregates in Mortar**

Apart from concrete, mortar is an important building material which is mainly used in plastering work. For such mixes, along with compressive strength; the adhesive characteristics of the mix also becomes an important parameter. Some researchers studied the effect of using marble powder in preparation of lean mortar mixes. Khyaliya et al. (2017) prepared lean mortar mix in 1:6 ratio (cement: sand) in which sand was systematically replaced by marble powder from 0% to 100%. The performance of mixes was monitored by compressive strength measurements, water absorption, drying shrinkage and resistance to outside exposure of sodium sulphate and acid.

The authors reported a decrease in water requirement for mixes having marble powder. In terms of compressive strength, maximum benefit of using marble powder was achieved at 50% replacement level. Water absorption, which is considered as more important parameter than compressive strength because of its utility as plaster for external walls, was found to be very low as compared to the control mix. The drying shrinkage of the mixes with marble dust was lower than the control mix, indicating lower chances of cracking of external surfaces. The author also reported lower effect of external aggressive exposures like sodium sulphate and acidic environments. The better mechanical performance of mortar mixes was also reported by Hebhouh et al. (2011) and Mohamadien (2012).

Keleştemur et al. (2014) prepared richer mortar mix by using cement and sand in the ratio of 1:3 by using very fine marble particles (<0.25 mm) as replacement to sand. The mixes were reported to have better compressive strength and split tensile strength, but had lower resistance to freeze-thaw cycles. The authors reported that the filler effect caused by the finer marble dust particles fill all minute pores; thereby not allowing easy expansion/ contraction in freeze-thaw cycles. In case of performance of mortar mixes in 1:3 proportions, only 10% replacement of fine aggregates with marble dust was recommended.

Corinaldesi et al. (2010), Khyaliya et al. (2017) and Rai et al. (2011) made 1:6 ratio mortar mix by replacing up to 40% of river sand with marble dust. The authors observed that better performance could be obtained only up to 20% replacement level, beyond which the finer particles of marble dust started interfering with cement particles in its penetration into finer pores, thereby affecting hydration of cement. The mortar brick adhesion quality was also found to decrease beyond 20% replacement level.

#### **2.4.4. Use of Marble Waste as Coarse Aggregates**

The marble waste generated during quarrying operations is generally larger in size and can therefore be used as coarse aggregates for making concrete. Some researchers have attempted such substitutions (André et al., 2014; Binici et al., 2008; Kore and Vyas, 2016).

Hebhoub et al. (2011) used upto 100% of marble aggregates to replace either natural coarse aggregates and fine aggregates to investigate the performance in terms of workability and mechanical strength. In terms of compressive strength, it was observed that as sand substitution, better performance was achieved upto 75% replacement level; while as gravel substitution, all mixes up to 100% replacement level performed better than the corresponding control mixes. The authors further reported that 50% replacement level was optimum for sand replacement, while higher replacement levels of 75% were most effective for coarse aggregate substitution.

André et al. (2014) also substituted upto 100% of primary aggregates with marble waste aggregates. The comparison of such mixes was made with the mixes having 100% basalt aggregates, 100% granite aggregates and 100% limestone aggregates. It was observed that the workability of the mixes with marble aggregates increased up to 20% replacement level, thereafter a decrease in workability was observed. Initial increase in workability was due to lower water absorption of marble aggregates as compared to other primary aggregates; while the modification in shape factor was responsible for the loss of workability at higher replacement levels. A slight increase in compressive strength was observed in mixes with marble aggregates, although water behaviour was found to be almost similar to the control mix. In terms of durability parameters, carbonation depth was reported to be similar for all mixes, while chloride migration coefficient was found to be higher for the mix with marble

aggregates. The authors attributed this to the low alumina content in marble aggregates.

Kore and Vyas (2016) made a lean concrete mix with water-cement ratio of 0.6 and the replacement of natural aggregates was made from 20% to 100% by weight. The performance of mixes was monitored in terms of workability, compressive strength, permeability and acid resistance of the mixes. For such lean mixes, marble aggregates demonstrated better performance than the natural aggregates; in which compressive strength was reported to be 38% at 80% replacement level. However, the penetrability of mixes also increased. The authors said that the increase in penetrability was due to inter connectivity of pores in marble aggregates. Also, the deterioration of concrete in acid exposure was also slightly higher than the mixes with marble aggregates.

Binici et al. (2008) attempted the substitution of both the conventional fine aggregates and coarse aggregates with the waste products for sustainable development. Fine aggregates were replaced by GGBS; while coarse aggregates were replaced by marble powder and granite. The results were monitored for fresh properties, hardened properties like compressive strength, flexural strength, split tensile strength, modulus of elasticity, abrasion resistance, chloride penetration and sulphate attack. The authors reported better workability of mixes having marble and granite waste aggregates due to their more cohesive nature. The mechanical strength also had significant improvement under addition of marble aggregates. The maximum benefit of using marble aggregates was reported in improvement in abrasion resistance of the mixes. It was reported to be around 60% lower than the control mix. The authors attributed it to the denser pore structure of the mix. In terms of durability performance, both chloride penetration and loss due to sulphate ion exposure was also lower in mixes with marble waste aggregates.

## **2.5. USE OF MARBLE WASTE IN SELF COMPACTING CONCRETE**

The high fineness of marble slurry can help in its use as filler in making self-compacting concrete. In order to explore this possibility, various researchers used marble powder as a substitute for cement or as a filler to improve fresh and hardened properties of self-compacting concrete. Some combinations of marble powder and other pozzolanic or filler materials was also attempted to compensate for the negative

effects of using marble powder. Some researchers provided a detailed mix design procedure for incorporating marble powder in self-compacting concrete.

For instance, Alyamaç and Ince (2009) proposed a mix design procedure for development of self-compacting concrete using additional inert particles of marble dust. The mixes were designed by using a monogram which allowed the design for two slump level allowing the mixes to be used for varying applications like reinforced concrete structures and columns. It also allowed the design of economical concrete mix using marble dust.

Gesoğlu et al. (2012) used both marble powder and limestone as filler along with some amount of fly ash in making self-compacting concrete. The binary and ternary mixes were designed for this purpose. In binary mixes, a combination of cement was made with either of the three additives, that is fly ash, marble or limestone; while in ternary mixes, a combination of fly ash and marble powder or fly ash and limestone was tried along with cement. The replacement level of fly ash was fixed at 30% as replacement of binder. The level of marble powder and limestone was varied from 5% to 20%. The prepared mixes were tested for fresh properties and hardened properties. The hardened properties included compressive strength, split tensile strength, sorptivity and electrical resistivity of the prepared mixes. It was observed that the addition of marble powder reduced workability of the mixes, thereby leading to the requirement of higher dosage of superplasticizer. However, the inclusion of fly ash helped in mitigating the negative effects on fresh properties. Also, the addition of both limestone and marble powder increased initial and final setting times of the mixes.

The compressive strength and split tensile strength registered a systematic decreased with increase in the amount of marble powder. Even, the strength values of the ternary mixes made by using fly ash and marble powder was lower than the reference mix. The authors thereby concluded that the addition of limestone has better effect on compressive strength than the incorporation of marble powder. In terms of sorptivity and chloride ion penetration, all the binary and ternary combinations were found to be better than the control mix. It gave an indication that the use of marble powder as a filler in self-compacting concrete could improve the durability parameters of the mix.

Topçu et al. (2009) used unprocessed marble waste as filler in making of self-compacting concrete, Marble powder used in the study was obtained from the

processing plant and was used without any further processing. The marble dust replaced the binder content from 0-300 kg/m<sup>3</sup>. The prepared self-compacting concrete was investigated for fresh and mechanical properties, including testing for compressive strength, flexural strength, porosity and capillary properties at 28 days. The fresh properties of the mix were improved by using marble waste dust at a dosage below 200 kg/m<sup>3</sup>. Also, the filling capacity and passing ability of the mixes was found to be within the acceptable limits up to the dosage level of 200 kg/m<sup>3</sup>. Use of dosage higher than this value had negative effects on both the filling and passing ability of the mix. The addition of marble dust further improved both early age and later age compressive strength of the mixes, due to their capability of filling up of the voids. The authors concluded that 200 kg/m<sup>3</sup> of marble dust could be used for best performance of self-compacting concrete in both fresh and hardened state.

Belaidi et al. (2012) investigated the effect of using natural pozzolana and marble powder as a substitute for cement on the properties of self-compacting concrete. The authors attempted up to 40% substitution of cement with marble powder. The results indicate that there was no negative effect of using marble powder on fresh properties of concrete. However, compressive strength of the mixes reduced with the use of marble powder. It was concluded that a suitable combination of natural pozzolana and marble powder can be attempted to get suitable strength at 28 days.

Sadek et al. (2017) investigated the effect of using granite and marble powder along with silica fume on both mechanical and durability performance of self-compacting concrete. In the first phase of experimental program, the optimum amount of marble powder that can be used for best performance of self-compacting concrete was investigated. It was observed that by using both granite powder and marble powder, the powder content in self-compacting concrete mixes can be increased from 400 kg/m<sup>3</sup> to 6000 kg/m<sup>3</sup>, without increasing the cement content. Then, the fresh state and hardened state properties of the mixes finalized in the first stage were accessed.

The results showed affinity of marble powder to take more water due to the angular particles and rough texture of marble particles, thereby increasing the dosage of either water or superplasticizer. The mix with only marble powder had lower compressive strength and split tensile strength. The compressive strength of the mixes with a combination of marble powder and granite powder was reported to be 40% higher

than the control mix. The water absorption of these mixes was also lowest amongst all the tested mixes. Further, the performance of the mixes under sulphate exposure was investigated. The performance of the mixes under sulphate attack was observed to be satisfactory, with better performance being registered by the mix having a combination of marble powder and granite powder. The authors suggested that a combination of marble powder and granite powder provides a dual benefit of a filler and pozzolanic effect; while the use of only marble powder could provide filler effect.

The performance of self-compacting concrete made with marble waste under external sulphate attack was also investigated by Tennich et al. (2017). The performance of the mixes was judged by changes in mass loss and dynamic modulus of elasticity. It was concluded that the mixes having marble powder increased compactness and reduced inter connection of pores which helped in decreasing the ingress of aggressive ions in concrete. The performance of the mixes with marble powder thereby increased under the external sodium sulphate exposure.

Similar observations were made by Vaidevi et al. (2020). The authors used marble powder as fine aggregates for self-compacting concrete. The percentage replacement was varied from 0-100%. The performance of the mixes was investigated under 5% sodium sulphate exposure and 5% hydrochloric acid exposure. The authors reported that up to 25% replacement of fine aggregates with marble powder could provide mixes with better performance under both the aggressive environments.

## **2.6. USE OF MARBLE WASTE FOR MAKING CELLULAR CONCRETE**

Zhang et al. (2020) prepared cellular concrete that is a special type of light weight concrete in which the pores are closed. In the concrete, both marble waste powder and silica fume were used as replacement of cement. The percentage replacement of marble waste powder and silica fume were up to 20% and 10% respectively. They observed negative impact of silica fume and marble powder on fresh properties of concrete. In terms of the mechanical properties, the authors reported that the highest compressive strength was exhibited by SF10M5, which was nearly 20% greater than the control mix. The authors suggested that a combination of 10% silica fume and upto 20% waste marble powder would lead to a green cellular concrete.

The durability performance of the mixes suggested that incorporation of waste marble powder increased water absorption of the mixes, while the addition of silica fume

decreased the water absorption. The water absorption of the specimen shaving 10% silica fume along with 5% marble waste powder was significantly lower than the control mix, suggesting that this combination was best in terms of mechanical and durability performance of concrete. A suitable combination of both silica fume and marble waste also helped in arresting the sulphate attack on the mixes. These mixes had denser microstructure that prevented ingress of aggressive ions in to the concrete.

## **2.7. USE OF MARBLE WASTE IN BRICKS**

Bilgin et al. (2012) used marble dust in the manufacture of bricks. The marble waste powder was grounded to <40 µm size before using in brick manufacturing. The waste material was used upto 80% in making brick mortar. The prepared materials were sintered at three different temperatures of 900°C, 1000°C and 1100°C. It was observed that better mechanical property of the mixes was obtained at lower replacement levels. However, at higher replacement levels, porosity of the mixes increased due to release of carbon dioxide gas during calcination process. The authors further suggested that the performance of bricks could be improved if the calcination of calcium oxide present in marble is done before the mixing process.

## **2.8. CONCLUDING REMARKS**

Marble waste has the potential to be used as a replacement of both cement and aggregates. If used as replacement of cement, the most favorable replacement levels are up to 15%. The use of even this amount of marble waste will lead to decrease in carbon dioxide gas emissions due to requirement of lesser amount of cement, thereby leading to sustainable development. As per one estimate, use of 15% marble waste in place of cement will lead to the overall saving of 10% in the production of concrete. It will also lead to around 1% reduced energy consumption and around 15% lower carbon dioxide production for every tonne of structural concrete produced (Singh et al., 2017).

When used as replacement of sand, the replacement levels of marble waste can be easily increased to 40-50% without having any serious detrimental effect of the properties of concrete or mortar mixes. Its environment impact will be huge since the illegal mining of sand from the river beds is eroding the river beds, damaging the natural course of rivers and having an irreparable impact on the natural ecosystem.

## **CHAPTER 3**

### **EXPERIMENTAL PROGRAMME**

#### **3.1. GENERAL**

In this chapter, the detailed experimental programme is discussed. Firstly, the properties of various materials used in the work are discussed, followed by the details regarding specimen preparations, casting and curing of specimens. Thereafter, the details of the tests carried out in the investigations are systematically underlined.

#### **3.2. MATERIALS**

The major materials used for making concrete are cement, fine aggregates, coarse aggregates and water. The relative proportion of each material used in a conventional concrete is shown in Fig. 3.1. Cement constitutes nearly 20 percent of the volume of concrete mix and acts as a binder. Aggregates form nearly 75 percent of the volume of concrete and is a relatively inert constituent. It imparts the bulk to concrete and negates the negative effects of using cement paste alone. The aggregates are used in two size ranges and are called coarse aggregates and fine aggregates. The coarse aggregates are used to provide bulk to concrete, while fine aggregates are used to achieve a uniform concrete mix. Water is used to make the mix workable and is responsible for hydration of cement.

In this study, along with the basic ingredients, marble waste was also used as replacement to conventional fine aggregates. All the materials were tested as per relevant codes of practice before using them in the test program. The details of the materials along with their properties are presented in the subsequent sections. The set of materials used were kept same throughout the investigations.

##### **3.2.1. Cement**

Ordinary Portland Cement conforming to BIS 8112-2013 equivalent to ASTM C150-17 was used in the investigation. The fresh batch of cement from the same brand was used in order to minimize the effect of change in brand.

The energy dispersive spectroscopy (EDS) along with the scanning electron microscopy (SEM) for OPC used in the present study is presented in Fig. 3.2. SEM images give the information regarding the compositional behaviour of the material.

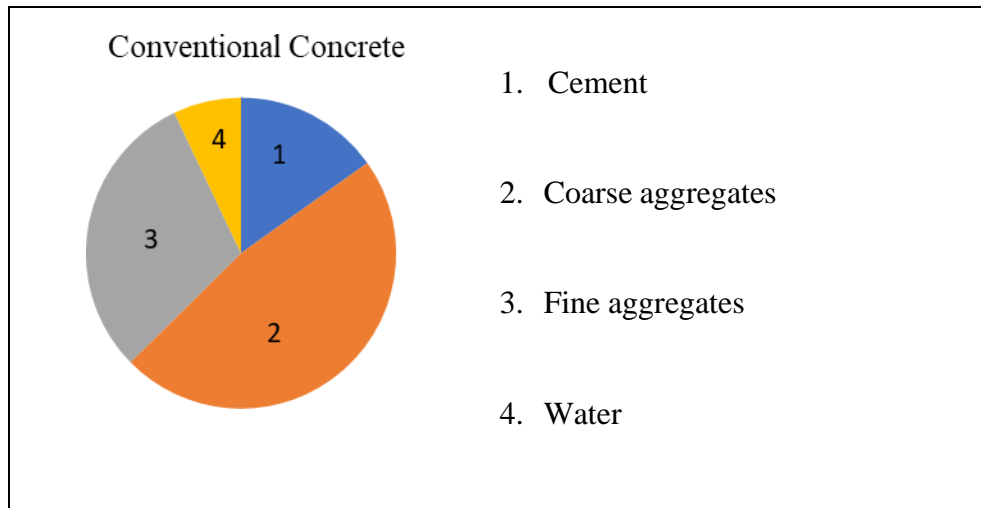


**Fig. 3.1: Relative material proportions in a conventional concrete**

From EDS, it is clearly observed that the major constituents of OPC are calcium oxide (CaO) and silicon dioxide (SiO<sub>2</sub>) along with the presence of other minor constituents. The chemical composition of the cement as supplied by the manufacturer is given in Table 3.1.

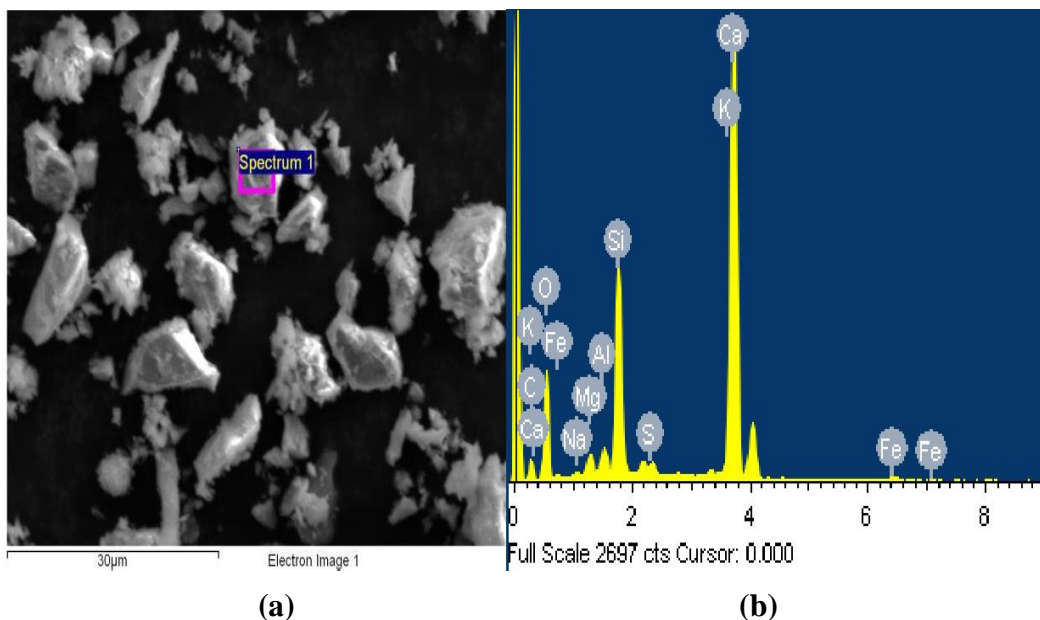


**Fig. 3.2: (a) Scanning electron microscopy (SEM) image and (b) Energy dispersive spectroscopy (EDS) of OPC cement**

**Table 3.1: Chemical composition of cement**

| <b>Composition (%)</b>                         | <b>OPC result</b> | <b>BIS Limit</b> |
|--|-------------------|------------------|
| Silicon dioxide (SiO <sub>2</sub> )            | 21.68             | -                |
| Aluminum oxide, Al <sub>2</sub> O <sub>3</sub> | 4.87              | -                |
| Ferric oxide, Fe <sub>2</sub> O <sub>3</sub>   | 3.35              | -                |
| Calcium oxide, CaO                             | 62.79             | -                |
| Magnesium Oxide, MgO                           | 1.73              | <6.00            |
| Sulfur trioxide, SO <sub>3</sub>               | 2.43              | <2.50            |
| Sodium Oxide, Na <sub>2</sub> O                | 0.21              | -                |
| Potassium oxide, K <sub>2</sub> O              | 0.69              | -                |
| Loss on ignition, LOI                          | 1.94              | <5.00            |
| Aluminum/Iron ratio                            | 1.45              | >0.66            |
| Lime saturation factor (LSF)                   | 0.88              | 0.66-1.02        |

**Table 3.2: Physical properties of cement**

| <b>Properties</b>                              | <b>OPC result</b> | <b>BIS Limit</b> |
|--|-------------------|------------------|
| Fineness (m <sup>2</sup> /kg)                  | 307               | >225             |
| Specific gravity                               | 3.10              | -                |
| Consistency (%)                                | 29                | -                |
| Initial setting time (min)                     | 130               | >30              |
| Final setting time (min)                       | 170               | <600             |
| <b>Compressive strength (N/mm<sup>2</sup>)</b> |                   |                  |
| 3 days   | 33.0              | >23              |
| 7 days   | 41.3              | >33              |
| 28 days  | 50.5              | >43              |

### 3.2.2. Fine Aggregates

Two types of fine aggregates are used in the present study. It includes the conventional river sand and marble waste. The details of both the materials used as fine aggregates are presented in the following sections:

### 3.2.2.1. River Sand

Locally available river sand fulfilling the requirements of BIS 383-2016 was used as fine aggregates. The physical properties of the aggregates were obtained by testing as per the relevant codal provisions and the values are provided in Table 3.3. Chemical composition of river sand is presented in Table 3.4. The SEM image of the river sand is presented in Fig. 3.3.

The sieve analysis results of fine aggregates used in the present study are presented in Table 3.5. From sieve analysis results, it can be seen that the percentage passing of fine aggregates satisfied the Zone –III recommendations and codal provision.

**Table 3.3: Physical properties of river sand**

| <b>Property</b>                           | <b>Natural River Sand</b> | <b>Standard followed</b> |
|---|---------------------------|--------------------------|
| Specific gravity                          | 2.59                      | BIS 2386 Part III- 1963  |
| Water absorption                          | 2.1                       | BIS 2386 Part III- 1963  |
| Fineness modulus                          | 2.26                      | BIS 2386 Part III- 1963  |
| Bulk density (kg/m <sup>3</sup> )         | 1510                      | -                        |
| Specific surface area (m <sup>2</sup> /g) | 0.210                     | -                        |
| Grading Zone                              | Zone III                  | BIS 383-2016             |

**Table 3.4: Chemical composition of river sand**

| <b>Constituent (%)</b>         | <b>River Sand</b> |
|--------------------------------|-------------------|
| CaO                            | 5.73              |
| SiO <sub>2</sub>               | 77.39             |
| Al <sub>2</sub> O <sub>3</sub> | 8.38              |
| Fe <sub>2</sub> O <sub>3</sub> | 2.39              |
| SO <sub>3</sub>                | -                 |
| MgO                            | 0.70              |
| K <sub>2</sub> O               | 0.02              |
| Na <sub>2</sub> O              | 0.005             |

The fine aggregates used were washed and removed of any silt content followed by drying for twenty-four hours in an oven. The oven-dried aggregates are used for casting of specimens for each type of concrete mix.

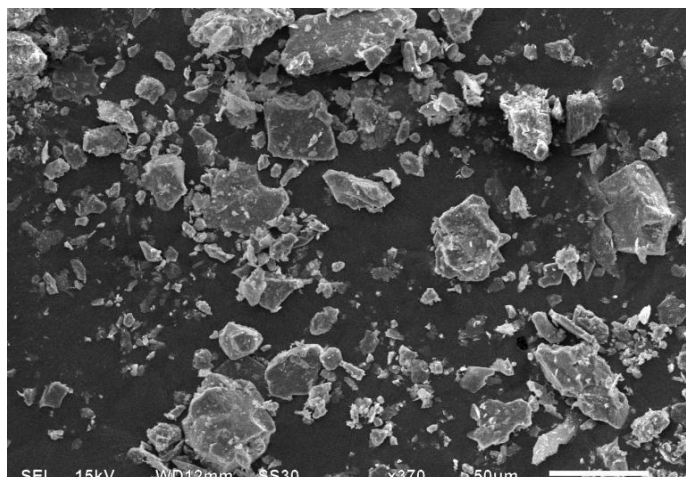


**Fig. 3.3: Scanning electron microscopy (SEM) image of river sand aggregates**

**Table 3.5: Sieve analysis results for river sand aggregates**

| IS-Sieve size (mm)  | Weight retained (%) | Cumulative weight retained (%) | Weight passing (%) | IS limits for Zone III |
|---------------------|---------------------|--------------------------------|--------------------|------------------------|
| 10 mm               | 0.0                 | 0.0                            | 100.0              | 100                    |
| 4.75 mm             | 5.2                 | 5.2                            | 94.8               | 90-100                 |
| 2.36 mm             | 5.5                 | 10.7                           | 89.3               | 85-100                 |
| 1.18 mm             | 8.5                 | 19.2                           | 80.8               | 75-100                 |
| 600 µm              | 9.7                 | 28.9                           | 71.1               | 60-79                  |
| 300 µm              | 41.0                | 69.9                           | 30.1               | 12-40                  |
| 150 µm              | 22.1                | 92.0                           | 8.0                | 0-10                   |
| Pan                 | 8                   | -                              |                    |                        |
| Total               |                     | 225.9                          |                    |                        |
| F.M. 2.26, Zone III |                     |                                |                    |                        |

### 3.2.2.2. Marble Waste

Marble waste collected from marble processing industry situated in Markanda area in Rajasthan (India) was used as partial replacement of fine aggregates. The waste was generated by cutting of marble slabs into required shapes and sizes using diamond

wires or a gang saw which uses multiple diamond-tipped blades to slice a marble block. The marble waste used in the present study was obtained from the bottom of first sedimentation tank which have marble particles of size suitable as fine aggregates. The obtained waste was dried in open, followed by oven drying to remove excess water.

Physical properties and the chemical composition of marble waste is presented in Tables 3.6 and 3.7 respectively. The sieve analysis results of marble waste used in the study are presented in Table 3.8. Sieve analysis results indicate that marble waste also belongs to Zone –III, as per the recommendations of BIS 383-2016.

**Table 3.6: Physical properties of marble waste**

| Property                                  | Marble waste | Standard followed       |
|---|--------------|-------------------------|
| Specific gravity                          | 2.88         | BIS 2386 Part III- 1963 |
| Water absorption                          | 1.1          | BIS 2386 Part III- 1963 |
| Fineness modulus                          | 2.23         | BIS 2386 Part III- 1963 |
| Bulk density (kg/m <sup>3</sup> )         | 1565         | -                       |
| Specific surface area (m <sup>2</sup> /g) | 0.249        | -                       |
| Grading Zone                              | Zone III     | BIS 383-2016            |

**Table 3.7: Chemical composition of marble waste**

| Constituent (%)                | Marble waste |
|--------------------------------|--------------|
| CaO                            | 28.67        |
| SiO <sub>2</sub>               | 4.66         |
| Al <sub>2</sub> O <sub>3</sub> | 0.21         |
| Fe <sub>2</sub> O <sub>3</sub> | 0.49         |
| MgO                            | 22.30        |
| K <sub>2</sub> O               | 0.05         |
| Na <sub>2</sub> O              | 0.06         |
| LOI                            | 43.7         |

**Table 3.8: Sieve analysis results for marble waste**

| IS-Sieve size (mm)  | Weight retained (%) | Cumulative weight retained (%) | Weight passing (%) | IS limits for Zone III |
|---------------------|---------------------|--------------------------------|--------------------|------------------------|
| 10 mm               | 0.0                 | 0.0                            | 100.0              | 100                    |
| 4.75 mm             | 0.2                 | 0.2                            | 99.80              | 90-100                 |
| 2.36 mm             | 0.25                | 0.45                           | 99.65              | 85-100                 |
| 1.18 mm             | 5.6                 | 6.05                           | 93.95              | 75-100                 |
| 600 micron          | 31.6                | 37.65                          | 62.35              | 60-79                  |
| 300 micron          | 49.5                | 87.15                          | 12.85              | 12-40                  |
| 150 micron          | 4.15                | 91.3                           | 08.70              | 0-10                   |
| Pan                 | 8.7                 | -                              | -                  | -                      |
| Total               |                     | 222.8                          |                    |                        |
| F.M. 2.23, Zone III |                     |                                |                    |                        |

X-Ray Diffraction (XRD) spectra of marble waste, shown in Fig. 3.4, indicate the presence of dolomite as the main crystalline mineral, along with small peaks of quartz and calcium carbonate. Also, SEM image of marble waste aggregates (Fig. 3.5) demonstrate the angular shape of marble particles.

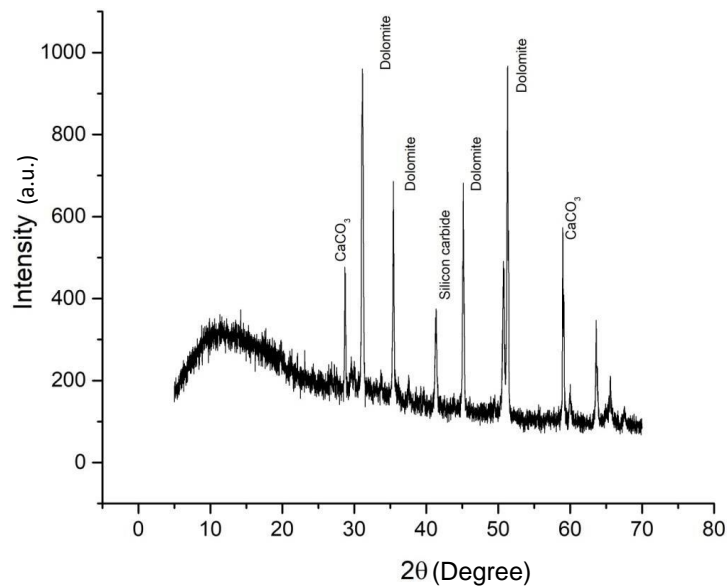


**Fig. 3.4: XRD spectra of marble waste**

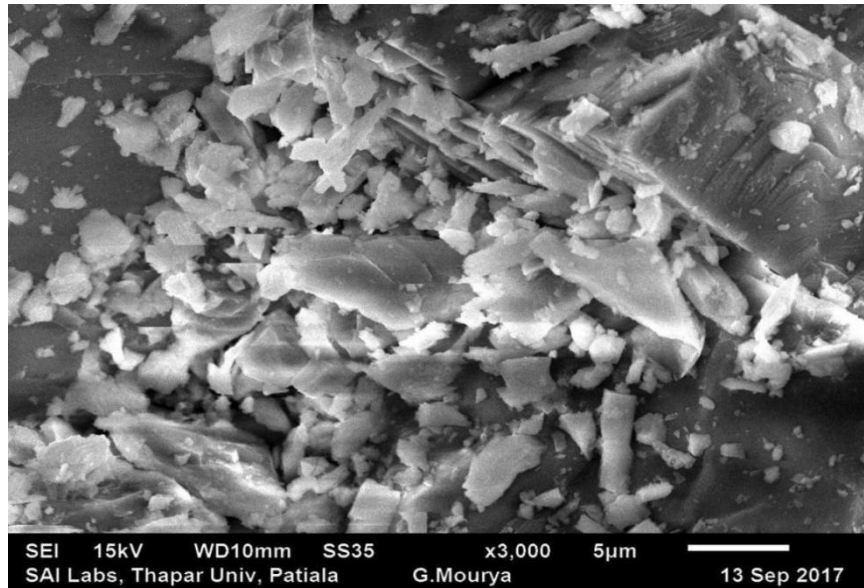


**Fig. 3.5: SEM image of marble waste**

### 3.2.3. Coarse Aggregates

Crushed gravel with nominal size of 20 mm and 10 mm was used as coarse aggregates. The physical properties of both these aggregates are listed in Table 3.9. EDS spectra along with SEM images for crushed gravel aggregates is presented in Fig 3.6. Through EDS analysis, it was observed that crushed gravel aggregates have silica as its major composition. The exact chemical composition of the used coarse aggregates is given in Table 3.10. Sieve analysis results for 20 mm and 10 mm crushed gravel aggregates are presented in Tables 3.11 and 3.12 respectively.

The coarse aggregates too were washed and removed of any silt and then dried for twenty-four hours in an oven. The oven-dried aggregates are then used for casting of specimens for each type of concrete mix.

**Table 3.9: Physical properties of coarse aggregates**

| Properties           | Coarse aggregates |       |
|----------------------|-------------------|-------|
|                      | 20 mm             | 10 mm |
| Specific gravity     | 2.63              | 2.65  |
| Water absorption (%) | 1.38              | 1.4   |
| Fineness modulus     | 6.99              | 6.18  |

**Table 3.10: Chemical composition of coarse aggregates**

| Constituent (%)                | Coarse Aggregates |       |
|--------------------------------|-------------------|-------|
|                                | 20 mm             | 10 mm |
| SiO <sub>2</sub>               | 85.16             | 86.12 |
| CaO                            | -                 |       |
| Al <sub>2</sub> O <sub>3</sub> | 9.24              | 8.29  |
| FeO                            | 1.86              | 2.03  |
| MgO                            | 0.75              | 0.79  |
| K <sub>2</sub> O               | 2.77              | 2.15  |
| Na <sub>2</sub> O              | 0.23              | 0.65  |

**Table 3.11: Sieve analysis of 20 mm crushed gravel coarse aggregates**

| IS-Sieve size (mm) | Weight retained (%) | Cumulative weight retained (%) | Weight passing (%) |
|--------------------|---------------------|--------------------------------|--------------------|
| 40                 | 0.00                | 0.00                           | 100.00             |
| 20                 | 3.73                | 3.73                           | 96.27              |
| 12.5               | 79.01               | 82.74                          | 17.26              |
| 10                 | 10.64               | 93.38                          | 6.62               |
| 4.75               | 6.58                | 99.96                          | 0.04               |
| Pan                | 0.04                | 100.00                         | 0.00               |

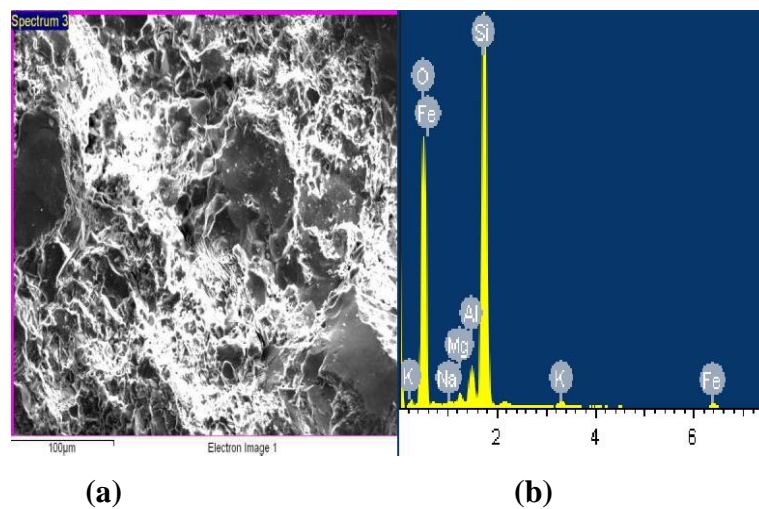


**Fig. 3.6: (a) Scanning electron microscopy (SEM) image and (b) Energy dispersive spectroscopy (EDS) for crushed gravel aggregates**

**Table 3.12: Sieve analysis of 10 mm crushed gravel coarse aggregates**

| <b>IS-Sieve size (mm)</b> | <b>Weight retained (%)</b> | <b>Cumulative weight retained (%)</b> | <b>Weight passing (%)</b> |
|---------------------------|----------------------------|---------------------------------------|---------------------------|
| 20                        | 0.0                        | 0.0                                   | 100.0                     |
| 12.5                      | 3.63                       | 3.63                                  | 96.37                     |
| 10.0                      | 8.41                       | 12.04                                 | 87.96                     |
| 4.75                      | 75.63                      | 87.67                                 | 12.33                     |
| 2.36                      | 12.31                      | 99.98                                 | 0.02                      |
| Pan                       | 0.02                       | 100                                   | 0.00                      |

The volume of water in each mix was adjusted to compensate for the water absorption of coarse aggregates and fine aggregates.

#### **3.2.4. Water**

For the preparation of specimens, potable ground water available in laboratory tap was used throughout the investigation. The composition of the tap water was tested and the values are presented in Table 3.13.

**Table 3.13: Properties of laboratory tap water**

| <b>Substance</b>       | <b>Concentration (mg/l)</b> |
|------------------------|-----------------------------|
| Total dissolved solids | 450                         |
| Total alkalinity       | 85                          |
| Total hardness         | 132                         |
| Chlorides              | 112                         |
| Sulphate               | 55                          |

### **3.3. MIX PROPORTIONS**

The investigations were carried out on concrete mixes, in which a partial replacement of fine aggregates with marble waste was attempted. The replacement ratios were set at 10, 20, 30, 40, 50 and 60% by weight of fine aggregates. Control concrete mix was designed as per the guidelines of BIS10262-2009, with a target 28 days compressive strength of 35 MPa. The water cement ratio of the control mix was kept as 0.5.

Further, in the subsequent mixes, fine aggregates of the control mix were replaced by equivalent amount of marble waste.

**Table 3.14: Mix proportions and nomenclature of mixes**

| Nomenclature | Mix proportions (Kg/m <sup>3</sup> ) |      |               |                   |       | Water |
|--------------|--------------------------------------|------|---------------|-------------------|-------|-------|
|              | Cement                               | Sand | Marble powder | Coarse Aggregates |       |       |
|              |                                      |      |               | 20 mm             | 10 mm |       |
| M0           | 372                                  | 621  | 0             | 707               | 472   | 186   |
| M10          | 372                                  | 559  | 69            | 707               | 472   | 186   |
| M20          | 372                                  | 497  | 138           | 707               | 472   | 186   |
| M30          | 372                                  | 435  | 207           | 707               | 472   | 186   |
| M40          | 372                                  | 373  | 275           | 707               | 472   | 186   |
| M50          | 372                                  | 311  | 344           | 707               | 472   | 186   |
| M60          | 372                                  | 249  | 413           | 707               | 472   | 186   |

The proportion of fine aggregates replaced was varied from 10 to 60%, with an increment of 10% in the subsequent mixes. It is to mention here that while doing the replacement, the difference in specific gravities of river sand and marble waste was considered by incorporating a correction factor, which developed by dividing specific gravity of river sand with the specific gravity of marble powder, the value of which was 1.115. This correction factor was multiplied with arithmetically calculated value. For instance, in Table 3.14, weight of 10% sand is 62.1g but value of marble powder is 69 g. This equivalent weight is arrived at by correcting value as per higher specific gravity.

Mix proportions of all the mixes, along with the nomenclature, are given in Table 3.14. The use of superplasticizer is avoided in the present study so as to reduce the number of variables affecting test results. The major focus of the study is to investigate the effect of replacement of river sand by marble waste on one-to-one basis.

### 3.4. CASTING AND CURING OF SPECIMENS

The test specimens were cast with the mix proportions given in Table 3.14. The desired mix was prepared in a rotating mixer of capacity 0.06 m<sup>3</sup>. To obtain the mix,

all the mix ingredients, viz. coarse aggregates, fine aggregates and cement were weighed in required proportions and mixed thoroughly for about two minutes to get a uniform mix in the dry state. After this, water was added to the dry mix in two equal proportions and a uniform mix was obtained by mixing for another three minutes. The prepared mix was poured in moulds of variable dimensions based on the tests to be performed. All the moulds were greased with oil before pouring of concrete in the moulds. The specimens of different sizes were cast corresponding to the evaluation of different strength properties.



**Fig 3.7: (a) Greasing and oiling of moulds (b) Casting of concrete mix**

It consisted of cubical specimens of size 150 mm to determine the compressive strength of mixes. The cubical specimens were also used in the durability studies related to compressive strength loss under variable exposure conditions like the acid attack and sulphate attack. 150 mm cube specimens were also used for water absorption test. Cylindrical specimens of dimensions 150 mm diameter  $\times$  300 mm height were cast to measure split tensile strength of the mixes. Cylindrical specimens of 100 mm diameter and 50 mm thickness were cast for the sorptivity test.



**Fig. 3.8: Curing of concrete specimens in the temperature-controlled curing tank**

For rapid chloride permeability test (RCPT), cylindrical samples of diameter 100 mm and 200 mm thickness were cast. These specimens were further cut in desired dimensions for the test. Prism specimens of size 75×75×285 mm were cast for the measurement of unrestrained drying shrinkage. For abrasion resistance measurements, specimens having size 65×65×30 mm were cast. After 24 hours of casting, all the specimens were demoulded and were water cured for the requisite days at temperature of 27±2 °C. Fig. 3.7 shows the casting of specimens, while Fig. 3.8 shows the curing of specimens in the temperature-controlled curing tank.

### **3.5. TESTING PROCEDURE**

The test programme consisted of examining fresh properties, strength and permeation characteristics and micro-structural analysis of the mixes. The test procedure adopted for studying each property is underlined in the following sections:

#### **3.5.1. Workability**

Workability of the concrete mixes was examined through the Slump test, conducted as per BIS 7320-1974. For conducting the test, slump cone was cleaned from inside and was greased with oil. Thereafter, the freshly mixed concrete was filled in the mould in three layers. Each layer was compacted by 16 mm diameter tamping rod. The mix was compacted by giving twenty-five strokes from the rounded end of the tamping rod. The compaction was done uniformly over the entire cross section of the mould. After filling the mould, the excess mass of concrete was struck off from the top layer with the help of trowel. The mould was then raised slowly and the concrete is allowed to settle under its own weight. The slump was measured by determining the difference between the height of the mould and the height of the specimen after subsidence of concrete. Fig. 3.9 shows the typical slump measurement.

#### **3.5.2. Compressive Strength**

Compressive strength of the mixes was determined as per BIS 516-2004 using 150 mm cubes. The compressive strength of each mix was measured at 7, 28, 90 and 365 days of casting. On the testing date, the cubical specimens were taken out of the curing tank and were kept in the laboratory environment for 2 hours. After that, the cube was placed under the platens of a compression testing machine of 5000 kN capacity.



**Fig. 3.9: Slump test apparatus**

The position of cube was such that the load was applied perpendicular to the as-cast position. The compressive load was applied through the hydraulic jack at a constant rate of 140 kg/cm<sup>2</sup>/min till failure. The test set-up is shown in Fig. 3.10(a). At each testing age, three specimens were tested as shown in Fig 3.10(b) and the average of three specimens was taken as the reference value.



**Fig. 3.10: (a) compression testing machine, (b) Compression test in progress**

Compressive strength of the mix was calculated according to the equation 3.1.

$$f_c = P / A \quad \dots (3.1)$$

where,

$f_c$  = Compressive strength (MPa or N/mm<sup>2</sup>),

$P$  = Maximum load (N),

$A$  = Cross section area of cube (mm<sup>2</sup>)

### 3.5.3. Split Tensile Strength

Split tensile strength of the mix was tested as per BIS 5816-1999 on cylindrical specimens of diameter 150 mm × 300 mm height. The split tensile strength was measured at 7, 28, 90 and 365 days of casting. For conducting the test at any desired age, the specimen was taken out of the curing tank and were allowed to air dry for two



**Fig. 3.11: Test set up and crack development in split tensile strength**

hours in laboratory. The test specimen was then placed horizontally between the platens of the compression testing machine and progressive compressive load was applied between the opposite generators of the test specimen as shown in Fig. 3.11.

The line was specifically marked on the cross-section of the cylinders in order to ensure that the load was applied along that line.



(a)



(b)

**Fig. 3.12: (a) Test arrangement for split tensile strength (b) Crushed split tensile strength test specimen**

As obtained from the elastic analysis, a fairly uniform tensile stress is produced over 2/3 of the loaded diameter of the cylinder because of applied line loading (Singh, 2012). The intensity of load at which the specimens fail by splitting into two halves along the loaded diameter is taken as the failure load. The test set-up used for split tensile strength test is shown in Fig. 3.12 (a), while the typical broken specimens are shown in Fig. 3.12 (b). The magnitude of split tensile strength was calculated from the failure load by using equation 3.2.

$$f_{st} = 2P/\pi dl \quad \dots (3.2)$$

where,

$f_{st}$  = Split tensile strength (N/mm<sup>2</sup>)

$P$  = Applied load at failure (N)

$d$  = Diameter of the cylinder (mm)

$l$  = Length of the cylinder (mm)

### 3.5.4. Permeation Characteristics of the Mixes

The permeation characteristics of the mixes were monitored by conducting rapid chloride permeability test (RCPT), sorptivity test and water absorption tests. All the tests were conducted at 28 and 365 days of casting.

#### 3.5.4.1. Rapid Chloride Permeability Test (RCPT)

Rapid chloride permeability test was conducted on cylindrical samples of 100 mm diameter and 200 mm thickness. The test was performed as per ASTM C1202-12.



(a)



(b)

**Fig. 3.13: (a) Rapid chloride ion penetration test apparatus; (b) Display sheet of the charge passed through concrete**

For conducting the test, specimens in the form of circular disc is shown in Fig. 3.13(a). Fig. 3.13(b) shows the display of charge passed through concrete during the test. Specimens in the form of circular disc of 100 mm diameter and 50 mm thickness was cut from the cylinder of 100 mm diameter and 200 mm height. The specimens were then kept in specially made cells that contain 3.0% sodium chloride solution and 0.3N sodium hydroxide solution. One end of the specimen was immersed in sodium chloride solution and the other end was immersed in sodium hydroxide solution. A potential difference of 60 V DC was maintained across the ends of specimen. Total electrical charge passed through 50 mm thick and 100 mm diameter size during 6 hours was measured. The average of total charge passed in coulombs through the three concrete specimens was reported as the RCPT value of that mix. The charge

passed is related to the resistance of the mix to chloride ion penetration and the rating is presented in Table 3.15.

**Table 3.15: Chloride ion penetration based on charge passed**

| <b>Charge passed (Coulombs)</b> | <b>Chloride ion penetration</b> |
|---------------------------------|---------------------------------|
| >4000                           | High                            |
| 2000 – 4000                     | Moderate                        |
| 1000 – 2000                     | Low                             |
| 100 – 1000                      | Very low                        |
| <100                            | Negligible                      |

The resistance to chloride ion penetration of concrete was rated as negligible, very low, low, medium and high as per Table 3.15. Prooveit data processor used in this study for measuring the chloride ion permeation is shown in Fig. 3.13(a). Fig. 3.13(b) shows the display of charge passed through concrete during the test.

#### **3.5.4.2. Sorptivity Test**

Sorptivity test is used to determine rate of water absorption by capillary suction. The test is performed to investigate the vulnerability of an unsaturated concrete specimen to the water infiltration. In the present study, the test was conducted as per ASTM C1585-13 at 28 days and 365 days of casting. For the test, cylindrical specimens of 100 mm diameter and 50 mm thickness were cast. After curing for the required number of days, the specimens were pre-conditioned in an oven at a temperature of  $50 \pm 2$  °C for three days. The specimens were then kept in a sealable container for 15 days. The circumference and the top surface of the specimens were covered with an epoxy, leaving only the bottom surface exposed.

The initial weight of the specimen was then measured by using a weighing balance with least count of 0.01g. Thereafter, the specimens were immersed in water to a depth of  $2 \pm 1$  mm in a pan, as shown in Fig.3.14. The change in weight of the specimen at 1, 5, 10, 15, 20, 30, 60, 120, 180, 240, 300, 360 minutes, 1, 2, 3, 4, 5, 6, 7 and 8 days of immersion was noted. A graph between the increase in mass per unit area over the density of water and the square root of time was plotted. The value of initial & secondary absorption was given by the slope of the best-fit line to initial and secondary curves, respectively. The slope of the best fit regression line of initial

absorption data was taken as sorptivity value of the specimen. While the constant of the best fit line equation gives the sorptivity coefficient. As per the codal provision, if the correlation coefficient (R) is less than 0.98, it indicates that linear relationship is not followed by the curve, then the water absorption rate cannot be determined.



**Fig. 3.14: Specimens kept for sorptivity test**

### 3.5.4.3. Water Absorption Test

Water absorption test is an indicator of porosity of the material and was performed as per ASTM C642-13 on cubical specimens of size 150 mm. For this test, after the required amount of curing, the concrete specimens were taken out of curing tank and were oven dried at a temperature of 110°C for a period of 24 hours. Thereafter, the specimens were cooled down to room temperature and weighed. The process was repeated until the difference in consecutive readings of weight of specimen taken at interval of 24 hours was less than 0.5 percent. Then the specimens were immersed in water for the period of 24 hours and the weight of specimens was noted after immersion. The value of water absorption was then calculated as per equation 3.3 as follows:

$$\text{Water absorption (\%)} = \left( \frac{B - A}{A} \right) \times 100 \quad \dots (3.3)$$

where

A = Weight of oven dried sample in air, (g)

B = Weight of saturated surface dry sample in air, (g)

### 3.5.5. Abrasion Resistance

Abrasion resistance was measured after 3, 7, 28, 90 and 365 days of curing as per BIS 1237-2012. For the test, concrete blocks of size 65×65×30 mm were prepared. The size of concrete block used in the test has minor modifications with respect to the dimensions prescribed in BIS: 1237-2012. The modifications were made so as to fit in the holding device available for conducting the test. The cross section under abrasion was same as adopted by the previous investigators (Siddique, 2013; Siddique and Khatib, 2010). The depth of specimens was kept in accordance with the requirements of holding device of the machine. The set up used for conducting abrasion test is shown in Fig. 3.15.

For conducting abrasion resistance test at a specified testing age, the specimens were taken out of the curing tank and were oven dried at 110±5°C for 2 hours. The specimen was then weighed accurately on a digital balance, having least count of 0.01 gram. Thickness of oven dried specimen was measured, with the help of vernier caliper having least count of 0.02 mm, at five locations (one at the center and other at four corners). The test specimen was then fixed in the holding device of the abrasion testing machine and loaded at the centre with a load of 300 N.

Thereafter, the specimen was grinded over the grinding machine rotating at a speed of 22 revolutions per minute. The grinding path of the disc of the abrasion testing machine was evenly distributed with 20 gram of abrasive (aluminum) powder. The abrasive powder was continuously spread on the grinding disc so that it remained uniformly distributed on the track corresponding to width of the test specimen (Siddique, 2013; Siddique and Khatib, 2010). Weight of the specimen was measured after each 22 revolutions and specimen was turned about the vertical axis through an angle of 90° in clockwise direction until the end of test (220 revolution). The extent of abrasion was determined from the difference in values of thickness measured before and after the abrasion test, by using the following formula as per equation 3.4.

$$t = \frac{(W_1 - W_2)V_1}{W_1A_1} \quad \dots (3.4)$$

where,

$t$ = Average loss in thickness (mm)

$W_1$ = Initial mass of specimen (gram)

$W_2$ = Final mass of abraded specimen (gram)

$V_1$ = Initial volume of the specimen ( $\text{mm}^3$ )

$A$ = Surface area of the specimens ( $\text{mm}^2$ )

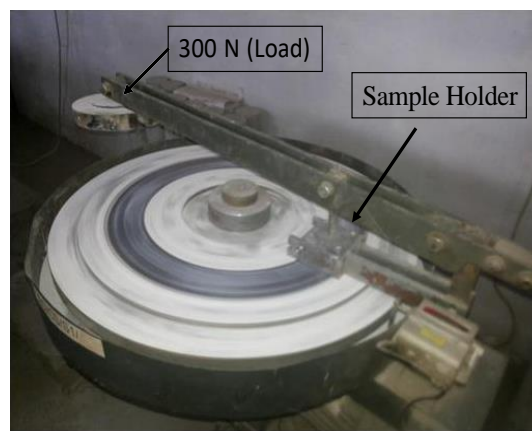


**Fig. 3.15: Experimental setup for measurement of abrasion resistance of concrete**

### 3.5.6. Drying Shrinkage

Drying shrinkage of hardened concrete was measured as per ASTM C157-17. The unrestrained drying shrinkage test is based on monitoring the variation in length of a specimen from the moment it is taken out of mould till its length stabilizes. The unrestrained shrinkage test set-up is shown in Fig.3.16. For measuring drying shrinkage, prism specimens were demoulded after 24 hours of casting and initial comparator readings, known as “initial CRD” for shrinkage was taken with the help of length comparator mounted with the dial gauge. The least count of the dial gauge was 0.01 mm. After that, the prism specimens were water cured for 28 days, followed by air drying for a period of 9 months in the laboratory environment, with relative humidity between 60–80 % air curing and having  $27\pm 2^\circ\text{C}$  temperature. The length comparator readings were taken at several intervals during the drying period, which were used to calculate drying shrinkage strain as per ASTM C157-17. During the first month of drying, the shrinkage strain was measured at 4, 7, 10, 14, 21 and 28 days of

drying. In the subsequent months, as shrinkage slowed down, drying shrinkage readings were taken at 15 days interval and the specimens were monitored till the drying period of 9 months. During air curing period, a clearance of 25 mm was maintained on all sides between the specimens.

Drying shrinkage strain was calculated according to equation 3.5.

$$\varepsilon_{sh} = \frac{\text{CRD} - \text{initial CRD}}{G} \quad \dots (3.5)$$

where,

$\varepsilon_{sh}$  = shrinkage strain ( $\mu\text{-mm/mm}$ )

CRD = Difference between the comparator reading of the specimen and the reference bar at any age

G = Gauge length = 250 mm



**Fig. 3.16: Unrestrained drying shrinkage test set-up**

### **3.5.7. Mineralogical and Microstructural Analysis**

The analysis of the mixes at micro structural level was done in order to understand the changes occurring at the micro scale in the mineralogical composition of the mixes upon addition of marble waste as replacement of river sand. The following studies were conducted:

### **3.5.7.1. Scanning Electron Microscopy (SEM) and Energy Dispersive Spectroscopy (EDS)**

To study the micro-structural characteristics of the prepared mixes, fractured small size pieces of specimens obtained after conducting compressive strength tests were collected and were used for Scanning Electron Micrographs (SEM) and Energy Dispersive Spectroscopy (EDS) analysis. The test was performed on JEOL JSM 6510 LV scanning electron microscope (SEM) at 20 Kn. SEM gives the information regarding the topographic and compositional behaviour of the material; while, EDS identifies the different phases present in the chemical composition.



**Fig. 3.17: Experimental set up for SEM and EDS spectroscopy**

SEM uses a high-energy beam of electron in a raster scan pattern to produce images of the surface topography of the specimen. Signal produced during the interaction of high energy beam with the specimen surface provides the information about the surface composition, topography and other properties. EDS works by measuring X-rays emitted from core electrons that move from higher energy levels to the ground state (Dodds, 2012). In this study, fractured small pieces of the specimens were mounted on the SEM stub and images were obtained using secondary electron (SE) image mode. To ensure electrical conductance, fractured small pieces of the specimens were coated with thin layer of gold. The set up used in the present study for SEM and EDS is shown in Fig.3.17. The SEM and EDS analysis was performed at 28 and 365 days of curing for all concrete mixes.

### 3.5.7.2. X- Ray diffraction (XRD)

The X- ray diffraction (XRD) technique is to identify the crystalline phases present in concrete, which includes calcium hydroxide, calcium-silicate-hydrate, ettringite etc. Along with this, the presence of aggregates result in the peaks corresponding to the minerals present in that aggregate. The various crystalline phases of any mineral has a unique diffraction image. The XRD investigation is carried out in a range of diffraction angles and a graph is then plotted between the diffraction angle ( $2\theta$ ) on abscissa and intensity of the diffracted radiation on ordinate.

In the present study, XRD technique was used to identify the phases present in various concrete mixes cast with variable percentages of marble waste. The XRD spectra of the mixes was recorded at 28 days and 365 days of casting. The broken concrete samples, obtained from the inner core of concrete obtained after compressive strength tests was taken. The broken pieces were crushed and were sieved through 90  $\mu\text{m}$  sieve. The test was performed on PW 1140/09 for diffraction angle  $2\theta$ , ranging from  $10^\circ$  to  $80^\circ$  in the steps of  $2\theta = 0.017^\circ$ . The diffraction pattern and relative intensities of diffraction peaks were noted. The obtained data was compared with the standard peaks of compounds in the diffraction database released by International Centre for Diffraction Data (ICDD). Fig 3.18 shows the X-Ray diffraction (XRD) instrument.



**Fig. 3.18: Experimental set up for X-Ray diffraction (XRD) instrument**

### 3.5.8. Acid Exposure

The adverse chemicals attack either concrete or rebar embedded in concrete. One of the most severe chemical exposure that affects the integrity of concrete is acid attack.

The concrete is highly susceptible to the acid exposure because it is highly alkaline in nature (with  $\text{pH} > 13$ ) and many of hydration products (for example calcium hydroxide, C-S-H etc.) are readily dissolvable in acids. Due to these chemical interactions, acid attack leads to loss of binding ability and strength of concrete and eventually to the loss of section.

There are numerous types of acids that can come in contact with concrete and cause its deterioration. The various sources of these acids are: marine environment (boric acid), acid rain (hydrochloric acid, sulphuric acid), ground water (carbonic acid), food products (acetic acid, tannic acid, phosphoric acid, oleic acid, lactic acid etc.), oil related products (sulphurous acid, carbolic acid) etc.

Out of all these types, sulphuric acid is considered to be one of the most deleterious acid (Hadigheh et al., 2017; Kwasny et al., 2018). It is because of the fact that sulphuric acid leads to combined deterioration due to attack by acid and sulphate (Hadigheh et al., 2017). The most common sources of sulphuric acid exposure to concrete are listed in Table 3.16.

In the present study, the focus is on the performance of concrete containing marble waste as fine aggregate replacement when the samples are exposed to 3% of sulphuric acid solution. The detailed test program is discussed in the following sections:

#### **3.5.8.1. Acid Solubility Index of Basic Ingredients**

Along with the basic tests, the acid solubility fraction of all the materials was tested as per relevant standards and is listed in Table 3.17. The procedure for determining acid solubility of the tested material involves taking 2.5 gm of dried and powdered sample and immersing it in a beaker with 75 ml of water and 25 ml of concentrated hydrochloric acid. The prepared solution was heated on a hot plate and was then left at room temperature for 2 hours.

Thereafter, the solution was filtered through medium porosity, fritted-disc crucible and the filtrate was collected in a flask. The filtrate was then dried at  $105 \pm 2$  °C over night. Then the sample was cooled for 2 hours in a desiccator and weigh to 0.0001 g accuracy.

**Table 3.16: Sources of sulphuric acid exposure to reinforced concrete structures**

| <b>S. No.</b> | <b>Source</b>  | <b>Process</b>  | <b>Vulnerable structures</b>   |
|---------------|--|---|--|
| 1.            | Acid rain:<br>Chatveera and Lertwattanakul (2014); Mahdikhani et al. (2018); Xie et al. (2004)   | Sulphur dioxide formed during incomplete combustion of industrial pollutants and burning of fossil fuels react with rain water and oxygen   | All structures falling in the zone of acid rain, especially monumental buildings |
| 2.            | Anaerobic and aerobic bacteria present in sewage: De Belie et al (2004); Huber et al. (2016); Lavigne et al. (2016); Scrivener and De Belie (2013) | Anaerobic sulphate reducing bacteria (SRB) attack sulphur compounds present in sewage to produce hydrogen sulphide (H <sub>2</sub> S).<br>Aerobic Sulphur oxidising bacteria (SOB) oxidises the H <sub>2</sub> S to form sulphuric acid | Sewer pipelines  |
| 3.            | Sulphate rich soils:<br>Bassuoni and Nehdi, (2007); Fattuhi and Hughes (1988a,b); Fattuhi and Hughes (1988); Hadigheh et al. (2017)                | Oxidation of pyrites and marcasite (sulphate rich minerals) present in soil oxidizes in the presence of the aerobic bacterium, Acidithiobacillus ferro-oxidans to form sulphuric acid   | Underground concrete structures  |
| 4.            | Industrial manufacturing processes:<br>Dyer (2014)   | Fertilizer industries use industrial grade sulphuric acid in the manufacturing process  | Industrial structures  |
| 5.            | Leakage and spillage of sulphuric acid in industrial environment   | -   | Industrial structures  |

The acid solubility (S) was then calculated using the

$$S(\%) = \frac{(m_s - m_{fs})}{m_s} \times 100 \quad \dots (3.6)$$

where

$m_s$  is the initial mass of the dried sample (in grams),

$m_{fs}$  is the mass of the treated and dried filtrate (in grams)

The values illustrate that the acid solubility fraction of portland cement and marble waste is very high; while the acid solubility fraction of river sand and gravel aggregates is very low. It clearly indicates that both cement and marble waste are highly soluble in acidic environment.

**Table 3.17: Acid solubility fraction of materials used in the study**

| Material       | Acid Soluble Fraction |
|----------------|-----------------------|
| OPC            | 99.6%                 |
| River sand     | 3.21%                 |
| Marble waste   | 99.9%                 |
| Crushed gravel | 0.2%                  |

### 3.5.8.2. Exposure Details

In order to study the acid resistance of various mixes, 150 mm size cube specimens were cast as per BIS 516-2004 for all the mixes. The specimens were demoulded after 24 hours of casting and were subjected to water curing at  $27 \pm 2$  °C for 28 days which ensured that all the specimens would reach a consistent level of hydration before subjecting them to aggressive solution (Goyal et al., 2009). Thereafter, the specimens were taken out of the curing tank and were dried at 25 °C at 50% relative humidity for 30 minutes to record the initial parameters (which includes measuring weight, compressive strength and making visual observations of the surface of specimens before the start of acid exposure). The specimens were then immersed in 3% sulphuric acid solution, so as to simulate severe environments in laboratory accelerated tests (Girardi and Maggio, 2011). The percentage of sulphuric acid led to the pH of nearly 1, which is categorized in the range of strong acid attack as per DIN EN 206 (EN 206-

1, 2000). The specimens were fully immersed in the aggressive media consisting of 3% sulphuric acid. The exposure was continuous till the testing age, with the samples being removed in between only for measuring mass at the specified time. The specimens of each group of mixes were dipped (fully immersed) in separate PVC containers so that similar acidic exposure is maintained for each mix. The solution was renewed monthly. The pH of the solution was checked at regular intervals to ensure that it is at a nearly constant level.

### 3.5.8.3. Test Method

The performance was monitored up to 180 days of immersion in acidic solution as per ASTM C267-01. The test method included visual observations, weight loss measurements, compressive strength loss measurements, SEM-EDS and XRD. On the testing day, required number of samples were taken out of the aggressive media and were rinsed thoroughly with the tap water. First of all, the samples were visually observed to record any changes in the surface appearance. Thereafter, they were left to dry for 30 minutes. The weight of each specimen was then noted by using a weighing balance of least count of 0.5 grams. The mass variation was calculated as per equation 3.7.

$$\text{Mass Loss (\%)} = \frac{(M_t - M_i)}{(M_i)} \times 100 \quad \dots (3.7)$$

Where

$M_t$  = Average initial weight of three specimens in grams

$M_i$  = Initial weight of the specimens before exposure to sulphuric acid solution, in grams

Afterwards, compressive strength test was performed on the specimens. Since the exposure to acid led to irregularities on the surface due to spalling, the surface of the specimens was finished by end capping to maintain uniformity of contact during loading. For end capping, a layer of cement mortar (1 part of cement and 3 parts of sand) was applied on the irregular load bearing surfaces. The compressive strength loss (CSL) was then calculated as per equation 3.8:

$$CSL = \frac{f_{ct} - f_{c28}}{f_{c28}} \times 100 \quad \dots (3.8)$$

Where,

$f_{ct}$  is the average compressive strength at the testing age

$f_{c28}$  is the reference 28 days compressive strength of the mix before immersion in the acid solution.

The weight loss measurements were taken at 7, 14, 28, 56, 90, 120, 150 and 180 days of exposure; while compressive strength test was conducted at 7, 28, 90 and 180 days of exposure. The mortar pieces were collected carefully from the surface of the broken concrete specimens at the end of exposure duration of 180 days and were examined by using JEOL JSM 6510 LV scanning electron microscope (SEM) to observe change in morphology of the mixes. The mixes were further analysed using EDX. Also, the powdered sample was taken from the collected mortar pieces and XRD was conducted on PW 1140/09 for diffraction angle ranging from 10° to 80°.

### 3.5.9. Sulphate Attack

Chemical attack by sulphates is a series of complex physio-chemical reactions between hydration products and sulphate ions which leads to the formation of harmful minerals in the pores of concrete.

In this study, the concrete specimens containing variable percentages of marble waste powder as partial replacement of fine aggregates were immersed in 5% sodium sulphate solution as per ASTM C1012-10. It is equivalent to 33,800 ppm of  $SO_4^{2-}$  ions and 16,200 ppm of  $Na^+$  ions (Goyal et al., 2009). The above exposure comes in the category of very severe exposure condition as per ACI committee 318-2011. In order to intensify the degradation process, the specimens were subjected to wet-dry cycles. There were four steps in the wet-dry cycle:

**Step 1:** Two days of air drying: In this the samples after 28 days of normal water curing were exposed to air curing in the controlled environment having  $27 \pm 2^\circ C$  temperature and 60-65% relative humidity. During air curing period, a clearance of 25 mm was maintained on all sides between the specimens.

**Step 2:** Five days by complete submergence in sulfate solution: In this, the specimens were stored in containers containing 5% of sodium sulphate solution.

**Step 3:** Two days of air drying: After 5 days exposure, the specimens were removed from the containers and above exposure of 2 days of drying in the controlled environment having  $27\pm 2^\circ\text{C}$  temperature and 60-65% relative humidity.

**Step 4:** Five days of immersion in 5% sodium sulfate solution.

**Step 5:** Two days of air drying: After the second immersion, the specimens were again left to dry for 2 days

**Step 6:** 12 days of immersion in 5% sodium sulfate solution. The last immersion period was perceptively kept longer in order to ensure that the specimens were in saturated state before measurements.

The sulphate solution was renewed monthly in order to maintain the pH of the solution, that may get affected due to the leaching of hydroxide ions from the specimens, that might increase the pH of solution. The specimens of each group of mixes were dipped (fully immersed) in separate tubs so that similar sulphate exposure was maintained for each mix. The specimens were stored in 200-litre capacity tubs with maximum of 6 specimens immersed in about 100-120 litres solution. The tests were completed in triplicate to confirm reproducibility of the test results.

The deterioration of the specimens was investigated at the end of 2, 4, 6, 8, 10, 12 upto 18 cycles of exposure. The test methods employed for judging performance of mixes included visual observations, weight loss measurement, compressive strength loss measurement, length change and microstructural analysis by SEM and XRD.

Visual observations were performed on the specimens at regular intervals for 18 months in order to note minute changes on the surface such as changes on the surface such as change in colour and texture, formation of any coating, cracking of corners etc. On the basis of visual observations, the damage was evaluated based on the deterioration scale, mentioned in Table 3.18 (Irassar et al., 2003; Sotiriadis et al., 2012).

For mass loss measurement, the specimens were taken out of the sulphate solution. The specimens were then washed with water and were cleaned gently to remove loose particles. The specimens were then left to dry for 30 minutes. The weight of each

specimen was then noted by using a weighing balance of least count of 0.01 grams. The mass variation was calculated as per equation 3.9.

**Table 3.18: Deterioration scale used for evaluating visual distress in concrete (Irassar et al., 2003)**

| <b>Deterioration Scale</b> | <b>Level of visual distress</b>             |
|----------------------------|---|
| 0                          | No sign                                     |
| 1                          | Slight attack on corners and edges          |
| 2                          | Deterioration at corners and edges visible  |
| 3                          | cracking at the corners                     |
| 4                          | cracking along the edges                    |
| 5                          | Extensive cracking and specimen expansion   |
| 6                          | Further expansion of specimen               |
| 7                          | Extensive expansion and spalling            |
| 8                          | Extensive deterioration with loss of pieces |
| 9                          | Specimen collapse                           |

$$\text{Mass Loss (\%)} = \frac{W_t - W_i}{W_i} \times 100 \quad \dots (3.9)$$

Where  $W_t$  = average weight of specimens at testing age (grams)

$W_i$  = initial weight of the specimens before exposure to sodium sulphate solution, in grams

Afterwards, compressive strength test was performed on the specimens. At each test age, the compressive strength of three specimens stored in test solution is determined and the average of these values is taken as the representative compressive strength. The compressive strength loss (CSL) was then calculated as per equation 3.10.

$$\text{CSL} = \frac{f_{ct} - f_{c28}}{f_{c28}} \times 100 \quad \dots (3.10)$$

Where

$f_{ct}$  is the average compressive strength at the testing age

$f_{c28}$  is the reference 28day compressive strength of the mix before immersion in the sodium sulfate solution.

The weight loss measurements were taken at 7, 14, 28, 56, 90, 120, 150 and 180 days of exposure; while compressive strength test was conducted at 7, 28, 90 and 180 days of exposure.

### **3.5.9.1. Length Change of Specimens**

Since the sulphate exposure is known to cause formation of expansive products, leading to the expansion of concrete, the prism specimens were cast and their change in length was monitored at regular intervals after exposure to sodium sulphate solution.

For this, the prism specimens were cast of dimensions  $75 \times 75 \times 285$  mm. The specimens were water cured for 28 days and were then subjected to wet-dry cycles for sulphate exposure. The length of specimens was monitored at the regular intervals and the length comparator readings were taken using the unrestrained drying shrinkage apparatus as per ASTM C1012-10 as per equation 3.11.

$$\Delta L = \frac{(L_x - L_i)}{L_g} \times 100 \quad \dots (3.11)$$

Where,

$\Delta L$  = Change in length at x age (%)

$L_x$  = comparator reading of the specimen at x age

$L_i$  = initial comparator of specimen

$L_g$  = nominal gauge length = 250 mm

### **3.5.9.2. Mineralogical and Microstructural Analysis**

The mortar pieces were collected carefully from the surface of the broken concrete specimens at the end of exposure duration and were examined by using JEOL JSM 6510 LV scanning electron microscope (SEM) to observe change in morphology of the mixes. The mixes were further analyzed by using EDX. Also, powdered sample was taken from the collected mortar pieces and XRD was conducted on PW 1140/09 for diffraction angle ranging from  $10^\circ$  to  $80^\circ$ .

## **CHAPTER 4**

### **RESULTS AND DISCUSSIONS**

#### **4.1. GENERAL**

In this chapter, the results obtained from the experimental programme are presented, followed by the discussion related to the effect of incorporating marble waste as a substitute to river sand for fine aggregates.

#### **4.2. CHARACTERIZATION OF MARBLE WASTE**

Marble waste used in the present study was collected from marble processing industry situated in Markrana area in Rajasthan (India). The waste is generated by cutting of marble slabs into required shapes and sizes using diamond wires or gang saw which uses multiple diamond-tipped blades to slice a marble block.

The fine particles of marble are produced during cutting operations and forms large volume of marble slurry, which is a mix of fine marble particles and water. This marble slurry is channelized through the series of sedimentation tanks (generally three), so that the coarser stone pieces are separated from slurry by settlement.

The slurry settled in the sedimentation tanks is of the size that can be used as fine aggregates in concrete. The remaining waste material consists of very fine particles impounded with water. The excess water from the slurry is extracted and is recycled, while the remaining mud like marble slurry, with 90% of the particles below 200  $\mu\text{m}$ , is disposed of in the open land. All these ranges of marble waste can be utilized as replacement of different constituents for making concrete.

The marble waste used in the present study was obtained from the bottom of first sedimentation tank which had marble particles of size suitable as fine aggregates. The obtained waste was dried in open, followed by oven drying to remove excess water.

Physical properties and the chemical composition of marble waste was compared with the river sand, so as to check its suitability for using it as replacement of river sand.

Physical properties of both the materials is presented in Table 4.1, while chemical composition is presented in Table 4.2. The sieve analysis results of both the materials

indicate that both river sand and marble waste belongs to Zone–III, as per the recommendations of BIS 383-2016.

**Table 4.1: Physical properties of natural river sand and marble waste**

| Property                                  | Fine Aggregates    |              | Standard Followed       |
|---|--------------------|--------------|-------------------------|
|   | Natural River Sand | Marble waste |                         |
| Specific gravity                          | 2.49               | 2.88         | BIS 2386 Part III- 1963 |
| Water absorption                          | 2.1                | 1.1          | BIS 2386 Part III- 1963 |
| Fineness modulus                          | 2.6                | 2.23         | BIS 2386 Part III- 1963 |
| Bulk density (kg/m <sup>3</sup> )         | 1510               | 1565         | -                       |
| Specific surface area (m <sup>2</sup> /g) | 0.210              | 0.249        | -                       |
| Grading Zone                              | Zone III           | Zone III     | BIS 383-2016            |

**Table 4.2: Chemical composition of natural river sand and marble waste**

| Constituent (%)                | Marble waste | Natural River Sand |
|--------------------------------|--------------|--------------------|
| CaO                            | 28.67        | 5.73               |
| SiO <sub>2</sub>               | 4.66         | 77.39              |
| Al <sub>2</sub> O <sub>3</sub> | 0.21         | 8.38               |
| Fe <sub>2</sub> O <sub>3</sub> | 0.49         | 2.39               |
| SO <sub>3</sub>                | -            | -                  |
| MgO                            | 22.30        | 0.70               |
| K <sub>2</sub> O               | 0.05         | 0.02               |
| Na <sub>2</sub> O              | 0.06         | 0.005              |
| LOI                            | 43.7         | -                  |

The physical properties of marble waste indicate that it can be easily used as replacement of natural river sand because both the materials have similar specific surface area, fineness modulus and grading zone.

The particle size distribution of both natural river sand aggregates and marble waste aggregates is presented in Fig. 4.1. As can be seen from the figure, marble waste aggregates have larger proportion of finer aggregates passing through 1.18 mm sieve

as compared to natural river sand. As can be seen from Table 4.1, the specific surface area of marble waste is higher than that of natural river sand. It indicates that the marble waste used in the study is slightly finer than the natural river sand, which might affect workability of the mixes. Also, the finer aggregates of marble waste is also expected to provide filler effect in concrete.

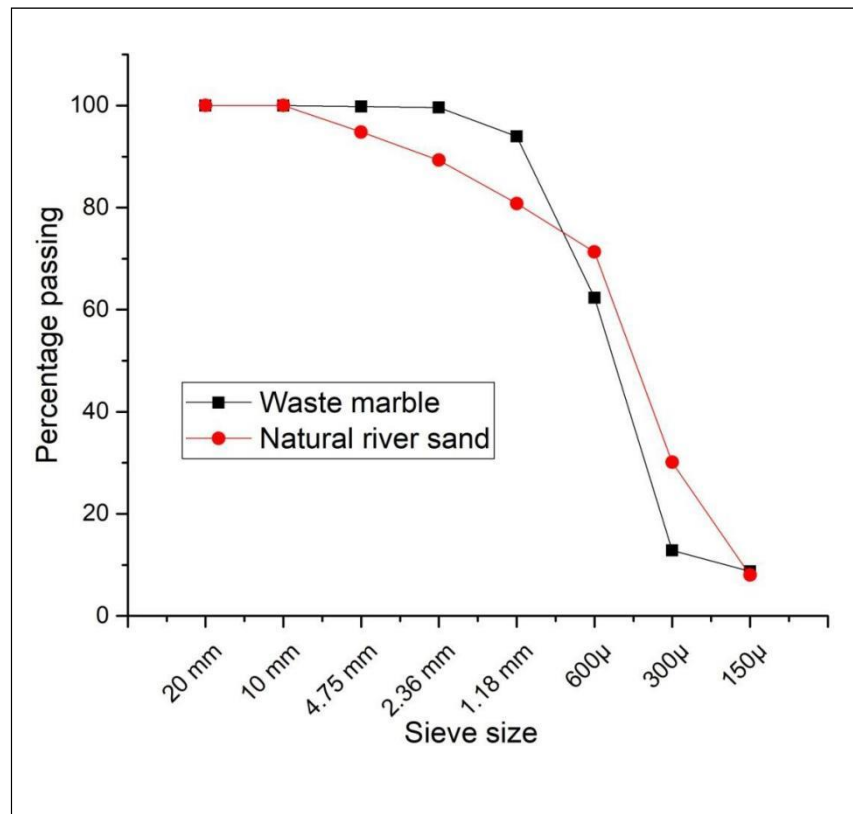


**Fig. 4.1: Particle size distribution of natural river sand and marble waste used as fine aggregates**

The values of water absorption of both the aggregates, as provided in Table 4.1 indicate that the water absorption of marble waste was very low as compared to the natural river sand. It is in agreement with the data presented by Ozcelik and Ozguven (2014), wherein it was reported that the least water absorbing natural building stone was marble, followed by granite, onyx and conglomerate. The lower water absorption was attributed to CaO content of marble waste.

Silva et al. (2013) also reported that marble waste fine aggregates have lowest water absorption. Most of the other researchers reported lower values of water absorption

for marble waste (André et al., 2014; Gameiro et al., 2014; Hebhouh et al., 2011; Khyaliya et al., 2017; Kore and Vyas, 2016).

X-Ray Diffraction (XRD) spectra of marble waste is shown in Fig. 4.2, indicate the presence of dolomite as the main crystalline mineral, along with small peaks of quartz and calcium carbonate. The chemical composition of marble waste shows that loss on ignition (LOI) of marble waste is very high. It can be attributed to the loss of carbon dioxide due to dissolution of calcite ( $\text{CaCO}_3$ ) and dolomite ( $\text{CaMg}(\text{CO}_3)_2$ ).

Higher LOI of marble waste is also reported by researchers investigating the effect of marble waste (Ashish, 2018; Belaidi et al., 2012; Buyuksagis et al., 2017; Ergün, 2011; Khyaliya et al., 2017; Kore and Vyas, 2016; Munir et al., 2017; Saboya et al., 2007; Sardinha et al., 2016; Topçu et al., 2009; Vardhan et al., 2015).

Also, SEM image of marble waste (Fig. 4.3) demonstrate the angular shape of marble particles.

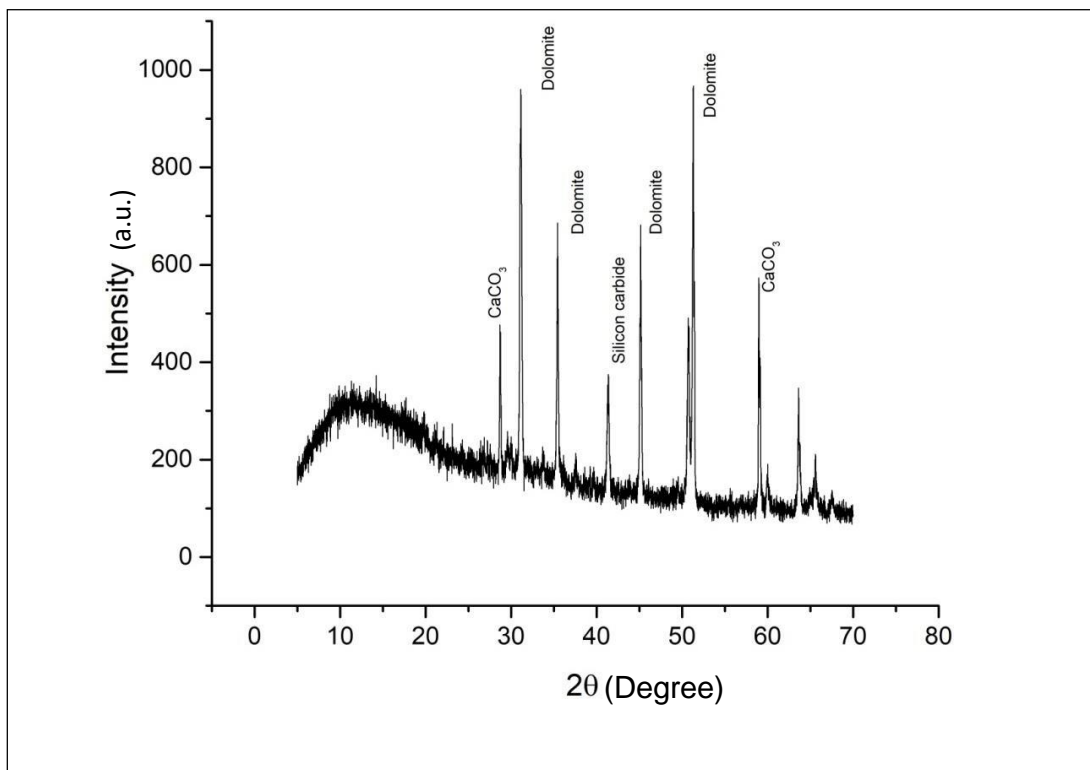


**Fig. 4.2: XRD spectra of marble waste**

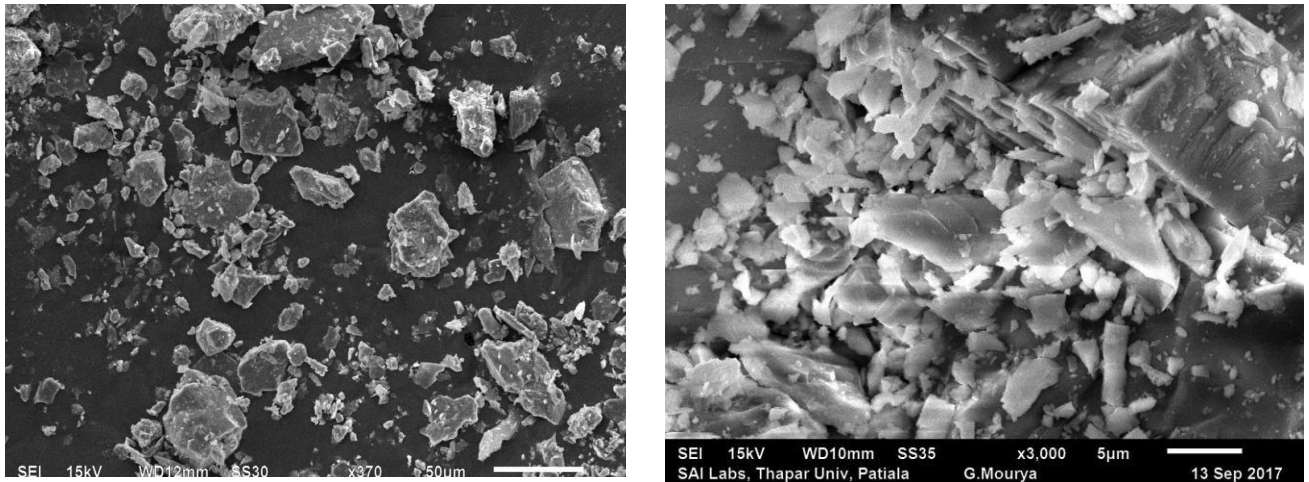


**Fig. 4.3: SEM image of (a) Natural river sand; (b) Marble waste**

### **4.3. WORKABILITY OF FRESH CONCRETE**

Workability of concrete is related to the consistency of the mix and defines the ease of placement of the mix, which is further related to rheology of the fresh concrete. It defines stability and compatibility of the mix. Slump test is one of the easiest and popular tests used for determining workability of mix. The test was conducted as per BIS 7320-1974. The slump values of all the mixes are presented in Fig. 4.4. It was observed that the workability of the mix decreased with the addition of marble waste as replacement of fine aggregates. The decrease occurred in spite of the fact that the water adsorption of marble was comparatively lesser than the water absorption of natural river sand.

Similar observations for the loss of workability with incorporation of marble powder were made by (Alyamaç and Ince, 2009; Binici et al., 2008; Corinaldesi et al., 2010; Hebhoub et al., 2011). It is known that the workability of concrete depends upon the characteristics of the material used, the grading and shape of fine aggregates. In the present study, both marble waste and natural river sand belonged to Zone III of BIS 383-2016; however the grading curve of both the aggregates show that marble waste had large proportion of finer aggregates, which will require more water to wet the surface of aggregates. The loss of workability with the incorporation of marble waste can also be attributed to the angular shape of marble waste aggregates (as shown in Fig. 4.3) and an increase in the surface area to be wetted, hence decreasing the workability. Also, it is reported that the addition of marble waste in a concrete mix makes the mix highly cohesive and less workable, thereby increasing the water

demand. The combined effect of increased cohesiveness of the mix and large surface area to be wetted led to loss of workability of the mix containing marble waste as replacement to fine aggregates. Actually, there were two properties that could have contradictory effect on workability of the mix. Lower water absorption could have led to increase in workability; while angular shape of particles along with higher surface area to be wetted could have decreased the workability. Out of the contradictory properties, the later ones seemed to be dominating in the present case, thereby decreasing the workability of the mixes.

In the present study, the mixes having slump in the range of  $80\pm 20$  mm were considered so that the mixes can be prepared without using any superplasticizer. That is why, the maximum percentage replacement of marble waste was limited to 60%, wherein the slump values in the desired range were obtained. Further, no chemical additives were planned to be used in the study in order to increase workability of the mixes because they might affect the sorptivity characteristics of the mixes (Alyamaç and Aydin, 2015).

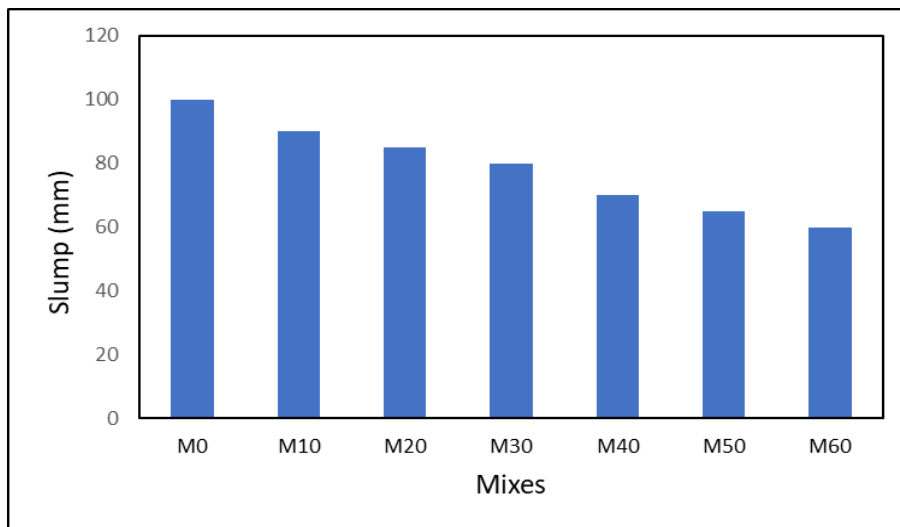


**Fig. 4.4: Slump of the mixes incorporating various percentages of marble waste**

#### **4.4. COMPRESSIVE STRENGTH**

The compressive strength results of all mixes at various ages are presented in Fig. 4.5. As can be seen from the figure, compressive strength of the mixes increased with the increase in marble waste in the mixes up to 40% replacement level, thereafter it got stabilized with no further change in strength. The 28-day compressive strength of the



Munir et al. (2017) also reported that calcite of marble powder reacts with  $C_3A$  to form calcium carbo-aluminate which is responsible for improving binding of concrete matrix, leading to better compressive strength of the mix incorporating marble waste. Bonavetti et al. (2001) also discussed the improved binding of mixes with marble powder and attributed it to the compact structure of carbo-aluminate.

The compressive strength improvement was not visible when the replacement level is increased beyond 40%, although the strength remains well above the strength achieved in the control mixes. The lack of improvement in strength beyond 40% replacement level can be due to loss of workability of the mix with the addition of marble waste, which could have adversely affected the packing of the constituent materials, hence leading to gradual reduction in strength.

Also, if the effect of curing age on compressive strength of mixes is considered (Fig. 4.6), it can be seen that the strength development of mixes incorporating marble waste is similar to that of the control mix. On comparing the compressive strength at different curing ages, maximum rate of increase of strength was observed at the age of 7 days of curing.

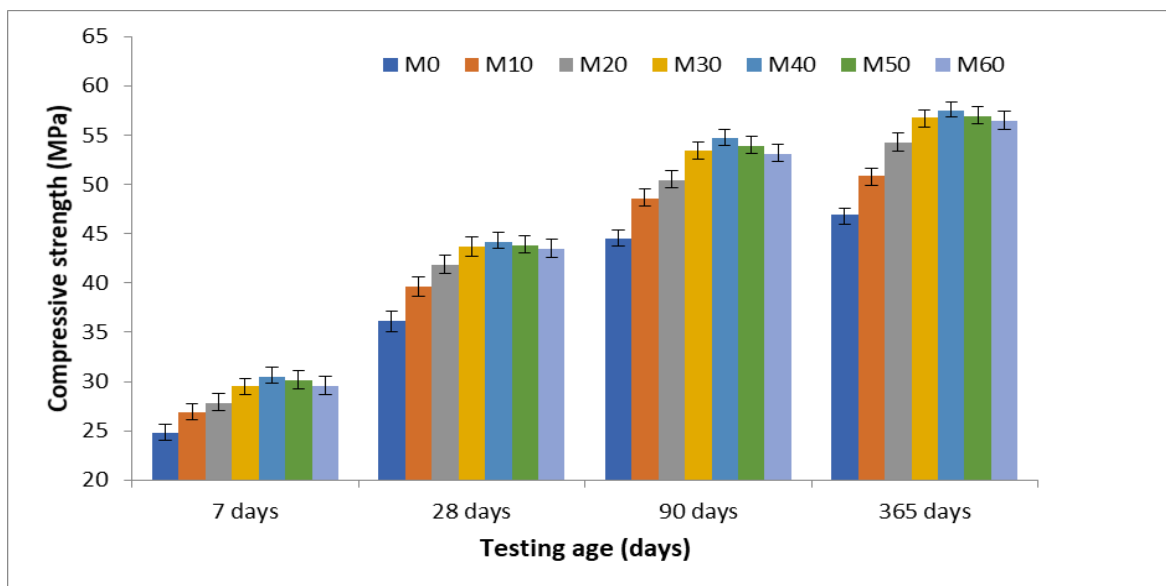


**Fig. 4.5: Compressive strength of mixes with varying percentages of marble waste**

All the mixes gained 68-70% of strength at 7 days as compared to their 28 days strength value. The final gain in strength at 365 days of curing was also similar for all mixes. The 365 days strength of all mixes was nearly 28-30% higher than their corresponding 28 days compressive strength.

It indicates that the addition of marble waste does not change the strength development pattern of the mixes. It is due to the inert nature of marble waste.

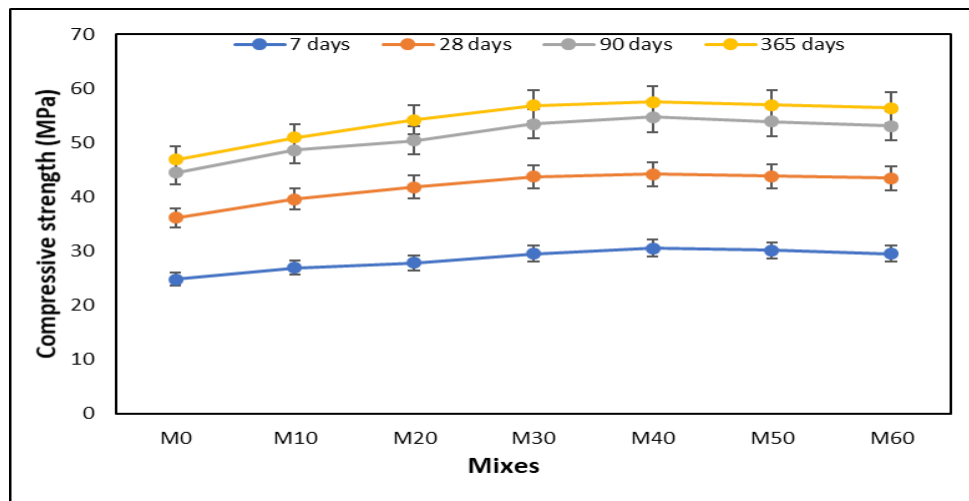


**Fig. 4.6: Compressive strength development of the mixes at various replacement levels of marble waste**

#### 4.5. SPLIT TENSILE STRENGTH

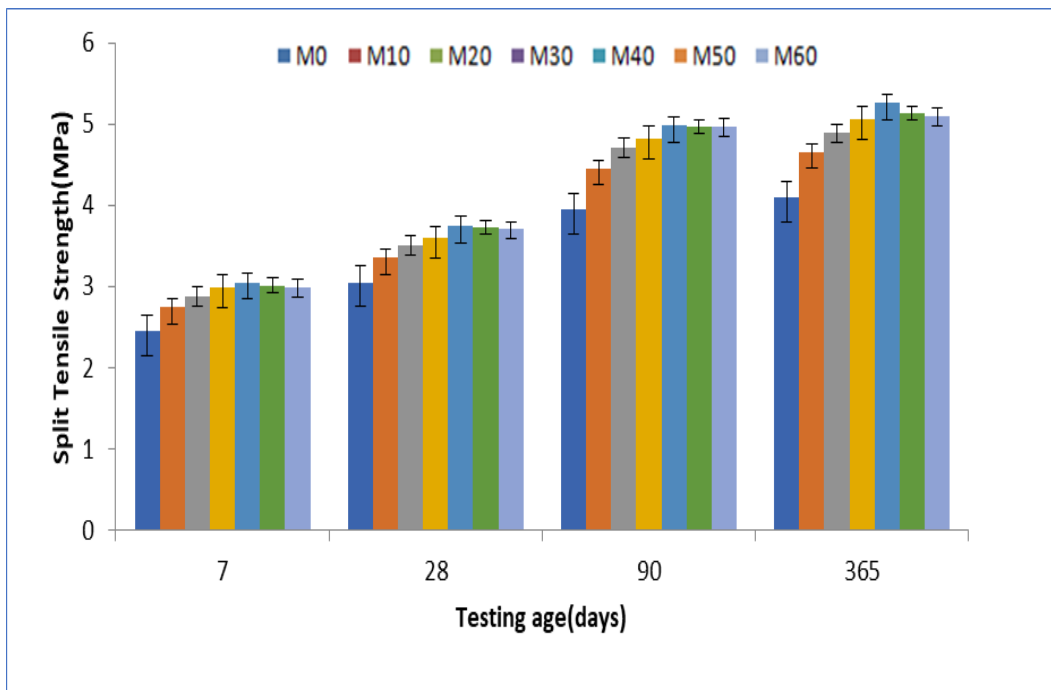
The split tensile strength of all mixes up to 365 days of curing has been presented in Fig. 4.7. Similar to the compressive strength results, split tensile strength also increased with the increase in marble waste as partial replacement of natural river sand, with the maximum increase in split tensile strength achieved at 40% replacement level, thereafter split tensile strength registered a small decrease. The 28 days split tensile strength of the mixes increased by 10.8, 17.1, 23.0, 25.3, 24.3 and 23.3% respectively for M10, M20, M30, M40, M50 and M60 mixes, as compared to the control mix M0.

Fig. 4.8 shows the split tensile strength development of the mixes at various curing durations. It can be seen that the strength development of mixes incorporating marble waste is similar to that of the control mix. For all mixes, maximum rate of increase of strength was observed at the age of 7 days of curing. All the mixes gained 79-81% of strength at 7 days as compared to their 28 days strength value. The final gain in strength at 365 days of curing was also similar for all mixes. The 365 days strength of all mixes was nearly 35-38% higher than their corresponding 28 days split tensile strength.

On comparing the compressive strength and split tensile strength results of the mixes, it can be seen that the percentage increase in split tensile strength is more than the corresponding increase in compressive strength for all mixes, irrespective of the curing age. The higher improvement in split tensile strength as compared to the compressive strength can be due to better bonding achieved by the shape of marble waste aggregates and formation of carbo-aluminates.

The angular marble particles help in providing better bonding along the crack path developed during split tensile strength test. The split tensile strength is known to be more dependent on the quality of the paste than the compressive strength (Singh and Siddique, 2013). The properties of fine aggregate influence the quality of paste, thereby affecting interfacial transition zones present in the concrete.

The ratio of split tensile strength to compressive strength for all mixes as presented in Table 4.3. The table shows that the percentage variation of split tensile strength varies from 9.9 to 10.4 %, 8.8 to 8.7 % and 8.9 to 9.3% as compared to the compressive strength at 7, 28 and 90 days respectively.



**Fig. 4.7: Split tensile strength of concrete with varying percentages of marble waste as fine aggregates**

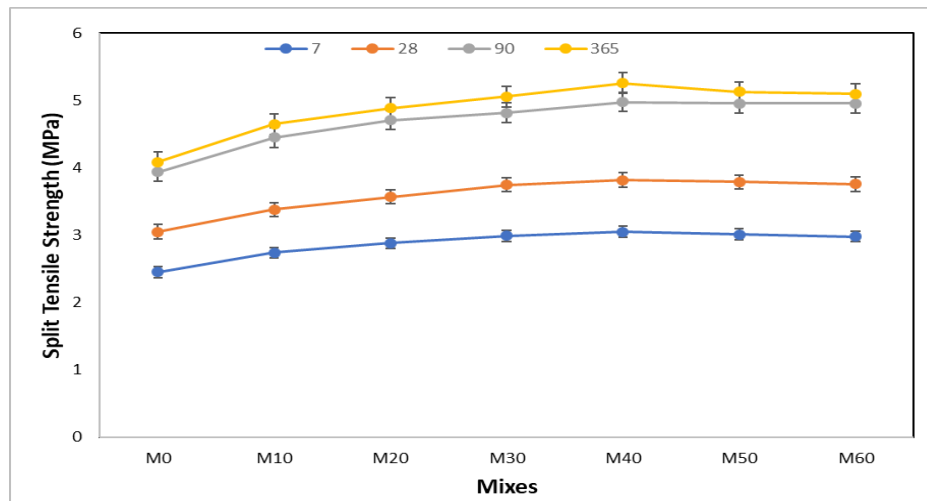


**Fig. 4.8: Split tensile strength development of the mixes at various replacement levels of marble waste**

**Table 4.3: Ratio of split tensile strength and compressive strength**

| Mix        | Split tensile strength / compressive strength (%) |        |        |
|------------|---|--------|--------|
|            | 7-day   | 28-day | 90-day |
| <b>M0</b>  | 9.9   | 8.4    | 8.9    |
| <b>M10</b> | 10.2  | 8.5    | 9.2    |
| <b>M20</b> | 10.4  | 8.5    | 9.3    |
| <b>M30</b> | 10.1  | 8.6    | 9.0    |
| <b>M40</b> | 10.0  | 8.6    | 9.1    |
| <b>M50</b> | 10.0  | 8.7    | 9.2    |
| <b>M60</b> | 10.1  | 8.7    | 9.3    |

#### 4.6. PERMEATION PROPERTIES OF THE MIXES

The permeation characteristics of the mixes were monitored by conducting rapid chloride permeability test (RCPT), sorptivity test and water absorption test. Rapid chloride permeability test was conducted at 28, 90 and 365 days of casting; while sorptivity test and water absorption test was conducted at 28 and 365 days of casting. The test results are presented in the following sections:

#### 4.6.1. Rapid Chloride Permeability Test (RCPT)

The resistance against ingress of chlorides is the most important parameter affecting deterioration of reinforced concrete structures due to rebar corrosion. RCPT evaluates the electrical chloride ion conductance of concrete and correlates it with chloride ion penetration. RCPT was conducted as per ASTM C1202-12 at 28, 90 and 365 days of casting. The charge passed for various mixes at different testing times is represented in Table 4.4. Based on the value of charge passed, the chloride ion penetration is specified to lie in certain penetration range, as specified. The obtained results and the respective penetration ranges are presented in Fig. 4.9.

It can be observed from the figure that the RCPT values decrease with the increasing curing age. At 28 days of curing, the mixes had chloride ion penetration in the range corresponding to moderate to low permeation category. At 365 days of curing, RCPT values for most of the mixes lie in the low chloride ion permeation category, with M40 mix registering RCPT values in ‘very low permeation’ range.

Also, at a given age of concrete, the RCPT values decrease with the increase in marble waste addition. For instance, at 28 days of curing the charge passed in the control mix was 2150 coulombs, which reduced to 1966 coulombs when 10% of marble waste was used. The charge passed further reduced to 1854, 1605 and 1492 coulombs for M20, M30 and M40 concrete, respectively. Thereafter, the charge passed started increasing for M50 and M60 concrete.

**Table 4.4: Charge passed through different concrete mixes in rapid chloride ion penetration test**

| Mix designation | Average charge passed (coulombs) at different curing age |        |         |
|-----------------|--|--------|---------|
|                 | 7-day  | 28-day | 365-day |
| M0              | 2510   | 2150   | 1810    |
| M10             | 2131   | 1966   | 1605    |
| M20             | 1991   | 1854   | 1410    |
| M30             | 1786   | 1605   | 1254    |
| M40             | 1582   | 1492   | 1012    |
| M50             | 1642   | 1510   | 1087    |

|     |      |      |      |
|-----|------|------|------|
| M60 | 1646 | 1544 | 1105 |
|-----|------|------|------|

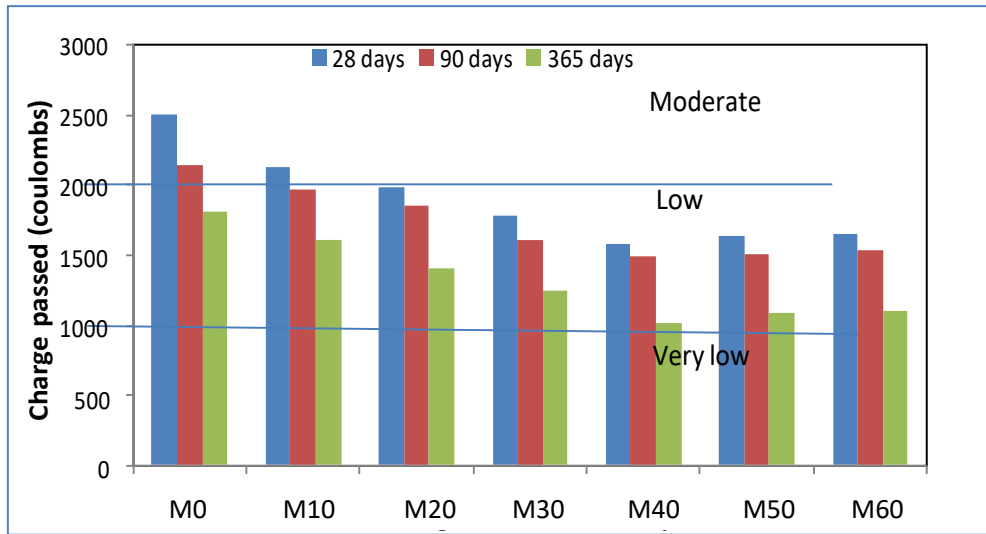


**Fig. 4.9: RCPT test results for concrete specimens at different testing ages**

At 28 days of curing, penetration of the control mix was in ‘moderate’ penetration range; while the penetration of all other mixes having marble waste was in ‘low’ penetration range; as specified in ASTM C 1202-12. M40 concrete registered least RCPT value among all mixes, irrespective of the curing age. The least RCPT value of M40 mix at all curing ages indicates its best performance.

#### 4.6.2. Sorptivity

Sorptivity test was used to determine rate of water absorption by capillary action. The test was conducted as per ASTM C1585-13. For obtaining sorptivity of the mix, the specimen was allowed to absorb water through one surface only and the mass gained due to capillary rise of water between the pore systems of specimen was noted. The change in mass of the specimen was recorded at 1, 5, 10, 20, 30, 60, 120, 180, 240, 300, 360 minutes and 1, 2, 3, 4, 5, 6, 7 and 8 days. A plot was then drawn between increase in mass per unit area over the density of water and the square root of time. The value of the initial or primary sorptivity was given by slope of the curve upto 6 hours and secondary absorption was given by the slope of the best fit line from 6 hours onward. The slope of the best fit line obtained by linear regression analysis of primary absorption data points is taken as the sorptivity value of the mix. The test was conducted at 28 and 365 days of curing for all mixes.

The absorption of different mixes at 28 days of curing throughout the test period is presented in Fig. 4.10; while the data points used for obtaining primary sorptivity are presented in Fig. 4.11. Similarly, Figs. 4.12 and 4.13 represents the absorption and data points for primary sorptivity obtained at 365 days of casting. The value of sorptivity obtained by best fit regression analysis is presented in Table 4.5. From Figs. 4.10 and 4.12, it can be seen that the slope of all mixes after 6 hours of absorption is nearly same at both the testing ages. It indicates that all the mixes have nearly same secondary sorptivity. The slope of water absorption upto 6 hours of testing varies significantly for all the mixes, and is therefore taken as the main parameter of study.

The value of primary sorptivity coefficient decreased systematically, as the amount of marble waste is increased in the mix. Initially, the value decreased rapidly up to 40% replacement level; thereafter the values became nearly constant and a small increase in sorptivity was registered. At 28 days of casting, the value of primary sorptivity was  $5.1 \times 10^{-3} \text{ mm/t}^{0.5}$  for the control concrete. The value decreased to  $3.6 \times 10^{-3} \text{ mm/t}^{0.5}$  for M40 concrete and then registered a small increase to  $4 \times 10^{-3} \text{ mm/t}^{0.5}$  for M60 concrete. Similarly, at 365 days of casting, the value of primary sorptivity was observed to be  $2.9 \times 10^{-3} \text{ mm/t}^{0.5}$  for the control concrete,  $2.0 \times 10^{-3} \text{ mm/t}^{0.5}$  for M40 concrete and  $2.1 \times 10^{-3} \text{ mm/t}^{0.5}$  for M60 concrete.

The obtained values of sorptivity indicates that the permeability characteristics of the concrete improved with the incorporation marble waste in the mix. Minimum sorptivity value was obtained for M40 mix at both 28 and 365 days of testing. The improved performance of mixes incorporating fine marble waste aggregates can be attributed to lower water absorption of marble waste aggregates, indicating lesser pores on the concrete surface and stronger bond between cement paste and the aggregates (Neville and Brooks, 2010). Along with this, the angular sizes of marble waste helped in better bonding, due to which more paste in interstitial transition zone (ITZ) of the resultant mix was required, which further improved aggregate - paste interface. This led to refinement in the pore structure network, thereby improving permeation characteristics of the mixes incorporating marble waste.

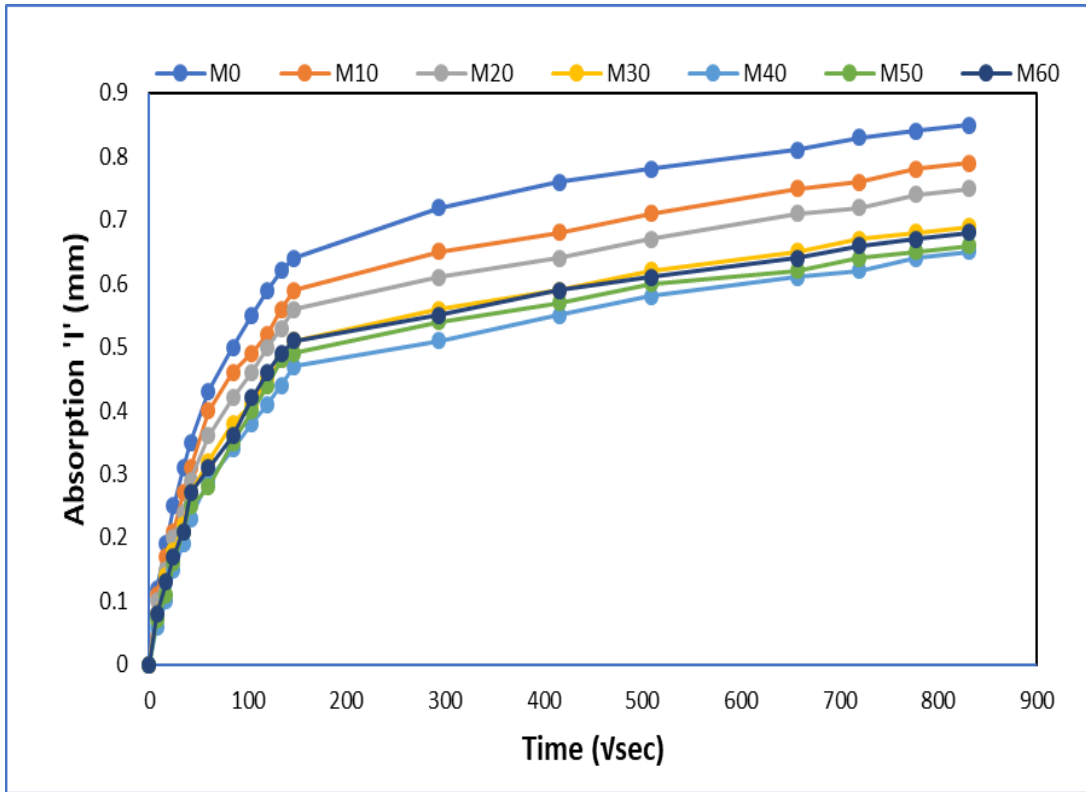


**Fig. 4.10: Absorption of mixes at 28 days of curing during sorptivity test**

Also, the permeability characteristics of all the mixes improved significantly with the increase in curing duration from 28 days to 365 days. Improved hydration resulted in decreasing capillary pores in the mix.

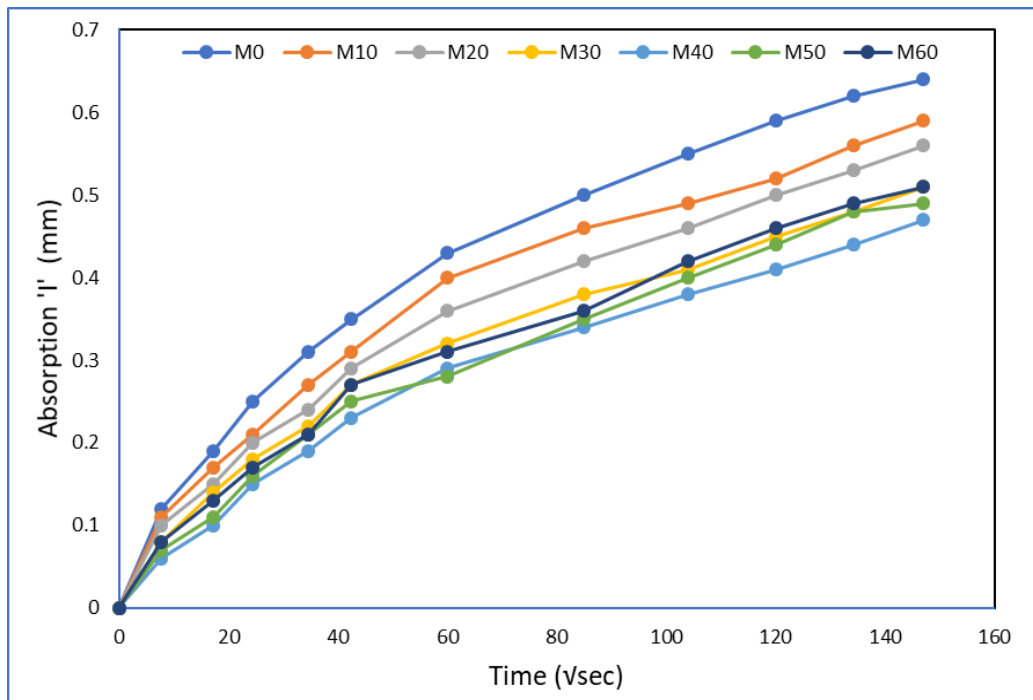


**Fig. 4.11: Primary absorption up to 6 hours for mixes at 28 days of curing**

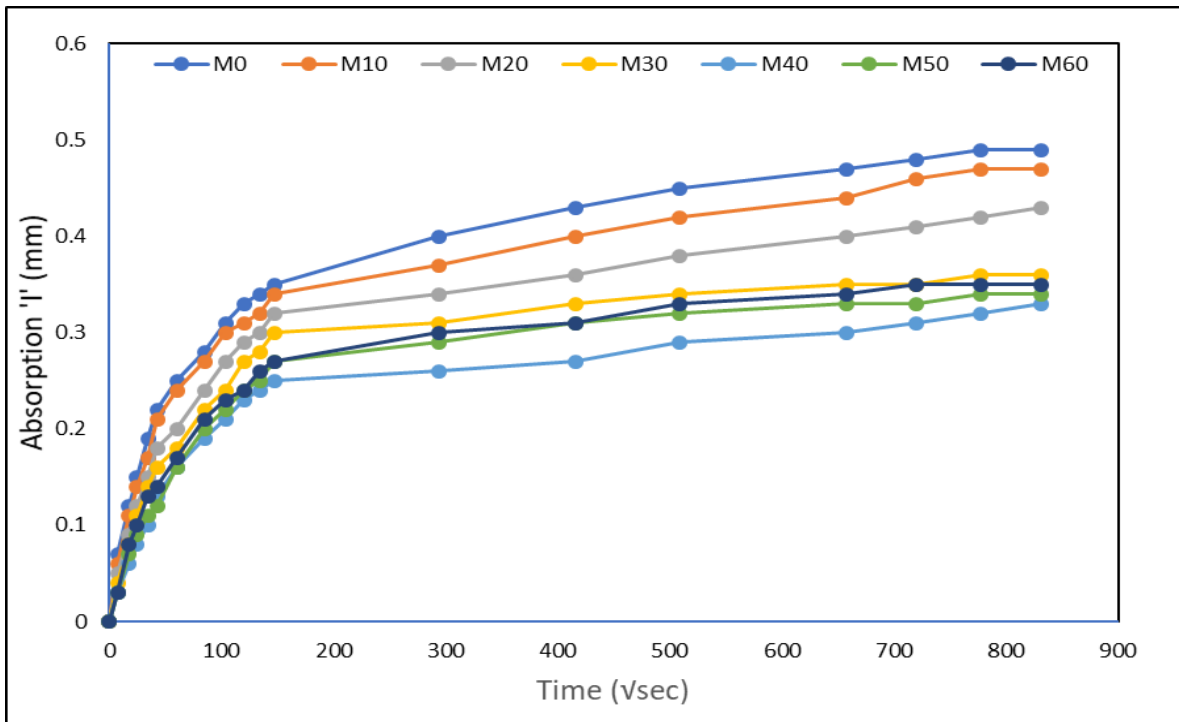


**Fig. 4.12: Absorption of mixes at 365 days of curing during sorptivity test**

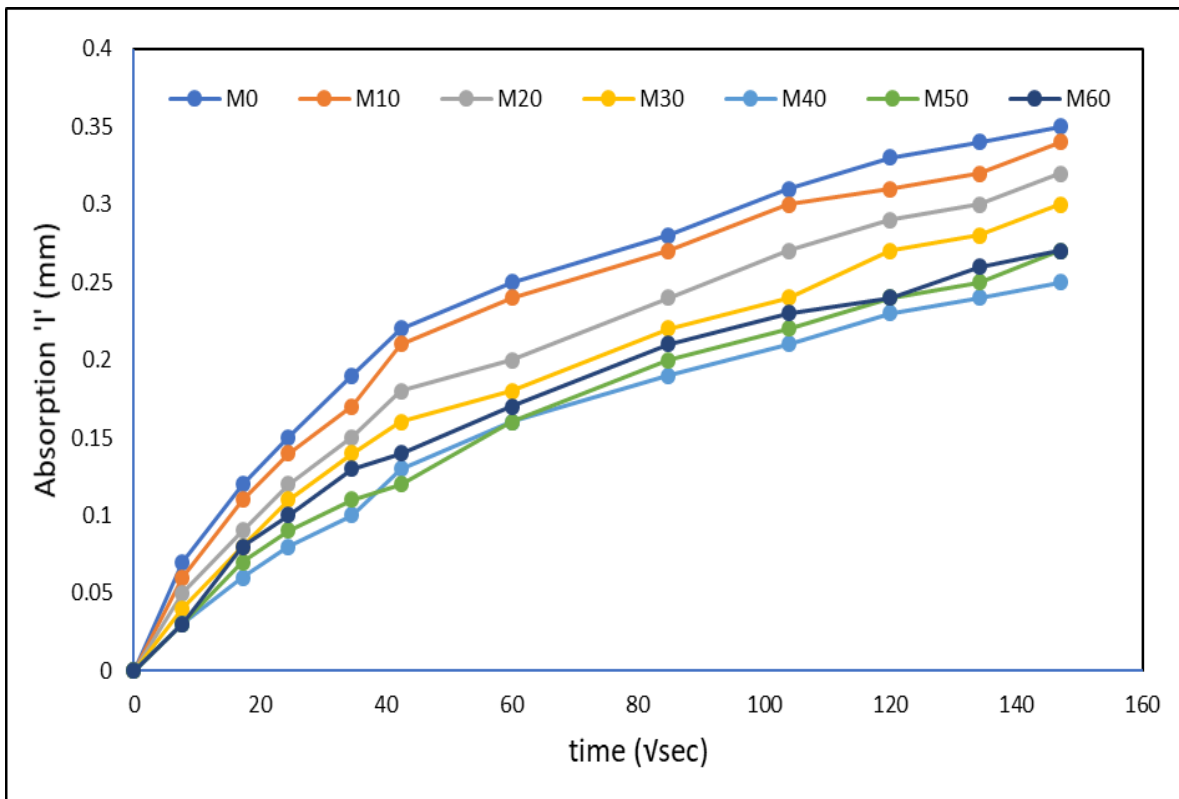


**Fig. 4.13: Primary absorption up to 6-hour for mixes at 365-day of curing**

**Table 4.5: Values of sorptivity coefficient of concrete mixes**

| Mix | Sorptivity coefficient ( $\times 10^{-3} \text{ mm/t}^{0.5}$ ) |         |
|-----|--|---------|
|     | 28-day   | 365-day |
| M0  | 5.11   | 2.9     |
| M10 | 4.6  | 2.8     |
| M20 | 4.4  | 2.5     |
| M30 | 3.9  | 2.3     |
| M40 | 3.6  | 2.0     |
| M50 | 3.8  | 2.1     |
| M60 | 4.0  | 2.1     |

**4.6.3. Water Absorption Test**

This test was conducted as per ASTM C642-13. Water absorption results of different mixes at 28 and 365 days of casting are presented in Table 4.6. The water absorption of the control mix is 5.10% and 2.68% at 28 days and 365 days respectively. As expected, water absorption decreased with the increase in curing age, indicating denser concrete matrix due to continuous hydration of concrete. Water absorption decreased with the addition of marble waste. Since water absorption is generally related to the structural pores, especially in the aggregate-interface zone; decrease in water absorption by marble waste addition confirms refinement of aggregate-interface zone, resulting in improvement of overall durability of the mix.

**Table 4.6: Water absorption of mixes at 28 days and 365 days of curing**

| Mix | Water absorption (%) |         |
|-----|----------------------|---------|
|     | 28-day               | 365-day |
| M0  | 5.10                 | 2.68    |
| M10 | 4.97                 | 2.56    |
| M20 | 4.44                 | 2.48    |
| M30 | 4.02                 | 2.30    |
| M40 | 3.79                 | 2.12    |
| M50 | 3.94                 | 2.26    |
| M60 | 4.05                 | 2.29    |

Least value of water absorption is observed in M40 mix, in which 40% of fine aggregates are replaced by marble waste. The results are in agreement with the strength and sorptivity results.

#### **4.7 MICROSTRUCTURE ANALYSIS**

The microstructural analysis of the mixes was carried out at 28 and 365 days of curing. It involved X-ray diffraction (XRD) analysis of the powdered specimens obtained from crushed specimens collected after conducting compressive strength test. Along with XRD, scanning electron micrographs (SEM) were obtained on the fractured pieces. The collected concrete pieces were mounted on SEM stub and the images were taken in the secondary electron image mode. To ensure electrical connectivity, the specimens were coated with a layer of gold before placing it on SEM stub. The results obtained are discussed in the following sections:

##### **4.7.1 XRD Analysis**

XRD analysis was performed in order to identify phases present in the resultant concrete mixes made by incorporating marble waste as replacement of fine aggregates. The investigations were performed on powdered concrete samples for diffraction angle ranging from  $10^\circ$  to  $80^\circ$ . XRD spectra of all specimens were obtained at 28 and 365 days of casting and are presented in Figs. 4.14 and 4.15, respectively. Since the trend of all mixes was same, the spectra of M0, M20, M40 and M60 are presented in the figures. The obtained spectra indicate that the major phases formed in all mixes remain same, irrespective of the replacement levels of marble waste with natural river sand as fine aggregates. It further strengthened the fact that marble waste is largely an inert material and has filler effect on the properties of the resultant mix. Major phases identified for all mixes are C-S-H gel, calcium hydroxide, calcium carbonate, dolomite and quartz. The XRD patterns show major presence of dolomite in concrete made with marble waste aggregates.

The intensity of dolomite peaks increased rapidly with an increase in percentage of marble waste beyond 40%. This indicates that dolomite was initially involved in reaction with  $C_3A$ . However, with a higher percentage of marble waste, much of the dolomite remained un-reacted and the same is observed in XRD analysis. The quartz

peaks have also diminished with the partial replacement of natural river sand with marble waste aggregates.

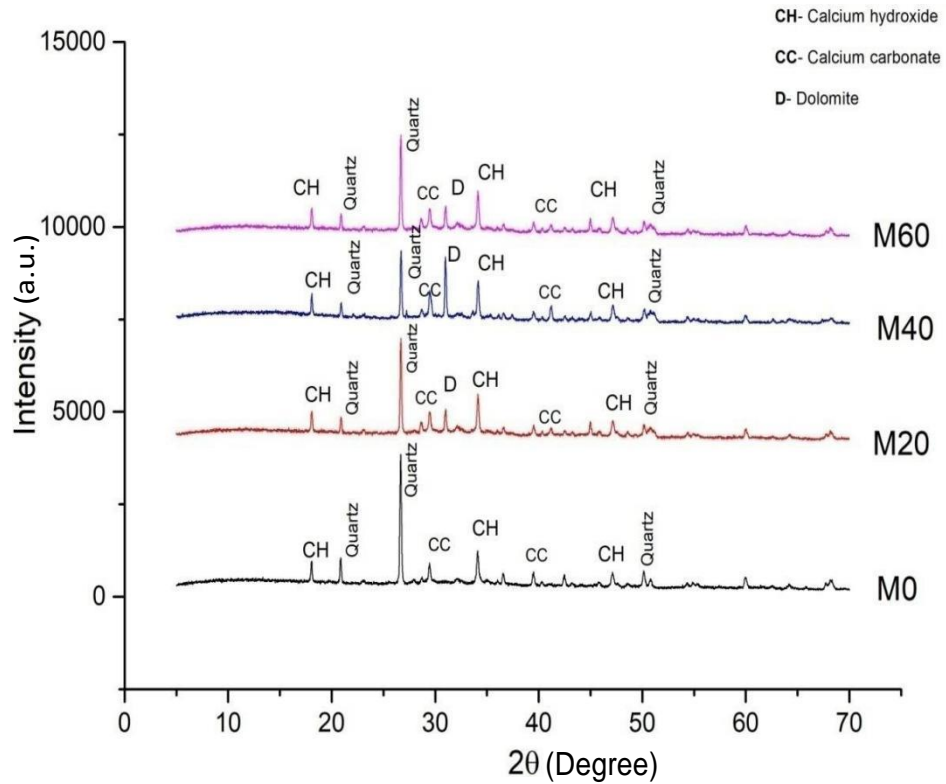


**Fig. 4.14: XRD spectrum of various mixes at 28 days of casting**

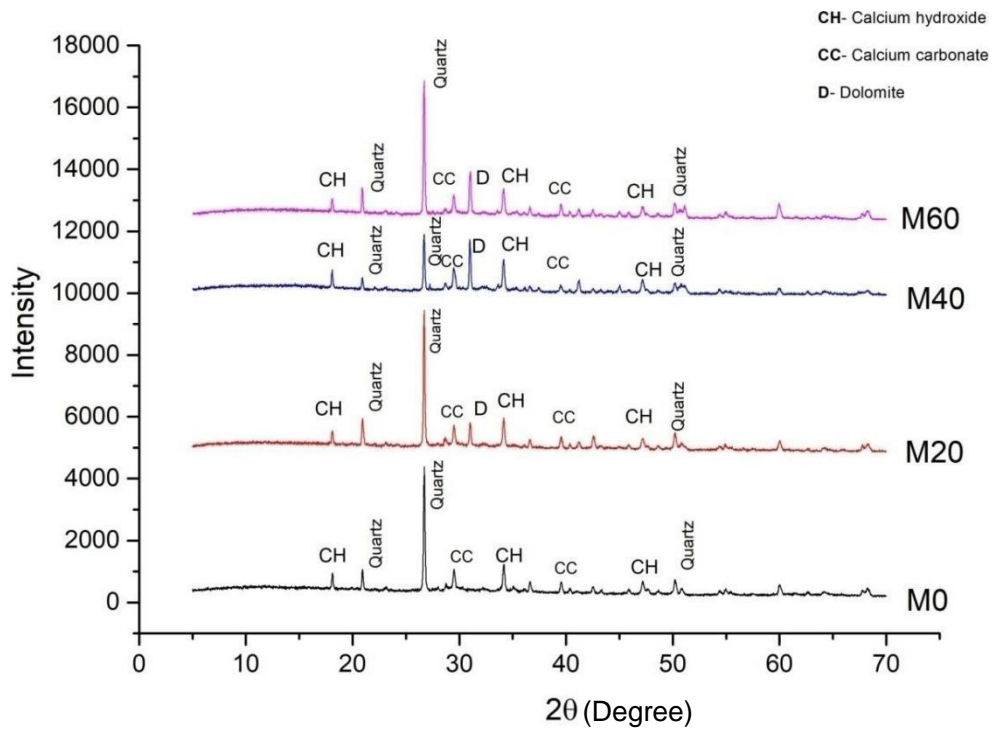


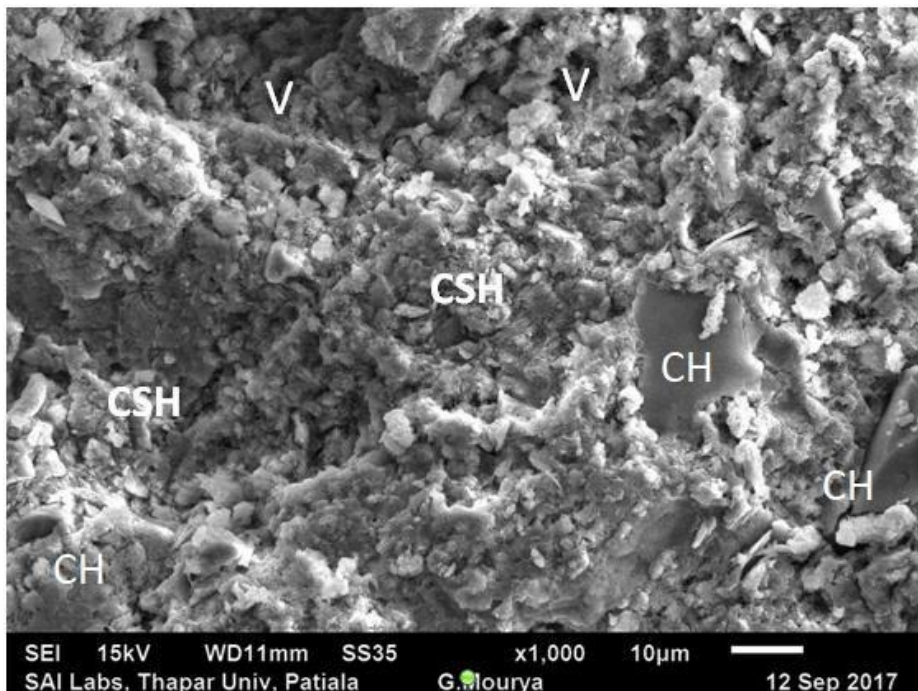
**Fig. 4.15: XRD spectrum of various mixes at 365-days of casting**

#### 4.7.2. Scanning Electron Micrographs

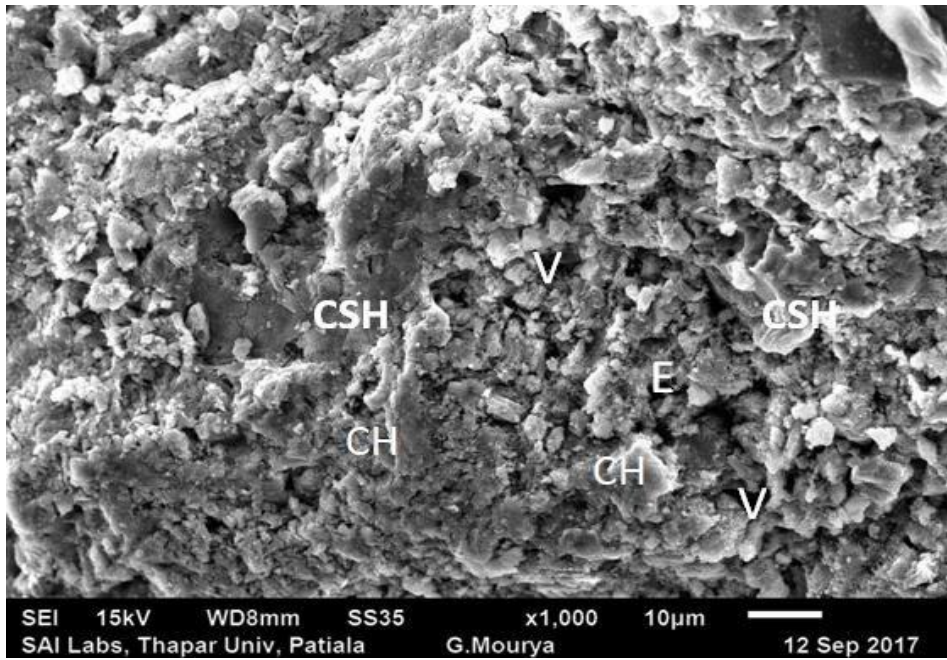
SEM images of broken concrete samples obtained from concrete mixes incorporating variable percentages of marble waste as fine aggregates and cured up to 28 days and 365 days were taken and are presented in Figs. 4.16 and 4.17 respectively.

In all the SEM micrographs, the amorphous phase of C-S-H and CH crystals are visible. CH crystals are noticeable in variable shapes and sizes like flat, prism-shaped and long crystals. Along with this, the voids are seen in all the micro graphs. Significant densification of the mix containing marble waste aggregates can be observed in SEM images, indicating the filler effect caused by incorporating marble waste. Also, the partial improvement in the binding ability due to presence of calcium carbo-aluminate phase can be the reason for dense and non-porous micro structure.

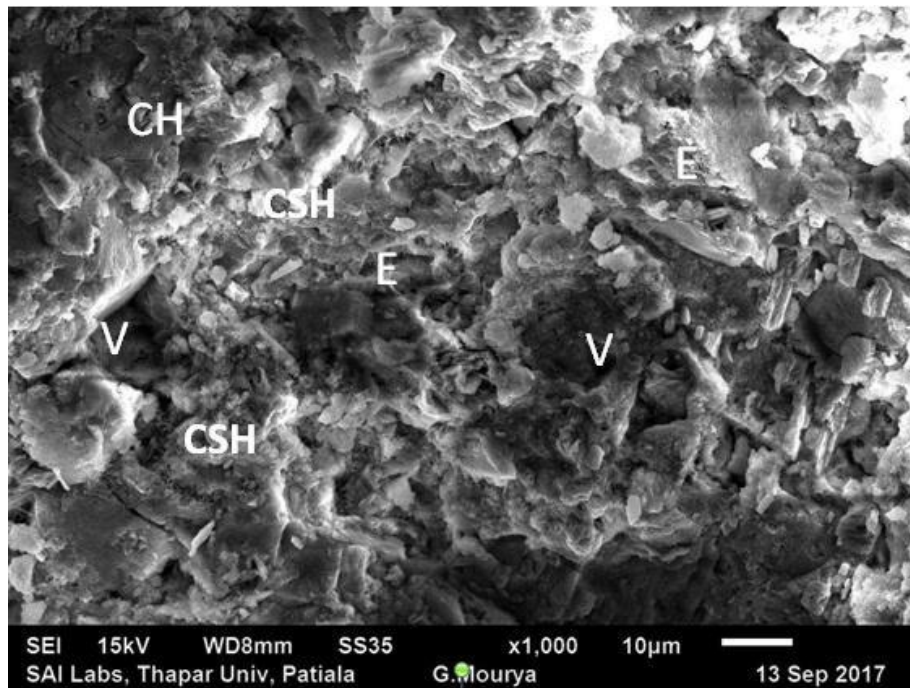
Similar observations were made by Singh et al. (2017) and Buyuksagis et al. (2017). Major phases, i.e. C-S-H gel and CH remain almost the same in all mixes, indicating that the incorporation of marble waste has not much influence on the hydration of cement. However, there is a better spread of C-S-H with the addition of marble waste. Thus, better mechanical properties of the mix can be explained by filler effect of marble waste aggregates and the densification of concrete matrix.



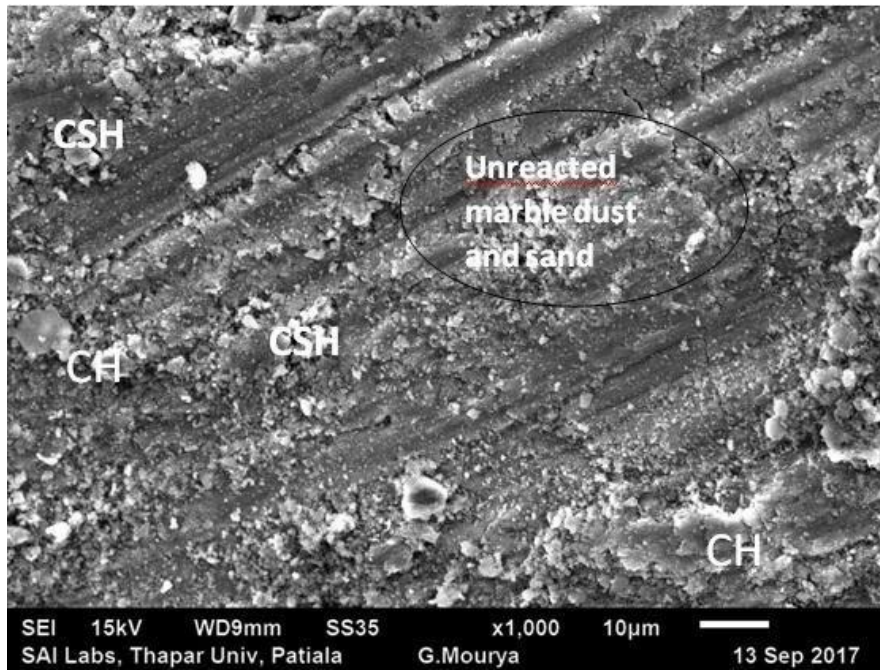
(a) M0 Mix



(b) M20 Mix

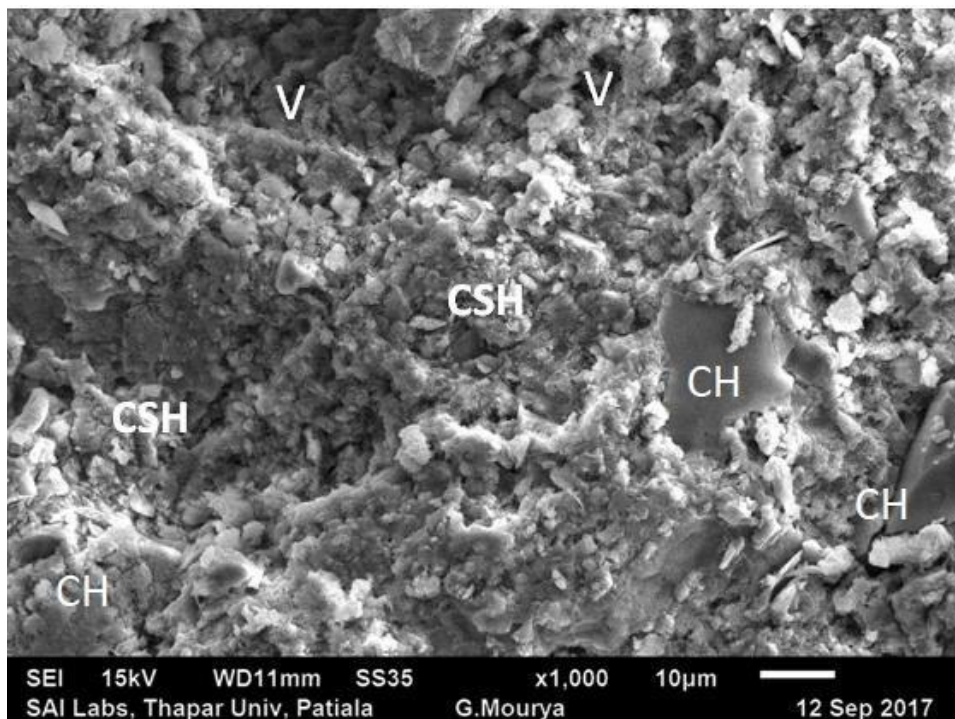


(c) M40 Mix

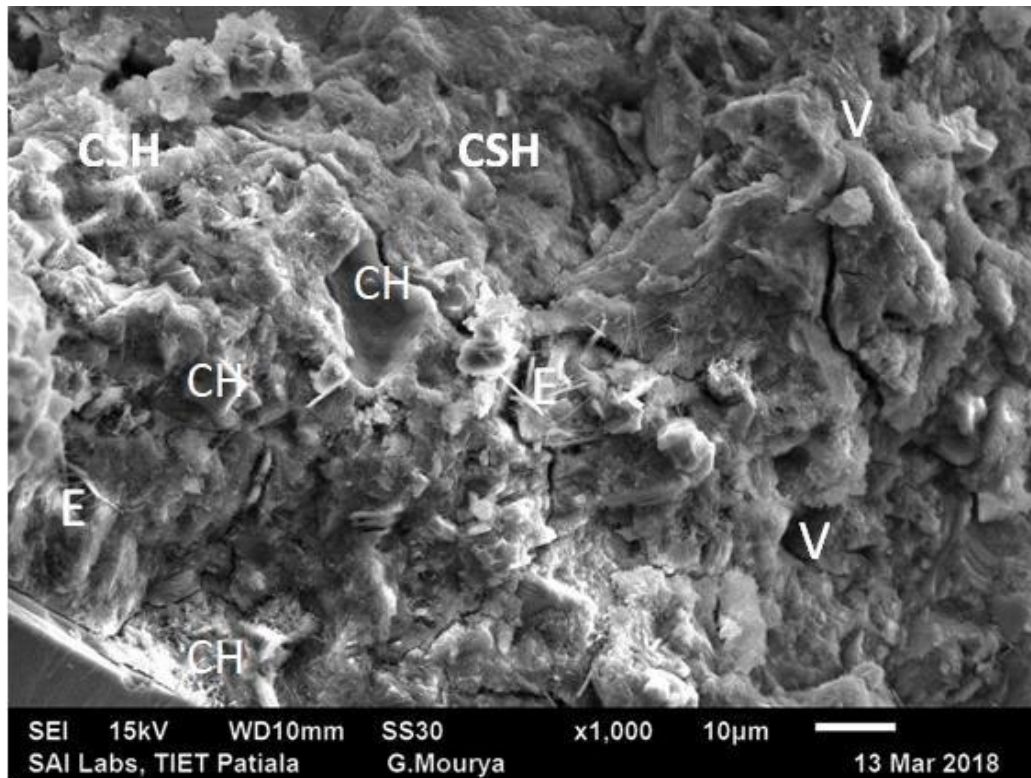


(d) M60 Mix

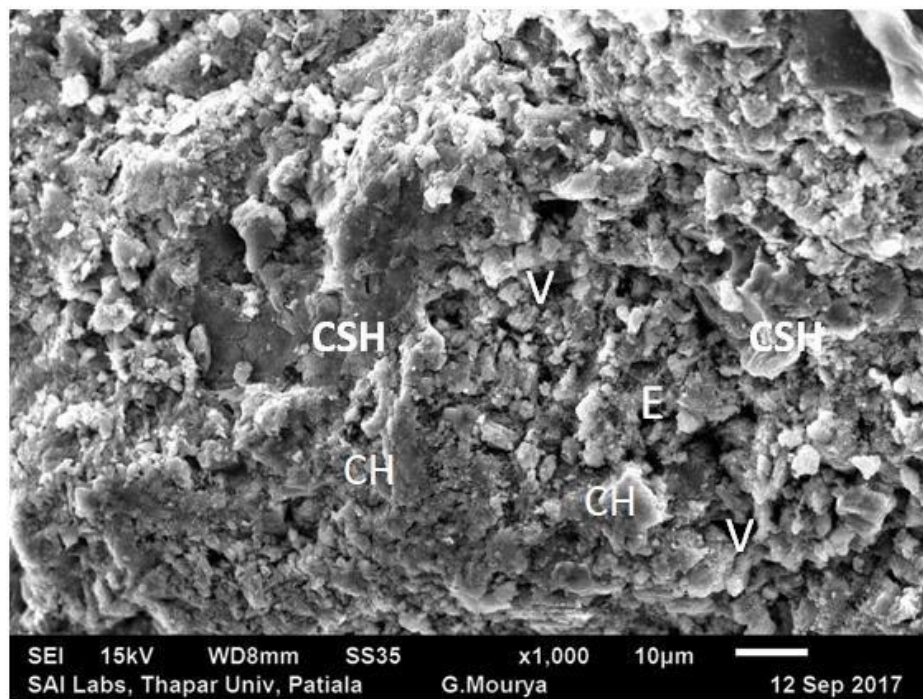
**Fig. 4.16: SEM images of concrete mixes containing varying percentage of marble waste as replacement of fine aggregates at the age of 28 days**



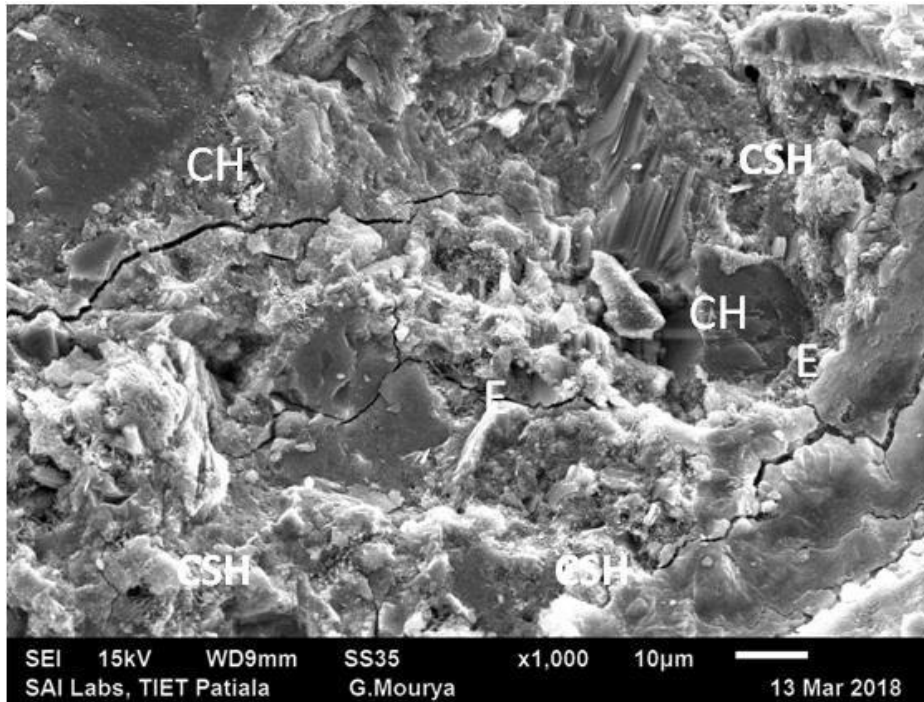
(a) M0 Mix



(b) M20 Mix



(c) M40 Mix



(d) M60 Mix

**Fig. 4.17: SEM images of concrete mixes containing varying percentage of marble waste as replacement of fine aggregates at the age of 365 days**

The test results clearly indicate that there is a definite relationship between various mechanical properties of the mixes. Also, a strong correlation can be observed between the compressive strength of the mix and the corresponding permeation parameter.

#### **4.8 STATISTICAL ANALYSIS OF MECHANICAL STRENGTH AND PERMEATION PARAMETER RESULTS**

The statistical analysis of data was performed and suitable models were generated between various tested parameters. These are discussed in the following sections:

##### **4.8.1. Relationship Between Compressive Strength and Split Tensile Strength**

It is observed from the test results that the split tensile strength is directly proportional to compressive strength of concrete. Also, both the strengths are observed to be dependent on the proportions of marble waste used as partial replacement of natural river sand as fine aggregates. The strength development is also known to be dependent on the age of concrete. Thus, it is expected that a realistic relationship between compressive strength and split tensile strength may also involve the

parameters corresponding to age of concrete and percentage of marble waste aggregates. Hence, the general form of the relation can be represented as:

$$f_{st} = f(f_c, t, p_m) \quad \dots (4.3)$$

where

$f_{st}$  is the tensile strength of concrete in MPa

$f_c$  is the cube compressive strength of concrete in MPa

$t$  is the age of concrete

$p_m$  is the proportion of marble waste used as partial replacement of natural fine aggregates.

Therefore, a model was developed through the multiple regression analysis, carried out by using the experimental data generated, considering the effect of compressive strength, age of concrete and percentage of marble waste used as fine aggregates on the split tensile strength. The following combined relationship was obtained:

$$f_{st} = 0.46 (f_c)^{0.57} \left( \frac{p}{100} \right)^{0.25} \left( \frac{t}{28} \right)^{0.047} \quad \dots (4.4)$$

where  $f_{st}$  is the split tensile strength of concrete in MPa,  $f_c$  is the compressive strength of concrete in MPa,  $t$  is the age of concrete in days and  $p$  is the percentage of marble waste used as partial replacement of fine aggregates. The coefficient of determination for this multiple regression analysis is 0.972.

In order to check the accuracy of the proposed model on a wider level, apart from the experimental results, data was collected from the literature with varying characteristics of cement, marble waste percentage and testing age.

The brief variability of the data is presented in Table 4.7. In all 85 data points were collected for validating the model. Also, a graph between the observed split tensile strength and the predicted value of split tensile strength by using the proposed model was plotted and is presented in Fig. 4.18.

For checking the accuracy of the obtained model, average ratio of observed and predicted values ( $\Delta O/P$ ) was obtained and the model is considered accurate depending on the closeness of the average ratio to unity.

Similar procedure was followed by Zain et al. (2002) and Goyal (2008) for validation of the proposed models. The average ratio was calculated to be 1.02, which clearly indicates that the proposed model can be used to estimate split tensile strength of concrete using marble waste as fine aggregates.

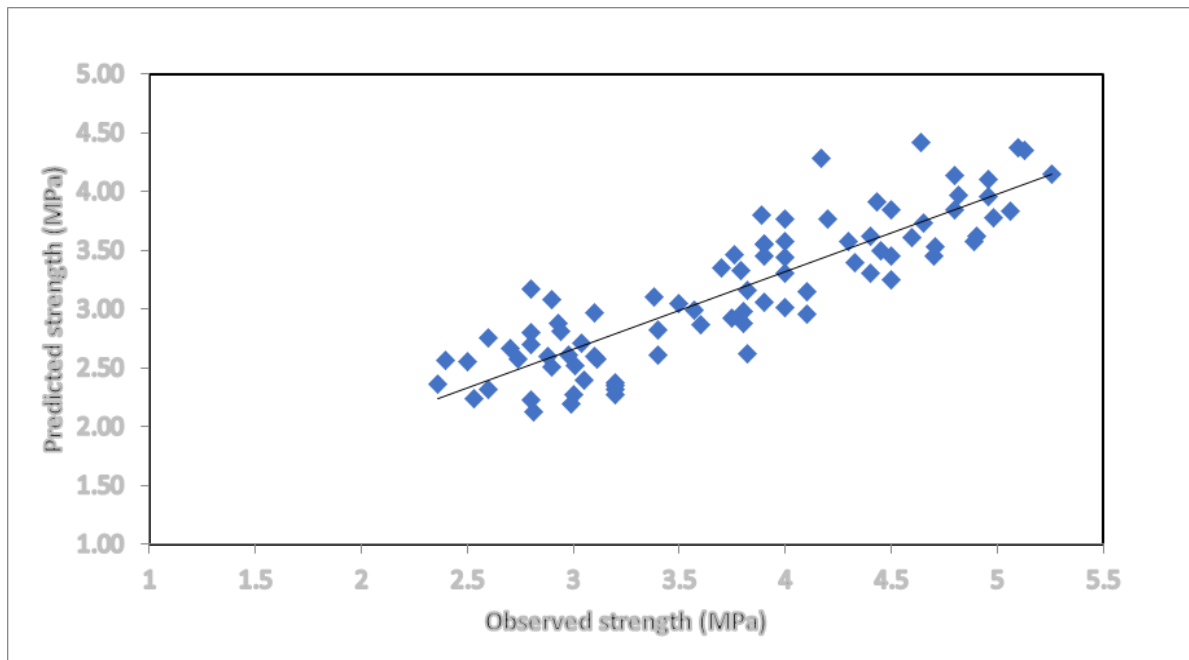


**Fig. 4.18: Relation between observed and predicted split tensile strength**

#### **4.8.2 Relationship Between Compressive Strength and Chloride Ion Permeability**

A correlation between concrete compressive strength and the corresponding charge passed in rapid chloride permeability test is attempted and is shown in Fig. 4.19.

The figure shows that the chloride ion penetration is inversely proportional to compressive strength, irrespective of the age of concrete. The level of correlation is good with  $R^2$  value of 0.743.

**Table 4.7: Description of data points used for checking the developed model for split tensile strength**

| <b>Author</b>             | <b>Compressive Strength Range (MPa)</b> | <b>Split Tensile Strength range (MPa)</b> | <b>Testing Time (days)</b> | <b>Marble waste as fine aggregate (%)</b> |
|---------------------------|---|---|----------------------------|---|
| (Aliabdo et al., 2014)    | 31.1 to 63.6                            | 3 to 5.5                                  | 7, 28, 56                  | 0 to 15                                   |
| (Keleştemur et al., 2014) | 50.3 to 60.3                            | 4.2 to 4.6                                | 28                         | 0 to 100                                  |
| (Alyamaç and Aydın, 2015) | 23.2 to 43.3                            | 2.4 to 3.2                                | 7, 28, 90                  | 0 to 90                                   |
| (Hebhoub et al., 2011)    | 10.3 to 35.6                            | 0.9 to 4.9                                | 2, 14, 28, 90              | 0 to 100                                  |
| (Ashish, 2018)            | 22.3 to 61.3                            | 2.2 to 5.2                                | 7, 28, 56, 90              | 0 to 15                                   |
| (Chavhan and Bhole, 2014) | 19.2 to 35.7                            | 2.8 to 5.9                                | 7, 14, 28                  | 0 to 50                                   |
| (Sakalkale et al., 2014)  | 9.8 to 35.5                             | 2.9 to 4.2                                | 3, 7, 28                   | 0 to 100                                  |

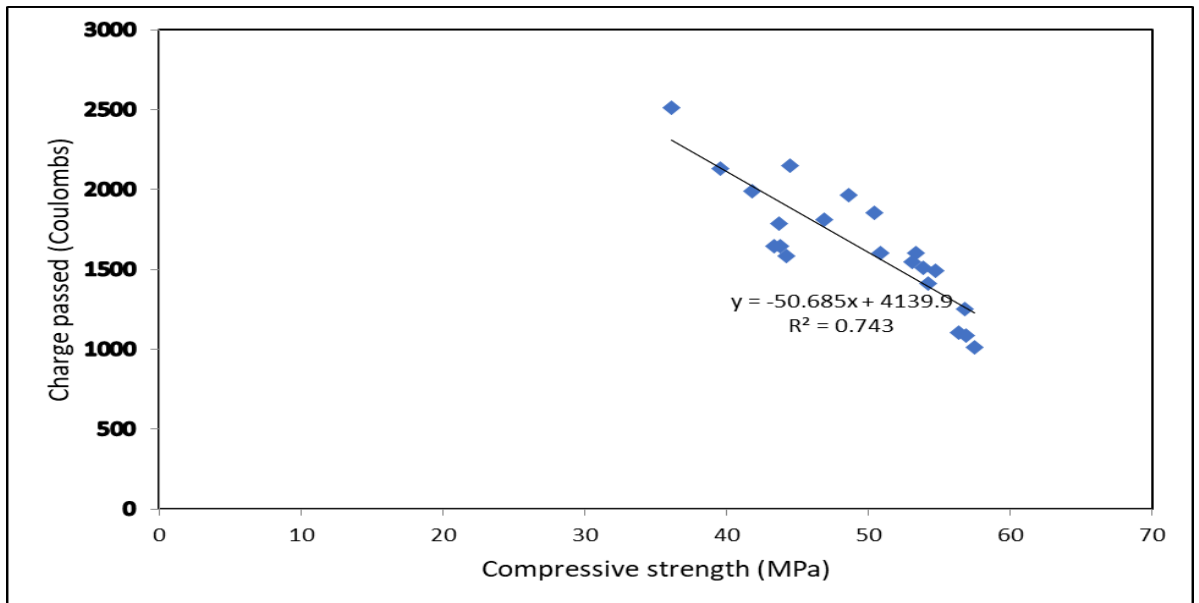


**Fig. 4.19: Relation between compressive strength and RCPT values**

## **4.9. ABRASION RESISTANCE OF CONCRETE**

This test was conducted as per BIS 1237-2012. Abrasion resistance of concrete is described as its ability to resist the wearing of the surface by rubbing and friction. It is an important durability property of concrete and is particularly important for concrete floors, concrete pavements and concrete dams. The property typically refers to the ability to resist wearing due to frictional movement between the surfaces of different characteristics. In the test, the abrasive particles are made to rub against stationary concrete block. The abrasive particles are provided with relative motion that creates shear force between particles and the concrete surface. The shear force so generated leads to formation of scratches on the surface. Also, a normal load of some value is put on the concrete block so that the abrasive particles penetrate into the concrete block. Both normal force and shear force ultimately leads to wearing away of concrete surface that is noted in terms of weight loss after the required number of revolutions.

### **4.9.1. Effect of addition of marble waste on abrasion resistance of concrete**

In the present study, abrasion resistance was measured in terms of depth of wear, which was also used by earlier researchers (Ghafoori and Sukandar, 1995; Naik et al., 2003; Siddique et al., 2013; Siddique and Khatib, 2010). The abrasion resistance of all mixes made by using marble waste as partial replacement of river sand was tested at 7, 28, 90 and 365 days of casting.

At a particular testing age, the specimen was subjected to wear from 20 gm of abrasive powder spread over a grinding machine, which was rotated at 20 rpm. The weight of specimen was measured after each 22 revolutions till the end of 220 revolutions. Two parameters were recorded from the measured data, which includes the progressive variation in depth of wear with each set and the final depth of wear at end of 220 revolutions. The final depth of wear after 220 revolutions for all the mixes is presented in Fig. 4.20; while the progressive depth of wear of each mix at 7, 28, 90 and 365 days of curing is shown in Figs. 4.21 to 4.24.

From Fig. 4.20, it can be observed that the curing age plays a vital role in improving the abrasion resistance of concrete. With the increase in curing age, the depth of wear decreased for all mixes. The maximum depth of wear was observed at 7 days of curing. It is due to incomplete hydration of cement products at this curing age.

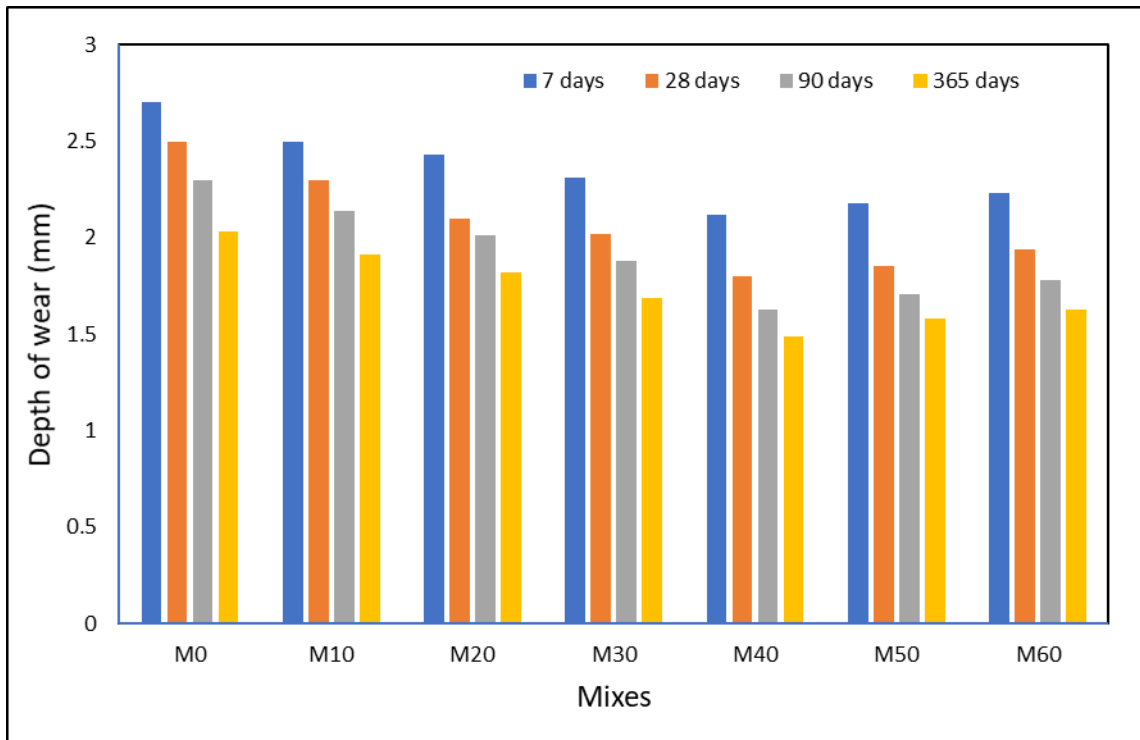


**Fig. 4.20: Final depth of wear of all mixes incorporating marble waste**

With the enhancement in curing age from 7 days to 28 days, the depth of wear decreased by nearly 15% which further reduced to 23 – 26% at 365 days of curing. Similar observations regarding decrease in depth of wear with the curing age is also made by other researchers (Khatib and Mangat, 1995; Kumar and Sharma, 2014; Siddique, 2013).

If the effect of addition of marble waste is analyzed, it can be seen that the addition of marble waste reduced the depth of wear as compared to the control mix at all curing ages. As the percentage of marble waste is increased, the depth of wear of the mixes decreased. As compared to the control mix, the depth of wear reduced by nearly 7-9% as the percentage replacement of marble waste was made 10%. The depth of wear reduced further to 14-16% at 20% replacement level of marble waste. The maximum improvement in depth of wear was observed at 40% replacement level, wherein the depth of wear reduced by 30% as compared to the control mix. The similar observation regarding the improvement in abrasion resistance of concrete mixes having marble waste was made by Binici et al. (2007, 2008); Alaymac and Aydin (2015).

The lower depth of wear achieved by using marble waste was due to the denser pore structure achieved due to better particle size distribution of marble particles, which

have more fines in the particle size range of 1.18 mm-300  $\mu\text{m}$ . Along with this, the angular sizes of marble waste aggregates helped in better bonding and improvement in interstitial transition zone (ITZ) of the resultant mix. Also, at the chemical level, marble waste improved the binding ability of the mix. The reaction between calcite present in marble with  $\text{C}_3\text{A}$  of cement provides a compact structure and helps in improving binding capability of the concrete matrix. Ulubeyli et al. 2016 further stated that the better hardness of marble aggregates led to improvement in abrasion resistance of concrete (Ulubeyli et al., 2016).

In order to further recommend the concrete mix to be used as tiles, BIS 1237-2012 provides the specifications with respect to the allowable depth of wear at 28 days of casting (Thomas et al., 2014). As per the IS provisions on depth of wear for different surfaces, it is recommended that for general purpose floors the depth of wear should not exceed 3.5 mm. Also, for heavy duty floors, the recommended depth of wear is 2 mm. The measured depth of wear at 28 days was 2.5 mm, 2.3 mm, 2.1 mm, 2.02 mm, 1.8 mm, 1.85 mm and 1.94 mm for M0, M10, M20, M30, M40, M50 and M60 mix, respectively. The values indicate that all the tested mixes could be used for general purpose floors; while mixes M40, M50 and M60 could even be used for heavy duty floors.

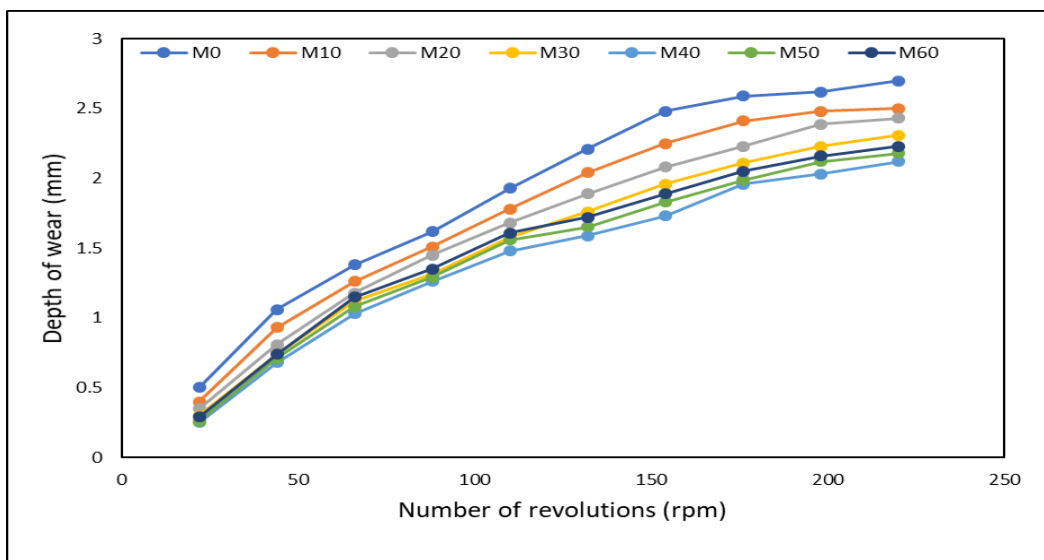


**Fig. 4.21: Progressive depth of wear versus number of revolutions for all mixes at 7 days of curing**

Figs. 4.21 to 4.24 shows the progressive increase in depth of wear with the increase in number of revolutions. It can be seen from the figures that the initial slope was higher for all mixes. It indicates that the wear was higher at initial revolutions. With the

increase in the number of revolutions, the rate of increase of depth of wear reduced. It indicates that the initial layer of concrete surface was softer and erodes at a faster rate. The erosion gets arrested once the hardened layers are reached. The similar observations regarding the progressive depth of wear was made by (Kumar and Sharma, 2014).

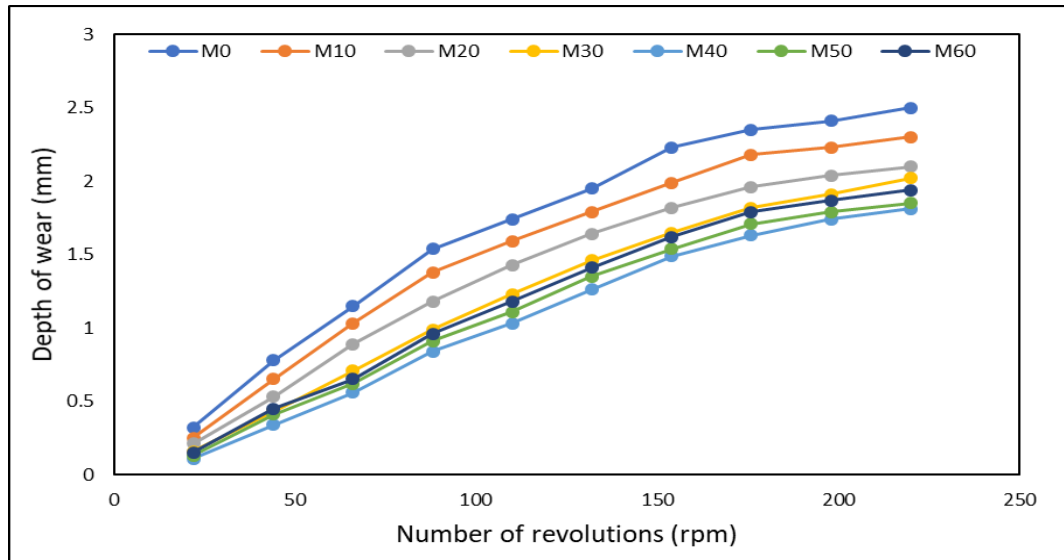


**Fig. 4.22: Progressive depth of wear versus number of revolutions for all mixes at 28 days of curing**

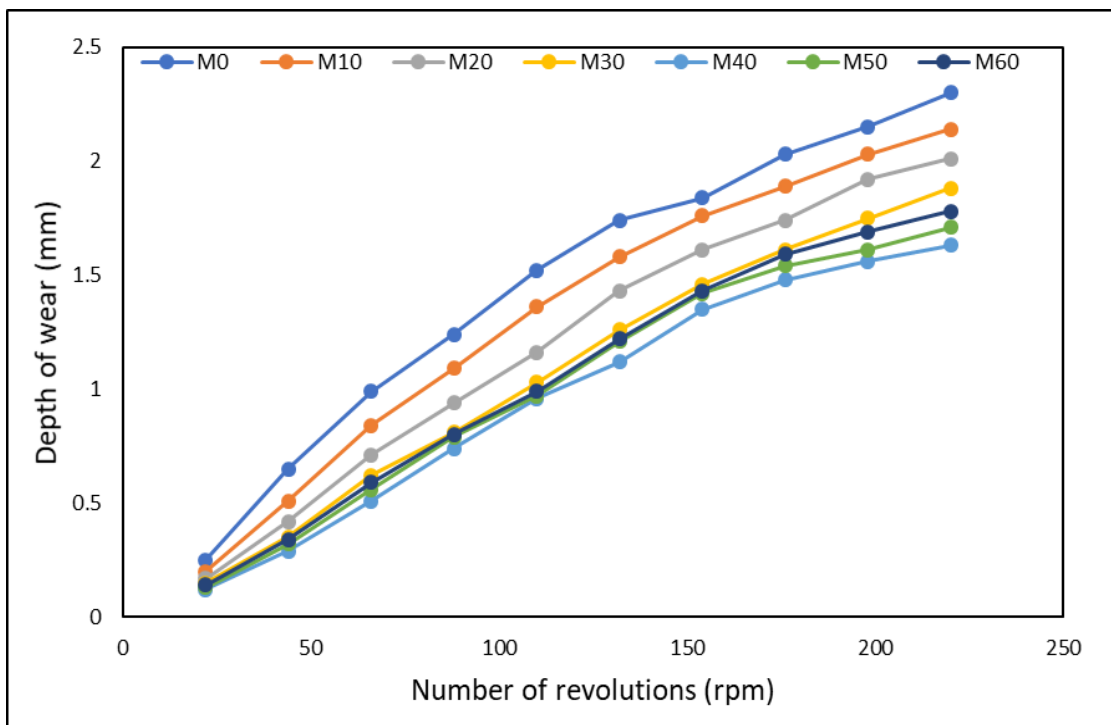


**Fig. 4.23: Progressive depth of wear versus number of revolutions for all mixes at 90 days of curing**

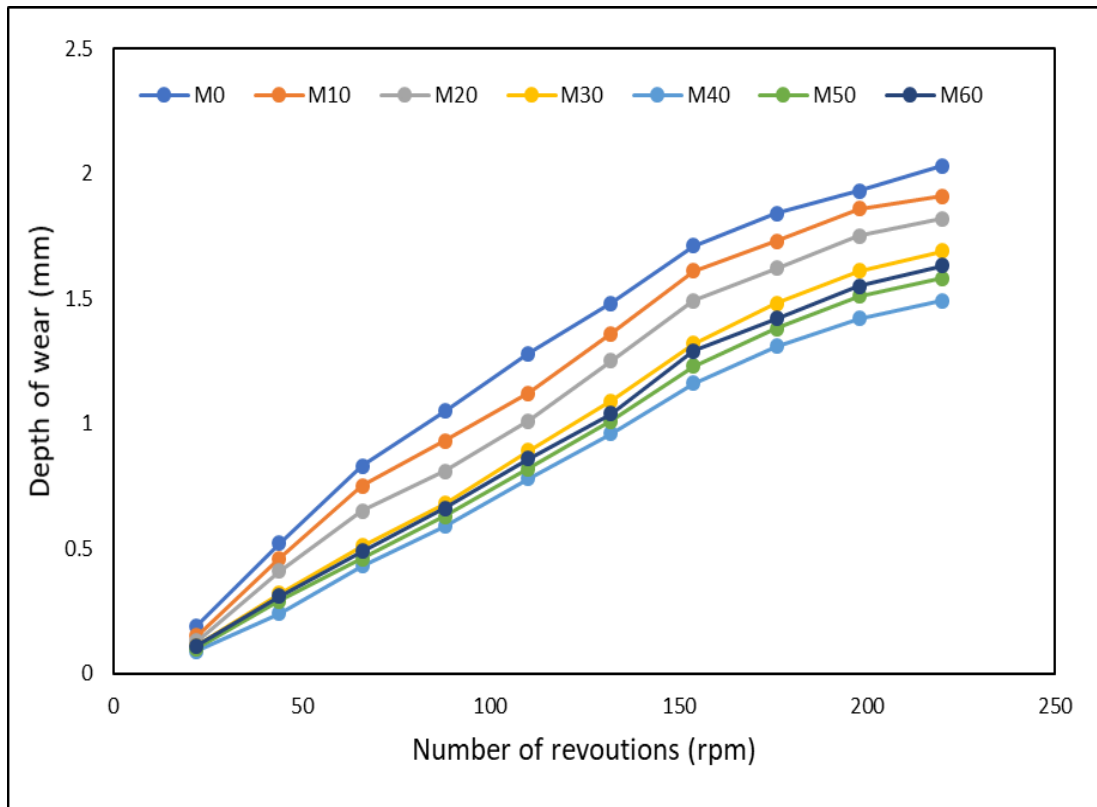


**Fig. 4.24: Progressive depth of wear versus number of revolutions for all mixes at 365 days of curing**

#### 4.9.2. Statistical Analysis of Abrasion Resistance Results

From the test results of mechanical properties and abrasion resistance of concrete, it can be observed that the abrasion resistance of concrete can be correlated with the mechanical properties of concrete. Therefore, a statistical analysis relating the abrasion resistance to mechanical properties is attempted.

Among all the mechanical properties of concrete generally tested, compressive strength is the most important factor governing other properties, including abrasion resistance of concrete (Rashad, 2013). Various regression models correlating the compressive strength with abrasion resistance have been proposed by different researchers.

Some of the researchers suggested polynomial relationship between these two properties (Ghafoori and Sukandar, 1995; Horszczaruk, 2005; Rashad, 2013). Some authors suggested a relationship between compressive strength and abrasion resistance in power format (Khatib et al., 2013; Konin and Kouadio, 2012; Naik, 2008; Siddique and Bennacer, 2012), while Topcu and Uygunoglu (2010) suggested

this relation in exponential format (Topçu and Uygunoğlu, 2010). The various relationships suggested by previous researchers for prediction of abrasion resistance based upon compressive strength results are summarized in Table 4.8.

From the table, it can be observed that most of the previous relationships were developed for conventional concrete containing fly ash as supplementary cementitious material. Most of the relations does not include the effect of type of aggregates. Apart from compressive strength other parameters like type of aggregates play a significant role in defining abrasion resistance of concrete (Li et al., 2011).

Therefore, an attempt has been made to develop a regression equation correlating compressive strength and depth of wear of concrete containing marble waste as fine aggregates. General trend of variation of compressive strength and depth of wear indicates that the depth of wear is inversely proportional to the compressive strength of the mix. The correlation between these two properties remains similar at all curing age.

Therefore, the relationship between these properties was attempted independent of the curing age. The data points corresponding to 28 days, 90 days and 365 days of curing were correlated and are presented in Fig. 4.25.

The exponential form of relationship was best suitable with the maximum regression coefficient ( $R^2$ ) of 0.88. The correlation equation (4.5) is as follows:

$$d_w = 4.49 e^{-0.02(f_c)} \quad \dots (4.5)$$

where,

$d_w$  = depth of wear (mm)

$f_c$  = compressive strength (N/mm<sup>2</sup>)

Similarly, the relationship between the depth of wear and split tensile strength was established, and is presented in Fig. 4.26 and equation 4.6 as follows. The regression coefficient of the developed equation is 0.88.

**Table 4.8: Details of existing relationship between compressive strength and abrasion resistance for conventional concrete**

| Source                       | Relationship  | Applicability  |
|------------------------------|---|--|
| Ghafoori and Sukandar (1995) | $d_w = 699 - 11670949 f_c + 67170315987 f_c^2$  | Conventional concrete with cement content ranged between 200-600 kg/m <sup>3</sup> |
| Rashad et al. (2014)         | $d_w = 0.0002 f_c^2 - 0.0223 f_c + 1.5159$  | High volume fly ash concrete   |
| Horszczaruk (2005)           | $d_w = a f_c^2 - b f_c + c$<br><i>a, b, c</i> are constant depends upon the testing duration with general range of <i>a</i> : 0.004-0.007; <i>b</i> : 0.843 -1.51; <i>c</i> : 45.126-81.649 | High strength concrete   |
| Topçu and Uygunoğlu (2010)   | $d_w = 60.47 e^{-0.0311 f_c}$   | Self-consolidating light weight concrete   |
| Siddique and Khatib (2010)   | $d_w = 40.202 f_c^{-0.8201}$  | High volume fly ash concrete   |
| Siddique et al. (2012)       | $d_w = 9.0256 f_c^{-0.5545}$  | High volume fly ash concrete   |
| Konin and Kouadio (2012)     | $d_w = 27.167 f_c^{-0.817}$   | Conventional concrete containing natural aggregates                                |
| Atiş et al. (2004)           | $d_w = -1.08 f_c + 2.75$  | Conventional concrete containing fly ash as cementitious material                  |

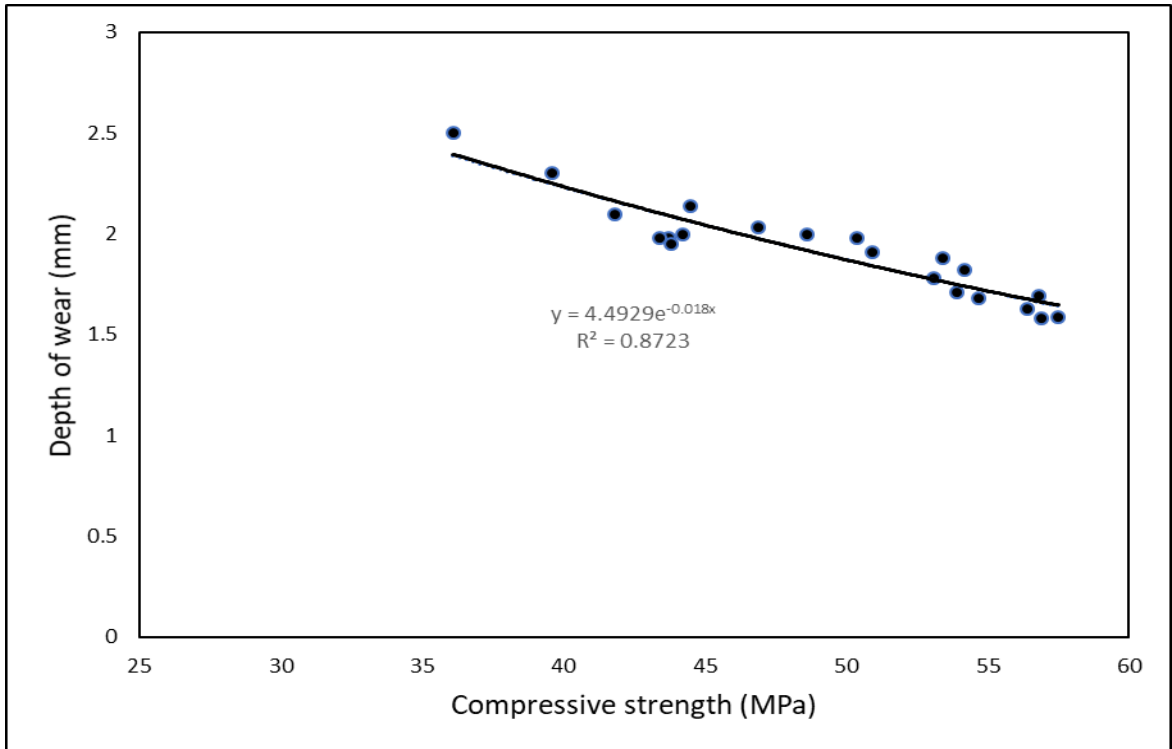


**Fig. 4.25: Relationship between depth of wear and compressive strength**

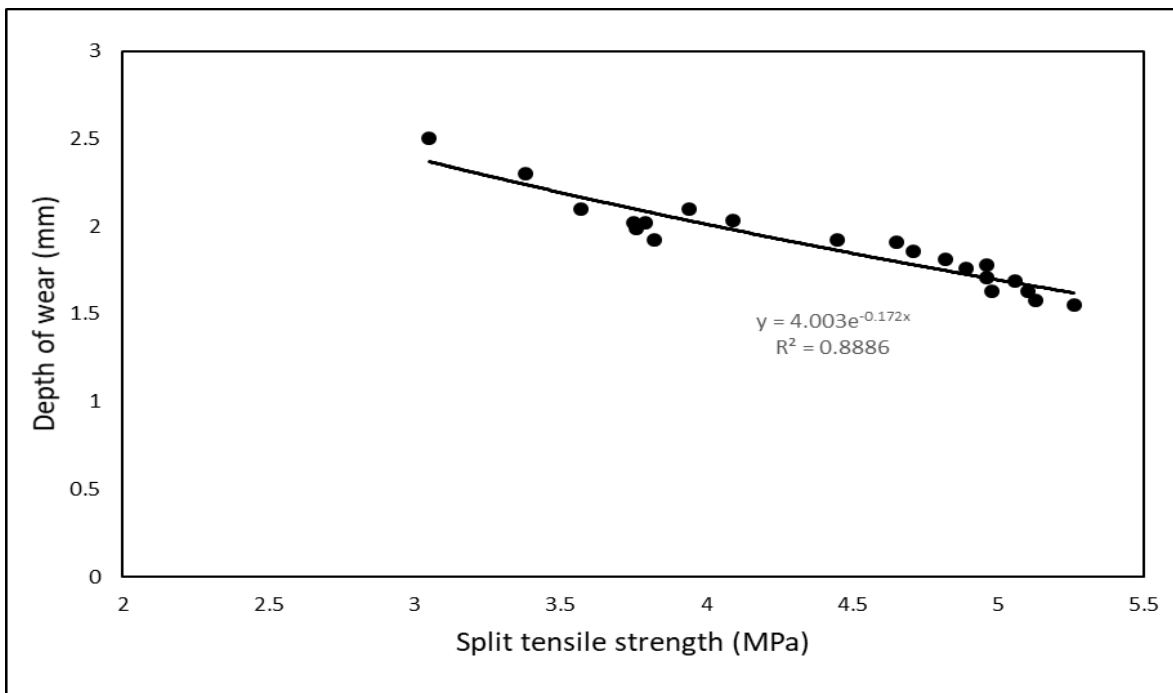


**Fig. 4.26: Relationship between depth of wear and split tensile strength**

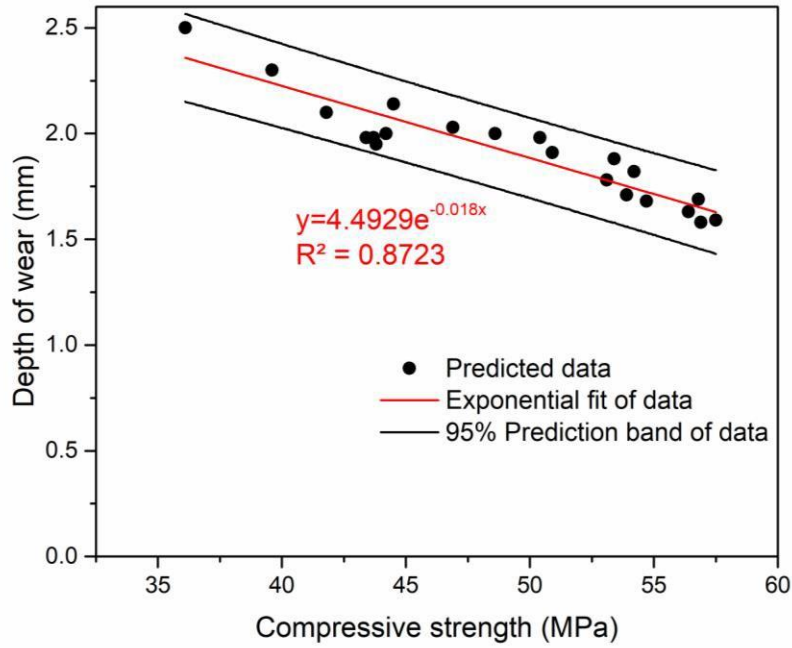


**Fig. 4.27: Comparison between observed and predicted depth of wear using developed relationship at 95% prediction band**

$$d_w = 4.0 e^{-0.017(f_{st})} \quad \dots (4.6)$$

where,

$d_w$  = depth of wear (mm)

$f_{st}$  = Split tensile strength (N/mm<sup>2</sup>)

Further, the predicted values of depth of wear based upon the above relationships was calculated and plotted in Fig. 4.27 against the experimental values. From Fig. 4.27, it can be observed that the predicted values of depth of wear are in good agreement with the experimental value at 95% prediction band.

#### 4.10 DRYING SHRINKAGE OF CONCRETE

Drying shrinkage of hardened concrete was measured as per ASTM C157-17. The unrestrained drying shrinkage test is based on monitoring the variation in length of a specimen from the moment it is taken out of mould till its length stabilizes. The unrestrained shrinkage test set-up is shown in Fig. 4.28. For drying shrinkage studies, initial comparator reading of the specimens was taken after 24 hours of casting with the help of dial gauge, by using length comparator instrument. After that, the prism

specimens were water cured for 28 days, followed by air drying for a period of 9 months in the laboratory environment, with relative humidity between 60-80%. The length comparator readings were taken at several intervals during the drying period, which were used to calculate drying shrinkage strain as per ASTM C157-17. During the first month of drying, the shrinkage strain was measured at 4, 7, 10, 14, 21 and 28 days of drying. In the subsequent months, as shrinkage slowed down, drying shrinkage readings were taken at 15 days interval and the specimens were monitored up to the drying period of 9 months.

Fig. 4.29 depicts the effect of addition of marble waste as partial replacement of natural river sand on drying shrinkage strain up to 270 days of drying period. The maximum drying shrinkage strain at 270 days of drying is referred to as ultimate drying shrinkage strain. From the figure, it can be observed that addition of marble waste reduced drying shrinkage strain of the mixes at all drying durations. The ultimate shrinkage strain of all mixes is well below  $600 \times 10^{-6}$  mm/mm, the value prescribed by ACI for concrete to be used in structural elements (ACI 224, 2001).



**Fig. 4.28: Unrestrained drying shrinkage test set-up**

#### **4.10.1. Effect of Marble waste as Fine Aggregates on Drying Shrinkage**

The maximum value of drying shrinkage was observed to be  $478 \times 10^{-6}$  mm/mm for the control mix at 270 days of drying, which reduced gradually as the percentage of

marble waste aggregates is increased. The ultimate drying shrinkage strain observed for the mix having 60% marble waste was  $332 \times 10^{-6}$  mm/mm. The ultimate shrinkage strain decreased by 7.7, 16.7, 22.0, 25.2, 27.6 and 30.5% respectively for M10, M20, M30, M40, M50 and M60 mixes, as compared to the control mix. The reduction in drying shrinkage with the addition of marble waste aggregates can be attributed to the pore refinement that occurred due to particle shape and pore size distribution of marble waste aggregates. The improvement in pore structure of concrete reduced evaporation of water through the capillary pores during drying; hence lowers the drying shrinkage. Similar observation of reduced drying shrinkage in concrete containing marble dust, with a particular physical characteristics, was made by (Gameiro et al., 2014). Khyaliya et al. (2017) also observed that the drying shrinkage of mortar mixes remained unaltered upto 50% substitution of river sand with marble powder. Further, it can be observed that the maximum improvement in drying shrinkage was observed up to 40% replacement level, thereafter the rate of decrease of drying shrinkage lowered. It can be due to the adverse effect of loss of workability on packing of concrete constituents.

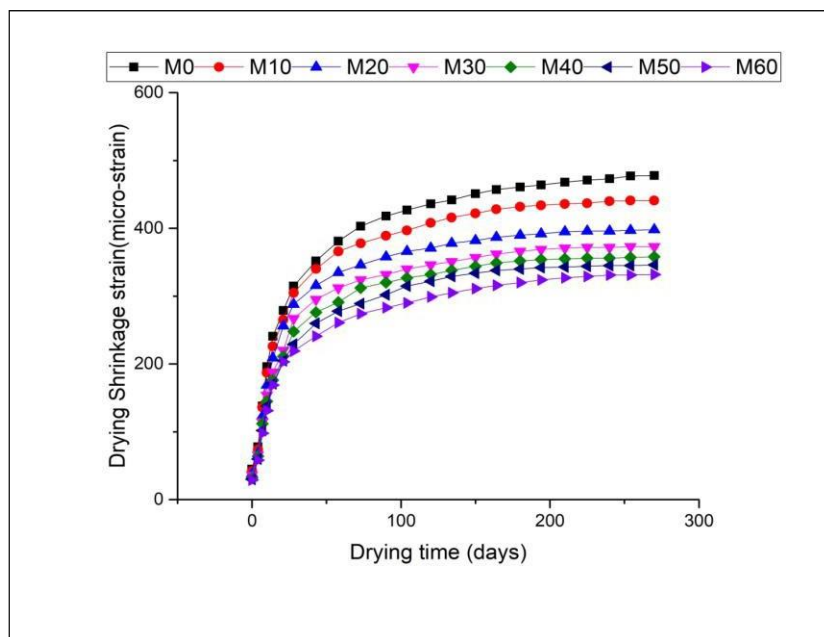


**Fig. 4.29: Shrinkage strain evolution with drying time for concrete mixes**

A close look at the shrinkage development curve plotted by using the drying shrinkage test results of a mix indicate that the shrinkage development curve consists of two phases; shrinkage occurred at faster rate during the first phase, followed by a

second phase where the shrinkage rate slowed down. These two phases could be observed for all mixes.

The demarcation between the two phases was made by calculating the days when the shrinkage of the mix reached half of the ultimate shrinkage strain value. The shrinkage-half time of all the mixes is presented in Table 4.9 and it was observed to be nearly equal to 14 days for all mixes.

Therefore, time up to 14 days of drying was taken as first phase of shrinkage in which almost 50% of ultimate shrinkage took place. Further, average rate of shrinkage was calculated in the first phase, and is presented in Table 4.9 for all mixes. It can be seen from the table, that the shrinkage rate was maximum for the control mix. The shrinkage rate decreased with the increase in percentage of marble waste aggregates.

However, the shrinkage rate was found to be nearly same for mixes having 40, 50 and 60% of marble waste as replacement of natural river sand. Lower rate of shrinkage by using marble waste aggregates indicates that the tensile stresses will take greater time to develop in the mixes incorporating marble waste aggregates, hence reducing the chances of development of drying shrinkage cracks in these mixes.

**Table 4.9: Ultimate shrinkage strain, shrinkage half-time and shrinkage rate of concrete mixes**

| <b>Mix</b> | <b>Ultimate shrinkage strain<br/>(<math>\mu</math>-mm/mm)</b> | <b>Shrinkage half-time<br/>(days)</b> | <b>Shrinkage rate in<br/>first phase</b> |
|------------|---|---------------------------------------|--|
| M0         | 478   | 13.8                                  | 17.21                                    |
| M10        | 441   | 13.4                                  | 16.14                                    |
| M20        | 398   | 13.6                                  | 14.92                                    |
| M30        | 373   | 13.8                                  | 13.43                                    |
| M40        | 358   | 14.0                                  | 12.57                                    |
| M50        | 346   | 14.1                                  | 12.21                                    |
| M60        | 332   | 14.1                                  | 12.07                                    |

#### **4.10.2. Shrinkage Strain Prediction Model**

*Existing Prediction models:*

Shrinkage of concrete is an important parameter that may affect the long-term performance of a structure. It is a complex phenomenon involving different factors related to the proportions and properties of constituent materials, environmental factors etc. (Shariq et al., 2016).

Many models have been proposed by various researchers to predict drying shrinkage strain of ordinary Portland cement concrete. Some of the models, which are easy to apply for the prediction of shrinkage strain are:

1. ACI-209 Model (ACI Committee 209, 2005; Mokarem et al., 2005)
2. Bazant B3 Model (Bazant and Baweja, 1995; Mokarem et al., 2005)
3. CEB-FIB Model (Khay et al., 2010; Mokarem et al., 2005; Shariq et al., 2016)
4. Gardner/ Lockman Model (Gardner and Lockman, 2001; Mokarem et al., 2005)

The details of the models, along with the conditions of applicability, are presented in Table 4.10. As can be seen, the models are applicable only for ordinary cement concrete using conventional materials. A comparison of the observed shrinkage strain with the easily accessible and well recognized models (ACI 209 model and Bazant B3 model) was attempted and is presented in Fig. 4.30. The solid lines in the figure were drawn corresponding to the values obtained for the control mix. However, the curves will not vary much because the variable corresponding to percentage replacement of fine aggregates is not considered in ACI 209 model and Bazant B3 model.

From the figure, it can be concluded that the existing well-established models for normal concrete using conventional materials did not fit well for the concrete using marble waste as fine aggregates. It indicates that the shrinkage model must incorporate a parameter based on percentage of marble waste aggregates used in the mix, along with the parameter of compressive strength and days of curing.

**Table 4.10: Details of shrinkage prediction models used for conventional concrete**

| <b>Prediction model</b>   | <b>Model description</b>  | <b>Range of applicability</b>   |
|---|---|---|
| ACI-209 Model<br>(ACI Committee 209, 2005;<br>Mokarem et al., 2005)   | $\varepsilon_{sh}(t) = \frac{(t - t_{sh,0})}{35 + (t - t_{sh,0})^{sh\infty}} \varepsilon_{sh\infty}$ <p>Where</p> <p><math>\varepsilon_{sh}(t)</math> : shrinkage strain at time t</p> <p><math>t_{sh,0}</math> : time at start of drying (days)</p> <p><math>\varepsilon_{sh\infty}</math> : ultimate shrinkage strain (in/in)</p> <p>t: time (days)</p>   | <ul style="list-style-type: none"> <li>• Type I and Type III cement, having cement content in the range of 280 to 445 kg/m<sup>3</sup>.</li> <li>• Predict shrinkage strain of normal and light weight concrete</li> <li>• Moist and steam curing conditions</li> <li>• Slump: 70mm</li> <li>• Air content: &lt;6%</li> </ul> |
| Bazant B3 Model<br>(Bazant and Baweja, 1995;<br>Mokarem et al., 2005) | $\varepsilon_{sh}(t) = -\varepsilon_{sh\infty} K_h S(t)$ $\varepsilon_{sh\infty} = \alpha_1 \alpha_2 \left[ 26(w)^{2.1} (f'_c)^{-0.28} + 270 \right]$ $K_h = 1 - h^3$ $S(t) = \tanh \sqrt{\frac{t - t_{sh,0}}{T_{sh}}}$ <p>Where</p> <p><math>\varepsilon_{sh}(t)</math> : Shrinkage strain at time t (in/in)</p> <p><math>\varepsilon_{sh\infty}</math> : ultimate shrinkage strain (in/in)</p> <p>w: water content (lb/ft<sup>3</sup>)</p> <p><math>K_h</math>: cross-section shape factor</p> <p>h: relative humidity (%)</p> <p>t : age of concrete (days)</p> <p><math>t_0</math>: age of concrete at beginning of shrinkage</p> <p><math>S(t)</math>: time function for shrinkage</p> | <ul style="list-style-type: none"> <li>• Concrete having 28 days cylinder strength (<math>f'_c</math>) in the range of 17 to 70 MPa</li> <li>• Cement content in the range of 160 to 720 kg/m<sup>3</sup>.</li> <li>• Water-cement ratio: 0.30 to 0.85</li> <li>• Aggregate-cement ratio: 2.5 to 13.5</li> </ul>              |

|   |  |  |
|---|--|--|
| <p>CEB - FIB Model<br/>(Khay et al., 2010; Mokarem et al., 2005; Shariq et al., 2016)</p> | $\varepsilon_{sh} = \varepsilon_s(f_{cm})(\beta_{RH})$ $\varepsilon_s(f_{cm}) = 160 + 10\beta_{sc}(9 - f_{cm}/1450)$ $\beta_{RH} = -1.55\beta_{ARH}$ $\beta_{ARH} = 1 - (RH/100)^3$ <p style="text-align: right;">Where</p> <p><math>\varepsilon_{cso}</math> : drying shrinkage of Portland cement concrete</p> <p><math>\varepsilon_s</math> : drying shrinkage obtained from RH-shrinkage chart</p> <p><math>f_{cm}</math>: 28-days compressive strength (psi)</p> <p><math>\beta_{sc}</math> : coefficient based upon type of cement</p> <p><math>\beta_{RH}</math> : coefficient based on relative humidity</p> | <ul style="list-style-type: none"> <li>• Ordinary concrete having 28 days cylinder strength in the range of 12 to 80 MPa</li> <li>• Cured at mean relative humidity of 40 to 100%</li> <li>• Cured at mean temperature of 5 to 30°C</li> </ul> |
| <p>Gardner/Lockman Model<br/>(Gardner and Lockman, 2001; Mokarem et al., 2005)</p>        | $\varepsilon_{sh} = \varepsilon_{shu}\beta(h)\beta(t)$ $\varepsilon_{shu} = 1000k \sqrt{\frac{4350}{f'_{cm28}}} 10^{-6}$ $\beta(h) = 1 - 1.18h^4$ $\beta(t) = \left[ \frac{(t - t_{sh,0})}{(t - t_{sh,0}) + 97(V/S)^{0.5}} \right] 10^{-6}$ <p>Where</p> <p><math>\varepsilon_{shu}</math> : ultimate shrinkage strain (in/in)</p> <p><math>\beta(h)</math>: correction factor for humidity</p> <p><math>\beta(t)</math>: correction factor for time</p> <p><math>t_c</math>: drying age commenced (days)</p> <p><math>t</math>: age of concrete (days)</p>  | <ul style="list-style-type: none"> <li>• Plain cement concrete having maximum 28-day compressive strength of 70 MPa.</li> <li>• Water-cement ratio: 0.4 to 0.6</li> </ul>  |

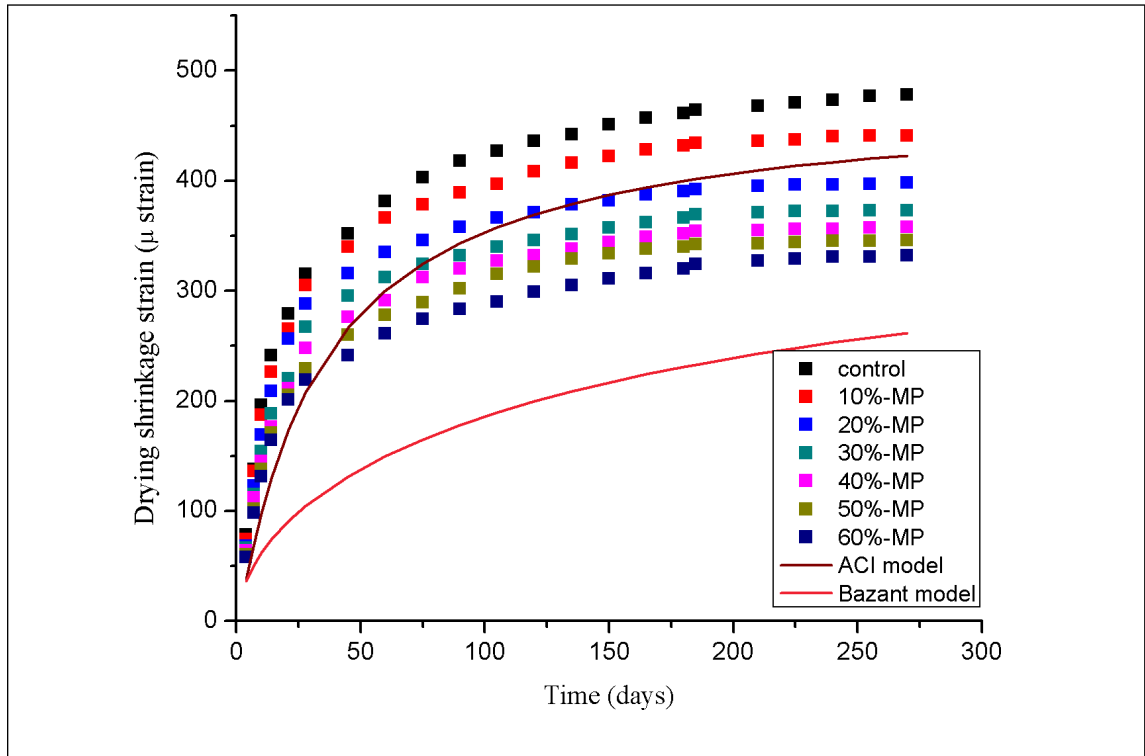


**Fig. 4.30: Comparison between observed shrinkage data with established prediction model**

***Multi-regression model for shrinkage prediction***

A multiple variable regression model was developed accounting for the effect of marble waste aggregate content, 28-day compressive strength of concrete and drying time on drying shrinkage strain of concrete. The model is developed with percentage of marble waste varying from 10 to 60% of fine aggregates and drying time up to 270 days. The proposed model is:

$$\epsilon_{sh} = \frac{1950 \left( \frac{t}{15+t} \right)^{1.1}}{(1+n)^{0.7} (f_c)^{0.86}} \quad \dots (4.7)$$

where,

$\epsilon_{sh}$  = shrinkage strain at time t (micro-strain);

$f_c$  = 28-day compressive strength (MPa) of the mix

$p$  = proportion of marble waste used as fine aggregate in concrete

$t$  = drying time (days)

Fig. 4.31 gives a comparative graph between the experimental shrinkage strain of concrete containing marble waste as fine aggregates and shrinkage strain predicted as per the regression model suggested in equation 4.7. The figure clearly indicates that the values obtained by using developed models are able to predict the drying shrinkage of mixes incorporating marble waste aggregates with a great accuracy. The predicted curve fitted well with a  $R^2$  value of 0.994. The results indicate the reliability of the proposed model to evaluate shrinkage strain of the mixes incorporating variable percentages of marble waste as fine aggregates. It further suggests that an additional parameter based on the proportion of marble waste used as fine aggregates should be adopted in the existing models to predict drying shrinkage of such mixes accurately.

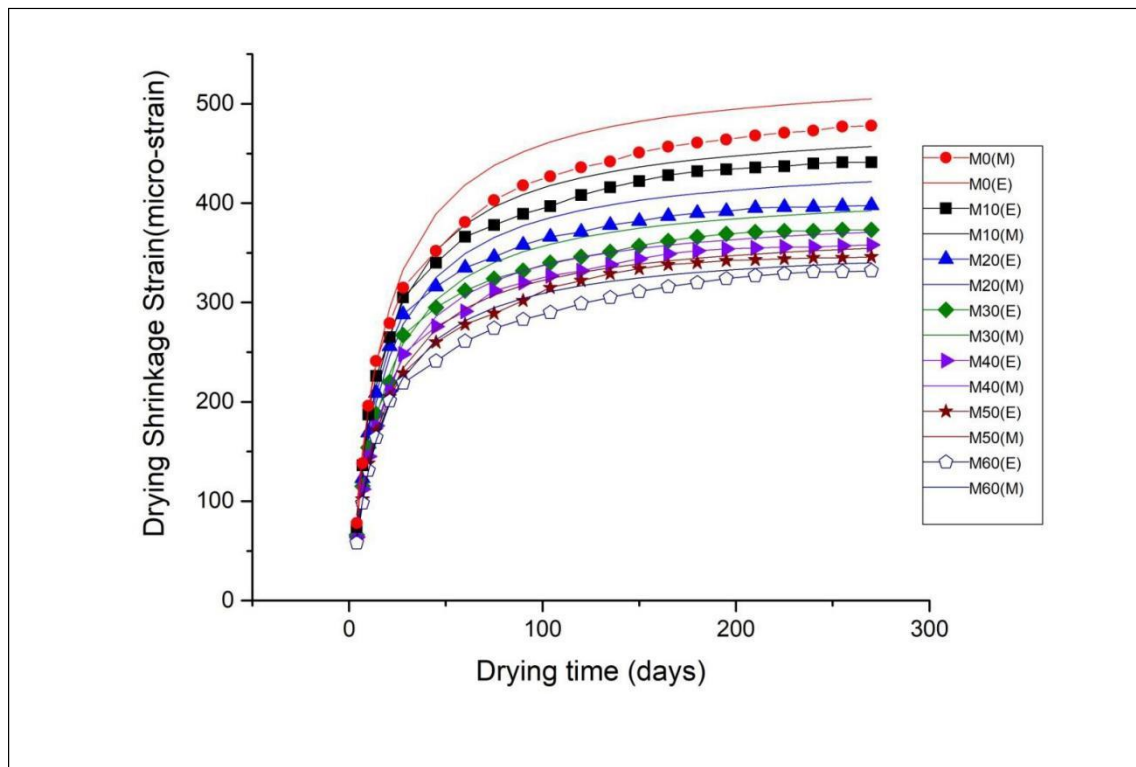


**Fig. 4.31: Comparison of shrinkage strain prediction by proposed model with experimental data**

The efficiency of the proposed model was further investigated by performing residual error percentage analysis. Residual error percentage is calculated as follows (Mokarem et al., 2005):

$$\text{Residual Error (\%)} = \frac{\text{Predicted shrinkage strain} - \text{Experimental shrinkage strain}}{\text{Experimental shrinkage strain}} \times 100 \quad \dots(4.8)$$

**Table 4.11: Residual error for mixes with marble waste as fine aggregates**

| Drying time (Days) | Residual error (%) |       |       |       |       |       |
|--------------------|--------------------|-------|-------|-------|-------|-------|
|                    | M10                | M20   | M30   | M40   | M50   | M60   |
| 7                  | 13.90              | 9.29  | -10.7 | 7.19  | 8.70  | 7.78  |
| 14                 | -1.98              | -0.80 | -5.2  | -3.12 | 1.13  | 0.89  |
| 28                 | -8.09              | -4.50 | -4.4  | -3.53 | -3.63 | -2.70 |
| 45                 | -6.30              | -3.61 | -5.2  | -2.07 | -4.18 | -4.24 |
| 60                 | -1.41              | 1.62  | -5.3  | 0.77  | -1.39 | -3.60 |
| 75                 | -3.22              | -5.39 | -6.4  | -3.13 | -0.26 | -0.03 |
| 90                 | 1.56               | 0.17  | -3.1  | 1.83  | 2.77  | 6.27  |
| 105                | 1.36               | 1.75  | -1.2  | 3.75  | 3.25  | 5.41  |
| 120                | 2.69               | 2.52  | -1.7  | 1.26  | 3.93  | 5.07  |
| 135                | 2.95               | 3.23  | -3.5  | 1.86  | 2.61  | 4.96  |
| 150                | 3.08               | 3.00  | -2.6  | 1.85  | 0.52  | 4.65  |
| 165                | 2.20               | 3.13  | -2.8  | 2.22  | 0.20  | 3.43  |
| 180                | 1.63               | 3.07  | -1.8  | 1.80  | -0.57 | 2.80  |
| 195                | 1.31               | 2.48  | -1.3  | 1.15  | -0.96 | 1.95  |
| 210                | 0.81               | 2.00  | -2.2  | 0.62  | -1.22 | 1.27  |
| 225                | 0.65               | 1.67  | -1.5  | 0.54  | -1.04 | 0.78  |
| 240                | 0.85               | 1.51  | -1.2  | 0.63  | -0.97 | 0.19  |
| 255                | 0.96               | 1.53  | -0.9  | 0.92  | -0.70 | -0.16 |
| 270                | 1.23               | 1.76  | -0.9  | 1.14  | -0.49 | -0.28 |

The sign of residual error indicates the ability of model to under estimate or overestimate shrinkage. Negative value of residual error strain indicates that model under estimates shrinkage, while positive residual error corresponds to over estimation of shrinkage strain. The corresponding number indicates the percentage by which model under estimates/overestimates drying shrinkage strain. From the table, it was observed that the higher residual error occurs during early drying age. With the

increase in drying time, the residual error decreases to a very small value. The percentage error for the prediction of long-term shrinkage strain by the developed model is reduced to nearly 2%. It can therefore be concluded that the proposed model can be used to evaluate shrinkage strain of concrete mixes containing marble waste with reasonable accuracy.

#### **4.11. ACID ATTACK**

The performance of prepared mixes containing marble waste as fine aggregate replacement was investigated when the samples are exposed to 3% of sulphuric acid solution as per ASTM C267-01. The observations were made in terms of visual observation, mass loss, compressive strength loss and microstructural analysis of concrete specimens after 180 days of aggressive exposure. The test results are discussed in the following sections:

##### **4.11.1. Visual Observations**

The specimens were visually examined at the end of exposure duration to record change in the appearance of the surface on exposure to sulphuric acid. It can be observed from Fig. 4.32 that among all the samples, the surface of control mix containing river sand was severely damaged and was highly rough. The surface had lost fine aggregates and cement hydration products. On the other hand, the specimens with marble waste had less damaged surface. The surface of these specimens was less rough, with some white patches, which can be due to the formation of gypsum (Bassuoni and Nehdi, 2007; Beddoe and Dorner, 2005; Torii and Kawamura, 1994). It clearly indicates that the incorporation of marble waste helped in restricting the damage caused by the aggressive sulphuric acid solution.



M0



M10



M20



M30



M40



M50



M60

**Fig. 4.32: Visual appearance of concrete cubes after 180 days of sulphuric acid exposure**

#### 4.11.2. Weight Loss

The weight of each specimen was noted at regular intervals and was compared with the initial weight before immersing the specimens in aggressive media. Fig. 4.33 shows the trend of weight loss as a function of time. It can be observed from the figure that there is an initial increase in weight of all specimens, followed by loss of weight with the progress in immersion time. The control mix gained weight up to 14 days of acidic exposure, followed by an abrupt decrease in weight thereafter. The specimens with marble waste recorded increase in weight for variable durations ranging from 7 to 28 days of immersion. The final weight loss of all the specimens is 30.56%, 27.3%, 23.46%, 19.4%, 13.5%, 12.03% and 10.01% respectively, for the mixes containing 0%, 10%, 20%, 30%, 40%, 50% and 60% marble waste.

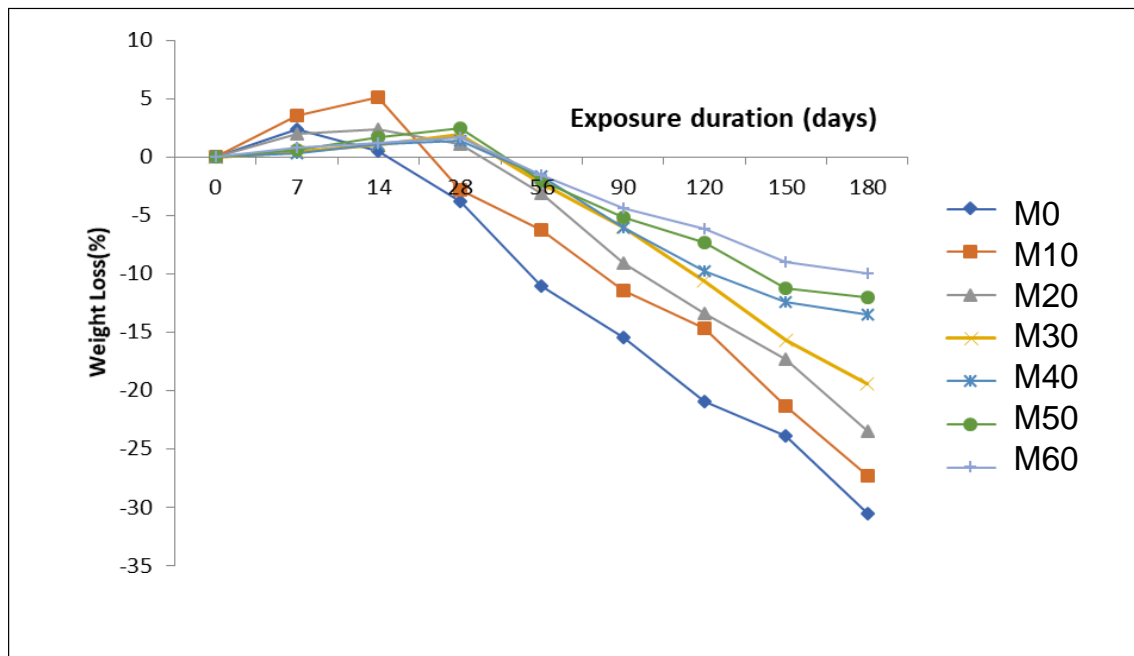


**Fig. 4.33: Weight loss of all the mixes subjected to sulphuric acid exposure**

The initial increase in weight is attributed to the formation of gypsum, which gets deposited in the pores of concrete matrix. The observation regarding initial increase in weight was also made by (Khyaliya et al., 2017; Mehta and Siddique, 2017; Zhuang et al., 2016). Actually, the solubility of gypsum is very low (0.22 grams of gypsum gets dissolved in 100 gram of water at 0° Celsius (Pavlík, 1994; Zivica and Bajza, 2001)). Due to low solubility, it occupies the space available in the voids of concrete matrix. However, with the increase in duration of exposure, gypsum gets further converted into ettringite. Both gypsum and ettringite are voluminous in nature, which

lead to development of tensile stresses in concrete, thereby leading to softening of outer surface and spalling of surface concrete (Chatveera and Lertwattanak, 2014; Girardi and Maggio, 2011).

Another factor that can lead to decrease in weight is leaching out of acid susceptible constituents of concrete, mainly calcium hydroxide, from the cement paste of hardened concrete (Nijland and Larbi, 2010). This action results in an increase in capillary porosity, loss of cohesiveness and eventually loss of strength. Therefore, both the chemical changes and leaching out of portlandite led to decrease in weight of the specimens.

It is clear from the test results that replacing river sand with marble waste makes the concrete less fragile, decreases the spalling of concrete surface and reduces the damage caused by aggressive sulphuric acid media.

#### **4.11.3. Compressive Strength Loss**

Compressive strength loss of all the mixes are presented in Fig. 4.34. As can be seen from the figure, there is a small increase in compressive strength during the initial immersion time ranging from 7 days to 28 days of exposure for all mixes, followed by the decrease in strength. The slope of strength loss increased with the increase in immersion period. However, the mixes with marble waste registered lesser compressive strength loss. The final strength loss of all the mixes were 36.79%, 32.42%, 25.33%, 15.74%, 12.76%, 9.66% and 7.81%, respectively, for the mixes containing 0%, 10%, 20%, 30%, 40%, 50% and 60% marble waste.

The surface of these specimens was less rough, with some white patches, which can be due to the formation of gypsum (Bassuoni and Nehdi, 2007; Beddoe and Dorner, 2005; Torii and Kawamura, 1994). It clearly indicates that the incorporation of marble waste helped in restricting the damage caused by the aggressive sulphuric acid solution. The surface of these specimens was less rough, with some white patches, which can be due to the formation of gypsum (Bassuoni and Nehdi, 2007; Beddoe and Dorner, 2005; Torii and Kawamura, 1994). It clearly indicates that the incorporation of marble waste helped in restricting the damage caused by the aggressive sulphuric acid solution.

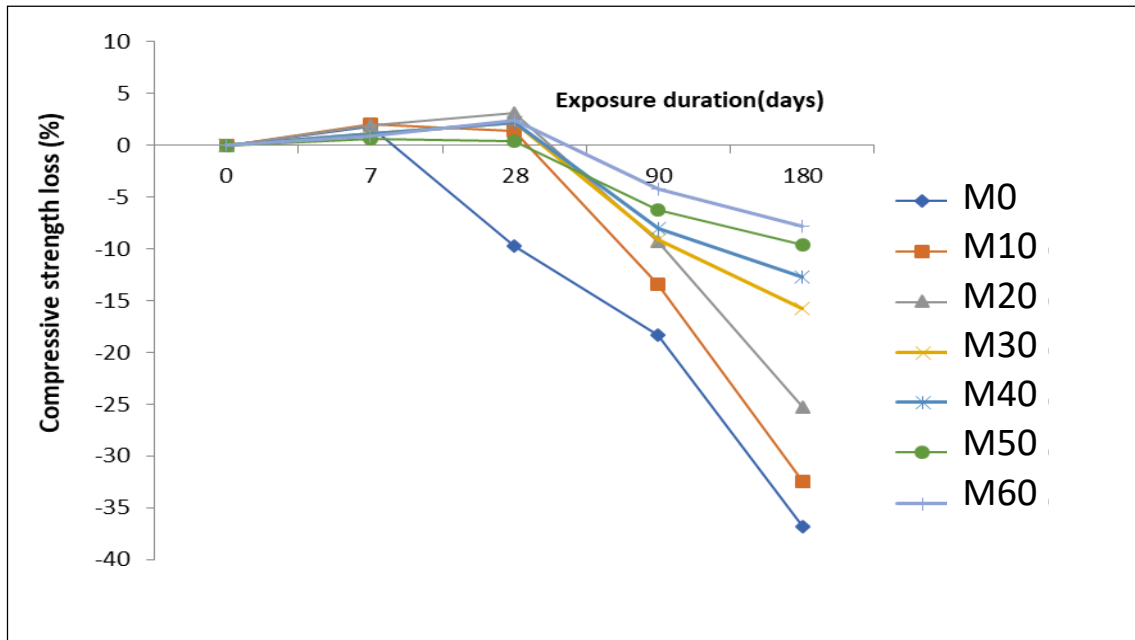


**Fig. 4.34: Compressive strength loss of all the mixes subjected to sulphuric acid exposure**

The acid soluble fraction of the marble waste used in the present study is found to be as high as 99%. Due to highly dissolvable carbonates present in marble waste, it will not allow the carbonates of cement compounds to dissolve initially. Therefore, in mixes containing marble waste, calcium carbonate present in marble waste reacts with sulphuric acid and helps in alleviating the cement hydration products from participating in the reaction at the first stage. Due to this, local neutralization of acid takes place and the acid required for attacking binder is decreased. The chemical equation of the reaction between marble waste and sulphuric acid is:



*(Calcareous Marble)*      *(Sulphuric Acid)*   *(Water)*                      *(Gypsum)*      *(Carbon Dioxide)*

The resulting sacrificial and neutralizing effect of marble waste reduces the local concentration of acid and hence arrests the damage caused by acid on concrete. The similar observations regarding the sacrificial behaviour of limestone aggregates is made by (Boubekeur et al., 2019; Chang et al., 2005; Samimi et al., 2018).

**Table 4.12: Acid solubility fraction of materials used in the study**

| Material       | Acid soluble fraction |
|----------------|-----------------------|
| OPC            | 99.6%                 |
| River sand     | 3.21%                 |
| Marble waste   | 99.9%                 |
| Crushed gravel | 0.2%                  |

#### 4.11.4: Microstructural Investigations

XRD analysis of all the mixes after 180 days of sulphuric acid exposure has been shown in Fig 4.35. Major phases present in XRD spectra at  $2\theta$  were calcium hydroxide ( $\text{Ca(OH)}_2$ )  $34.1^\circ$ , quartz ( $\text{SiO}_2$ ) at  $20.85^\circ$ ,  $26.65^\circ$ ,  $50.14^\circ$ , gypsum at  $31.1^\circ$  and  $43.4^\circ$ , ettringite at  $36.5^\circ$  and calcium carbonate ( $\text{CaCO}_3$ ) at  $43.15^\circ$ .

The phase composition showed same phases for all the mixes. However, mixes containing marble waste showed prominent peaks at  $2\theta$  pertaining to gypsum at  $31.1^\circ$  and  $43.4^\circ$  and of  $\text{CaCO}_3$  at  $43.15^\circ$ . As the percentage of marble waste is increased in the mix, greater formation of gypsum is observed from higher intensity of the peaks in the respective spectra. A careful examination of XRD peaks indicate that the peaks of both gypsum and portlandite are higher in the mixes incorporating marble waste.

It clearly indicates that gypsum was formed but portlandite is not consumed. It is possible only due to reaction of marble waste with sulphuric acid, thereby allowing portlandite and other cement hydration products to remain intact even after severe acid exposure. The peaks of calcium carbonate are also seen but they have very low intensity, indicating that calcium carbonate is consumed in reaction with sulphuric acid.

SEM-EDS analysis of various mixes after acid exposure of 180 days has been shown in Fig. 4.36. The microstructure of all the mixes has been observed to be deteriorated due to acid attack. The morphology of the mixes indicated presence of  $\text{Ca(OH)}_2$  (identified by flat crystals), cotton shaped CSH gel, gypsum (prismatic shape crystals) and ettringite (needle like crystals). EDS shows major peaks of Ca, S, Si and Al. The presence of Ca and S peaks in the EDS confirms the formation of gypsum on acid

attack. Mixes containing higher content of marble dust showed greater formation of gypsum as was observed in XRD spectra. Higher content of marble waste (M50 and M60) provides more content of  $\text{CaCO}_3$  to react upon acid attack, hence more formation of gypsum is observed in these mixes.

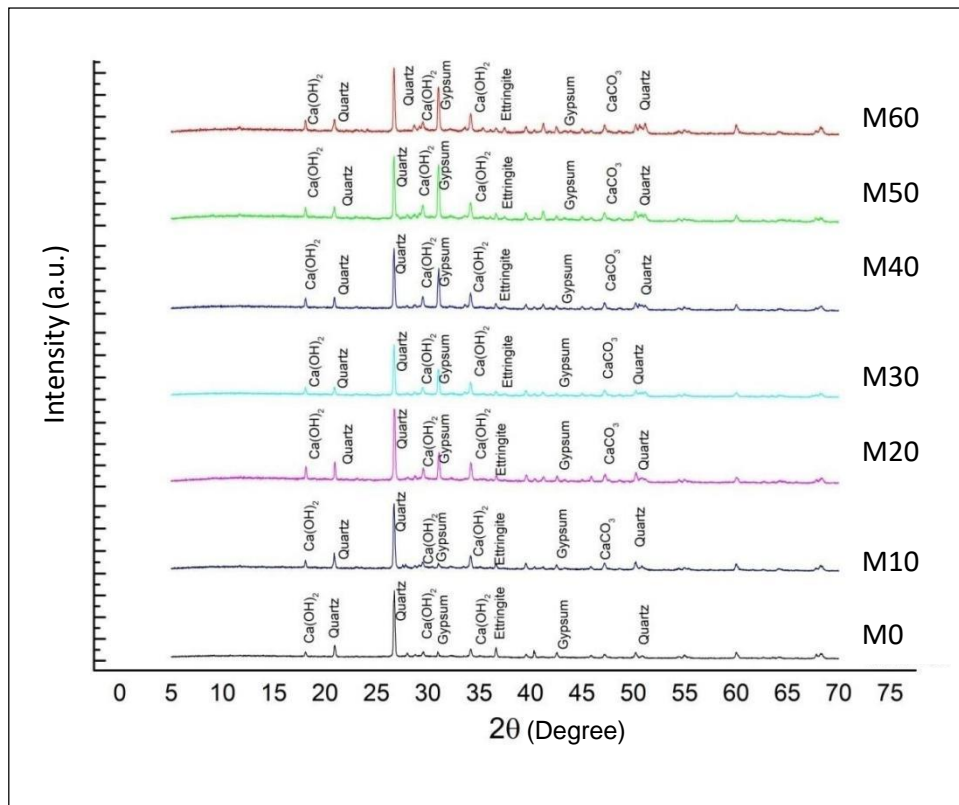
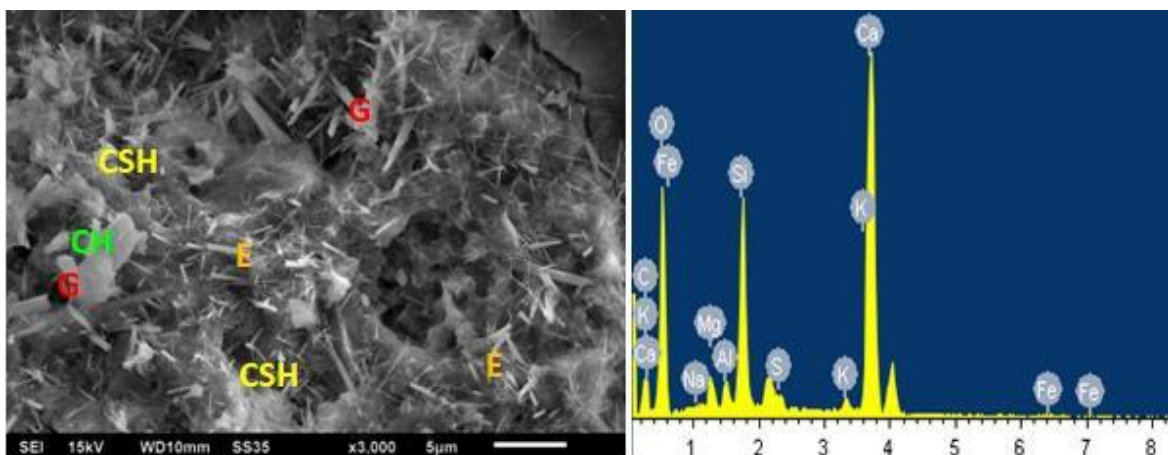
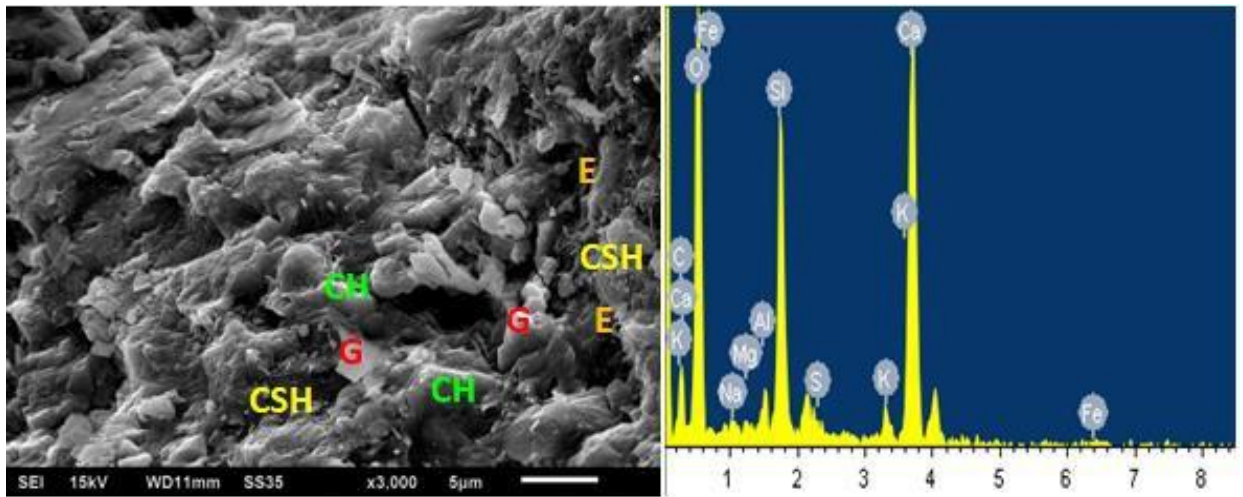


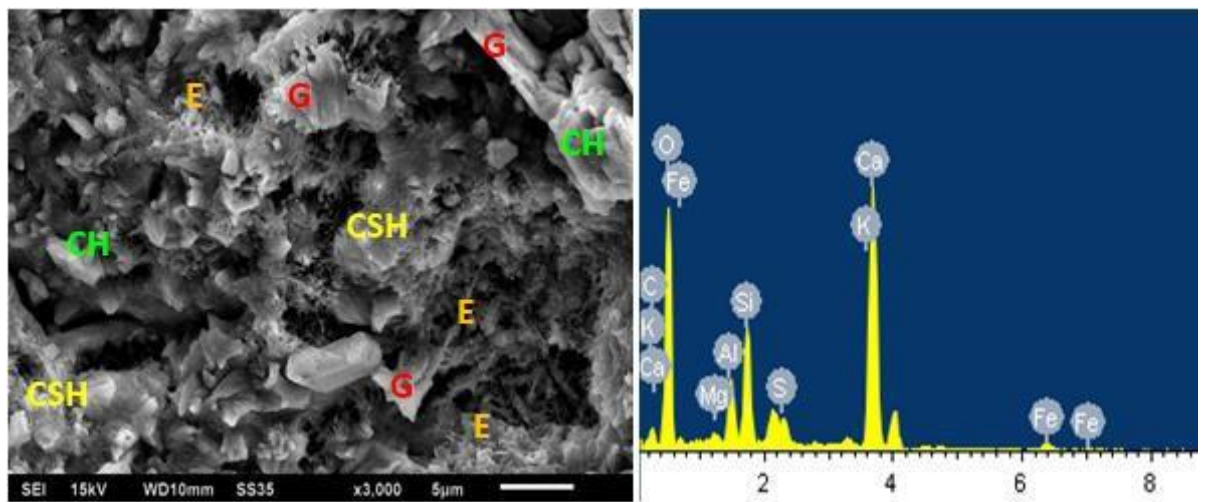
**Fig. 4.35: XRD patterns of mixes upon exposure to sulphuric acid solution for 180 days**



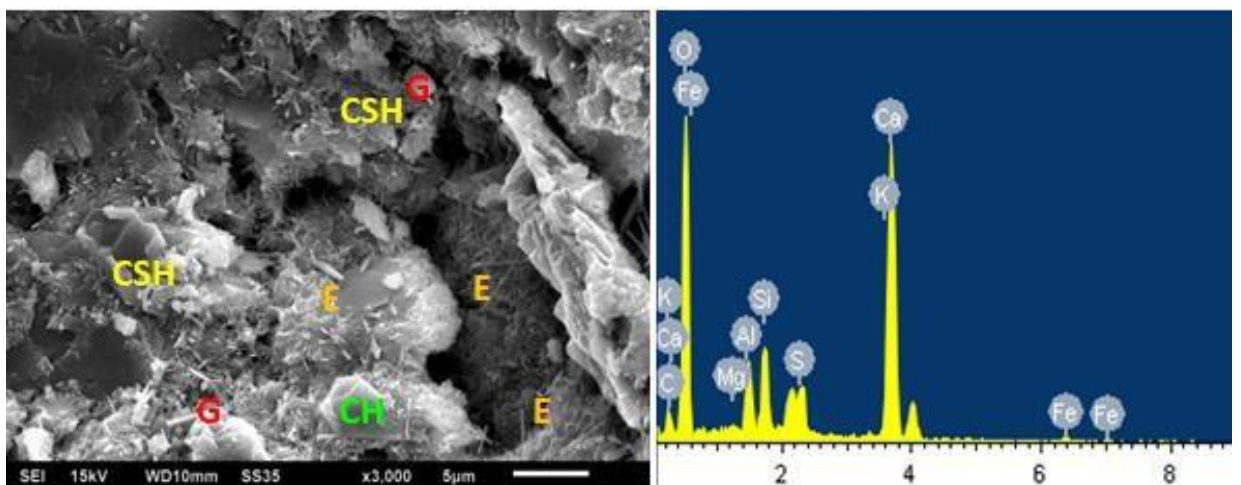
M0



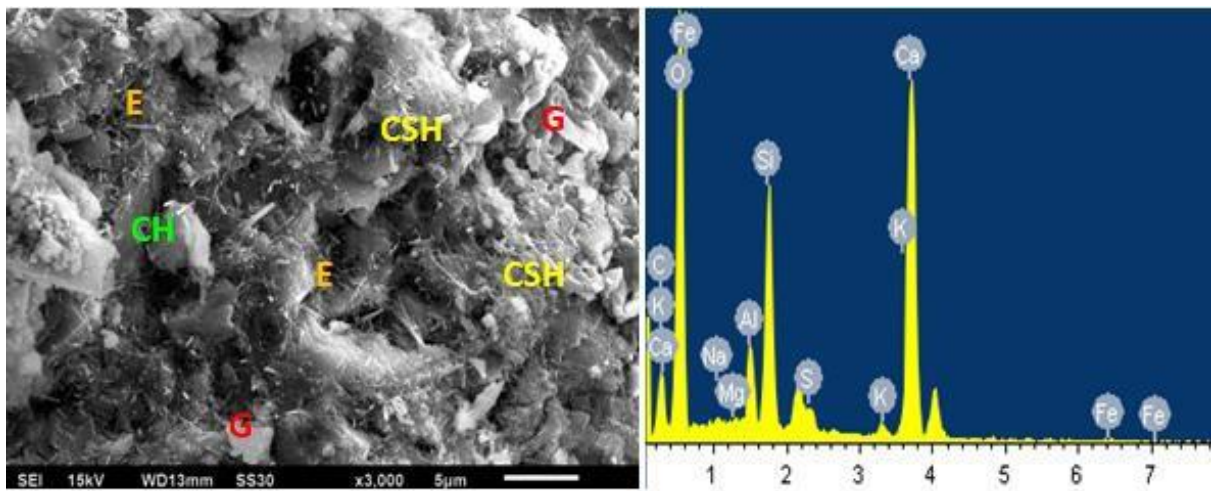
M10



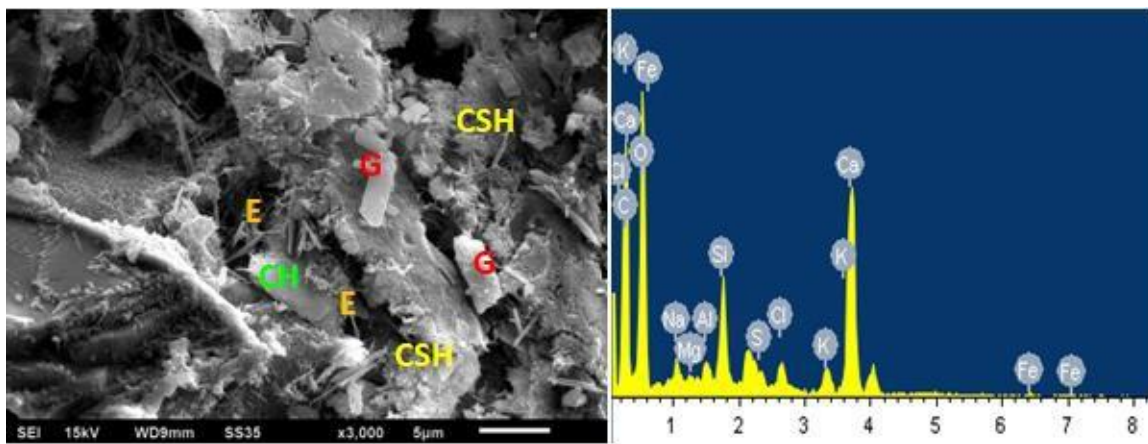
M20



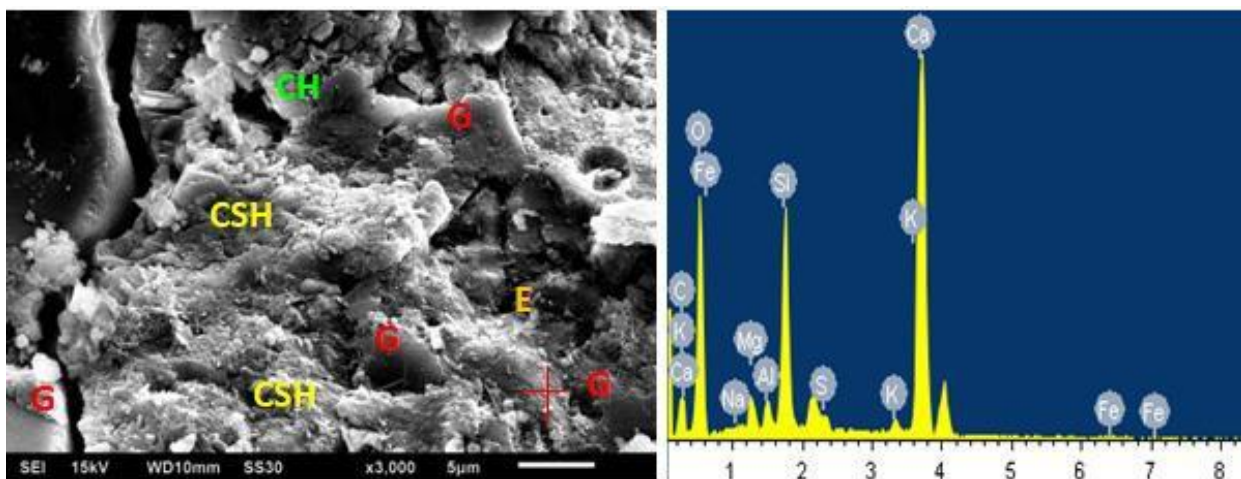
M30



M40



M50



M60

**Fig. 4.36: SEM images and EDS analysis of concrete mixes after exposure to sulphuric acid solution for 180 days**

## 4.12. SODIUM SULFATE EXPOSURE

The sulphate exposure to concrete is one of the major durability concerns. In the present study, all seven concrete mixes were exposed to 5% sodium sulphate salt as per ASTM C1012-10 in order to investigate their performance in the presence of sulphate ions. The test methods employed for judging performance of mixes included visual observations, weight loss measurements, compressive strength loss measurements, length change and microstructural analysis by SEM and XRD. The following sections deal with the results and discussions on the changes in various parameters after sodium sulphate exposure:

### 4.12.1. Visual Observations

Before subjecting the specimens to destructive compressive strength tests, the surface of specimens was carefully examined to observe significant changes on the surface; such as extra deposition, cracks, change in colour and the level of deterioration. The deterioration of the surface was further categorized based on the deterioration scale provided in Table 4.13. The common observation for all mixes was that the deterioration invariably started from the corners followed by the deterioration of the edges. Later on, as the extent of deterioration increased, it was observed that the deterioration was visible on the complete surface.

**Table 4.13: Deterioration rating observed from visual appearance of specimens under 5% sodium sulfate exposure**

| Exposure cycles | Level of deterioration for various mixes |     |     |     |     |     |     |
|-----------------|--|-----|-----|-----|-----|-----|-----|
|                 | M0                                       | M10 | M20 | M30 | M40 | M50 | M60 |
| 2               | 0  | 0   | 0   | 0   | 0   | 0   | 0   |
| 4               | 0  | 0   | 0   | 0   | 0   | 0   | 0   |
| 6               | 0  | 0   | 0   | 0   | 0   | 0   | 0   |
| 8               | 1  | 0   | 0   | 0   | 0   | 0   | 0   |
| 10              | 2  | 1   | 1   | 0   | 0   | 0   | 0   |
| 12              | 3  | 1   | 1   | 1   | 0   | 0   | 1   |
| 14              | 4  | 2   | 2   | 1   | 1   | 1   | 1   |
| 16              | 5  | 3   | 3   | 2   | 1   | 1   | 2   |
| 18              | 6  | 4   | 4   | 3   | 2   | 2   | 2   |

Large deterioration of the corners and edges was due to larger sulphate concentration in these areas as the simultaneous intrusion took place from the adjacent faces (Al-Amoudi 1995).

Among the samples with different concentrations of marble waste, maximum deterioration was noticed in the control mix having river sand as fine aggregates. The use of marble waste as replacement of river sand reduced the deterioration of specimens caused due to sodium sulphate exposure. It can be due to decrease in porosity of mixes having marble waste. Also, the less deterioration of marble waste mixes indicates that chemically the concrete made with marble waste was not reactive with aggressive sodium sulphate media.

#### 4.12.2. Weight Loss/Gain

The weight of specimens was noted after two cycles of monthly exposure to sodium sulphate and the values were compared with the initial weight of the specimens prior to the sulphate exposure. The values of weight loss / gain as a function of time are presented in Fig. 4.37 for all mixes, while Fig. 4.38 shows the final weight loss achieved in all mixes. A gradual rise in weight was observed in all the specimens, followed by the weight loss with the increase in exposure duration. Among all the tested mixes, maximum weight loss was observed in the control mix having river sand as fine aggregates.

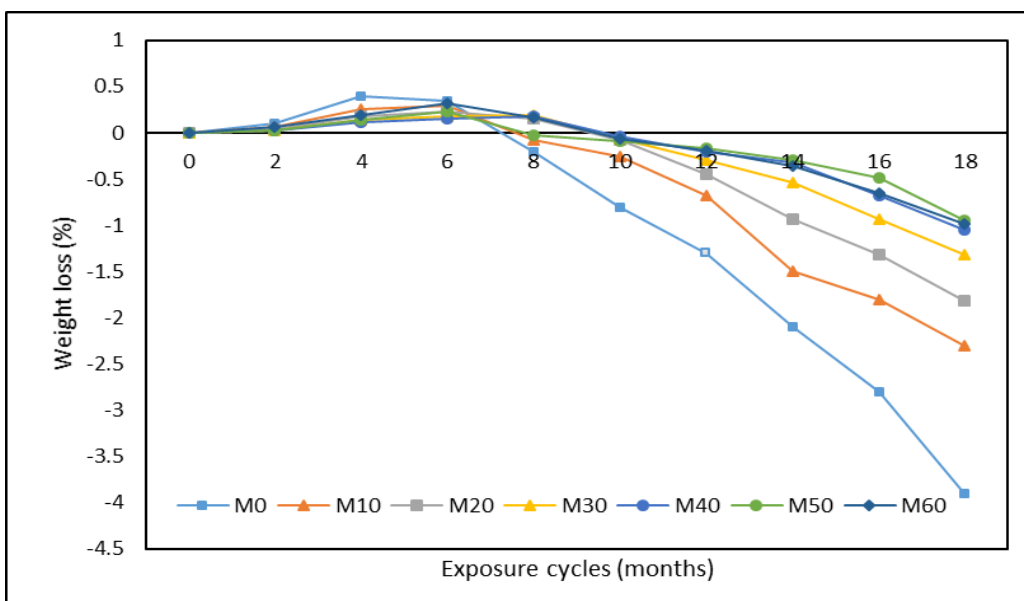


**Fig. 4.37: Progressive weight loss/gain of various concrete mixes under cyclic exposure to 5% sodium sulfate solution**

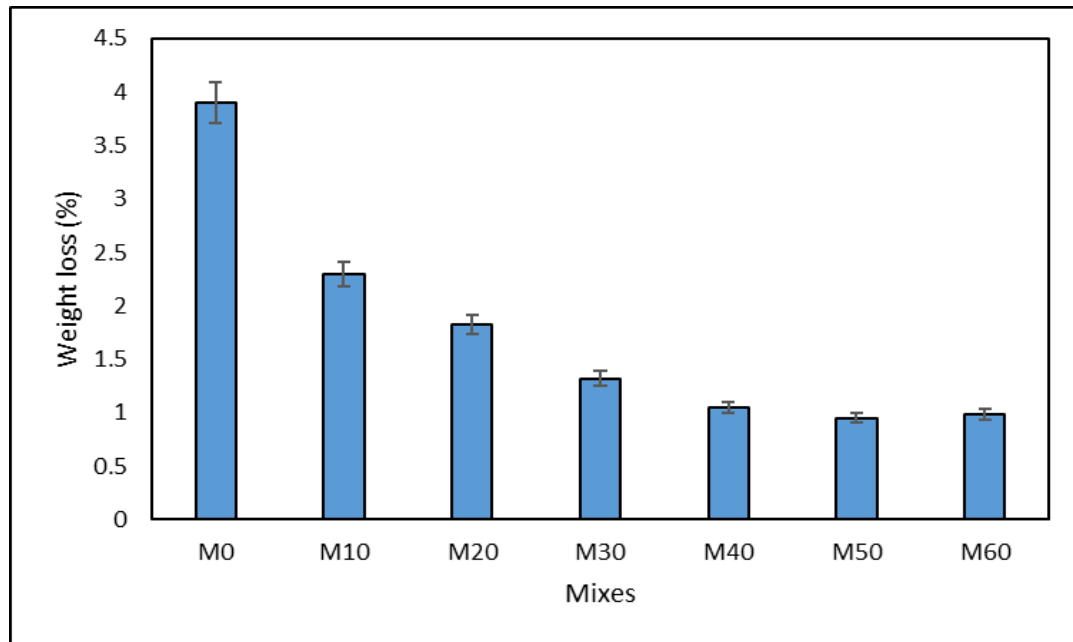


**Fig. 4.38: Final weight loss of mixes at the end of 18 monthly cycles of sodium sulfate exposure**

The mixes incorporating marble waste as partial replacement of river sand as fine aggregates registered lower weight loss. The weight loss decreased as the incorporation level of marble waste was increased from 10% to 40%. With further increase in percentage of marble waste, the weight loss of the mixes became almost stagnant at the values obtained for M40 mix.

The initial increase in weight of mixes indicated filling up of the pores existing in the concrete matrix. It resulted in densification of concrete matrix. With increase in exposure duration, the disruption of concrete matrix took place due to tensile stresses created by the expansive products formed during the sodium sulphate exposure.

As the percentage of marble waste is increased, the porosity of the mixes got reduced, which helped in restricting the attack to the surface only. The aggressive solution was not allowed to penetrate through concrete, thereby restricting the deteriorating reaction between cement hydration products and the aggressive solution. Also, the major chemical composition of marble was  $\text{CaCO}_3$ , which does not participate in reaction with sodium sulphate, thereby acting as inert material under this exposure.

#### **4.12.3. Compressive Strength Loss/Gain**

Similar to the observations made in weight changes in sodium sulphate exposure, compressive strength of the mixes was also noted. Fig. 4.39 shows the changes in

compressive strength loss/gain with progressive exposure to 5% sodium sulphate solution; while the final compressive strength loss after 18 monthly cycles of exposure is presented in Fig. 4.40. Similar to the trend of weight loss/gain, the compressive strength also registered an initial increase followed by decrease in strength with the increase in exposure duration. Maximum compressive strength loss was observed in the mix made with river sand as fine aggregates. The strength loss was as high as 32%. However, the compressive strength loss was reduced when marble waste was incorporated in mixes as partial replacement to river sand as fine aggregates. The final compressive strength registered was 28.6%, 24%, 21%, 19.4%, 18.8% and 20.6% for mixes having 10%, 20%, 30%, 40%, 50% and 60% of marble waste, respectively. It clearly indicated that the incorporation of marble waste helped in arresting the sodium sulphate attack.

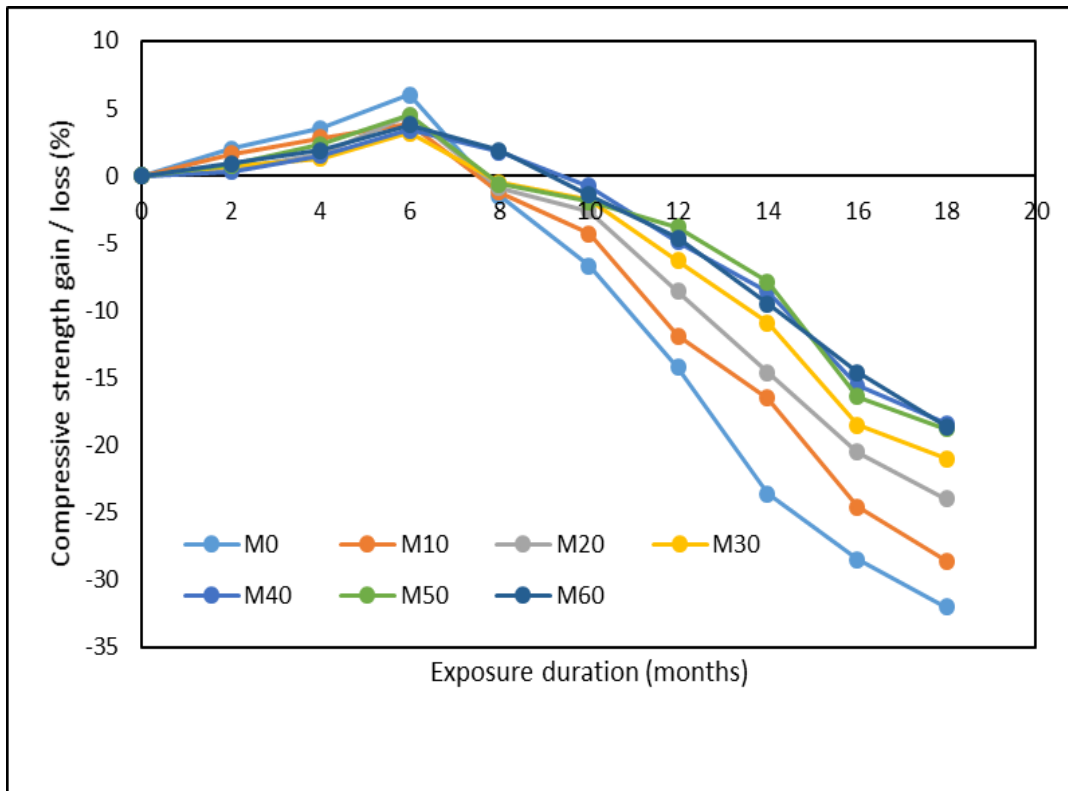


**Fig. 4.39: Progressive compressive strength loss / gain of various concrete mixes under cyclic exposure to 5% sodium sulfate solution**

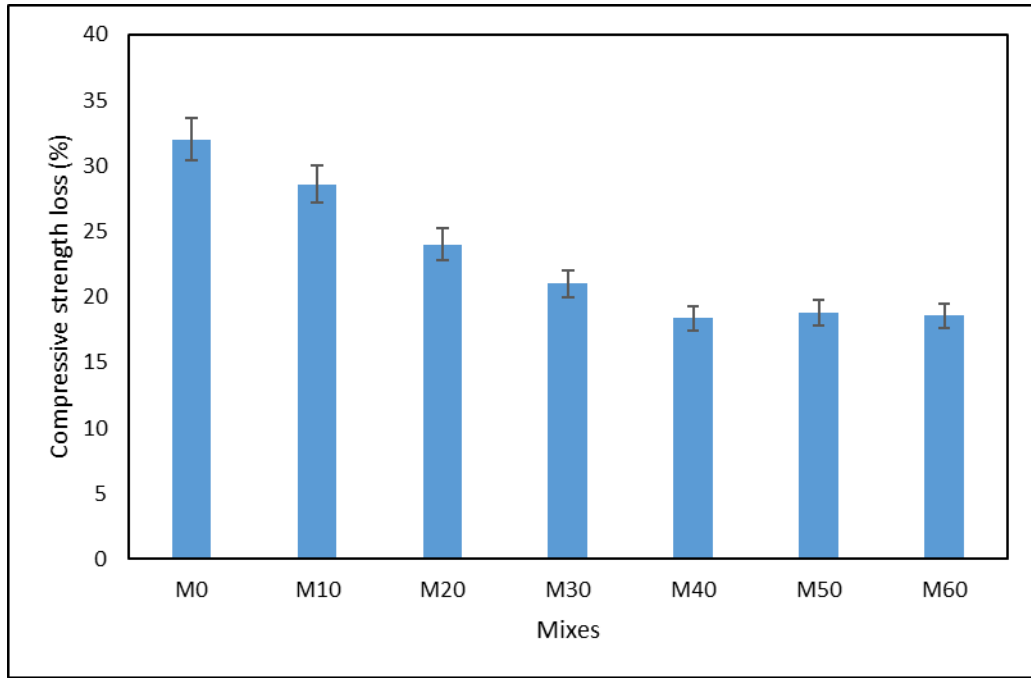


**Fig. 4.40: Final compressive strength loss of mixes at the end of 18 monthly cycles of sodium sulfate exposure**

#### 4.12.4. Linear Expansion

Along with the weight loss/gain as well as compressive strength loss/gain measurements, the dimensional changes that occur due to sodium sulphate exposure was also monitored by using prism specimens of size 75 mm x 75 mm x 285 mm. The prisms were subjected to continuous sodium sulphate exposure for a period of 18 months. The unrestrained expansion of prisms was measured using the test set up of unrestrained drying shrinkage. The expansion was compared with the corresponding expansion in specimens stored in water at  $25 \pm 2$  °C.

Percentage expansion was then calculated as:

$$\text{Expansion (\%)} = \frac{(\Delta L)_{\text{NS}} - (\Delta L)_{\text{water}}}{(\Delta L)_{\text{water}}} \times 100 \quad \dots (4.10)$$

The values of linear expansion obtained for all mixes are presented in Fig. 4.41. It was observed that the control specimens had expansion as high as 2.8% upon exposure to sodium sulphate. However, when marble waste was incorporated in the mixes, the expansion of the mixes reduced drastically. The maximum expansion registered at the end of 18 months of exposure for mixes incorporating 10%, 20%, 30%, 40%, 50%

and 60% of marble waste was 1.5%, 1.2%, 0.7%, 0.35%, 0.46% and 0.56% respectively. It clearly indicated that the lesser amount of expansion products, viz. gypsum and ettringite were formed in the mixes incorporating marble waste. It could be due to the availability of calcium ions in marble waste mixes which reduced the chances of attack on cement hydration products under sodium sulphate exposure. Also, for all the mixes, the rate of initial expansion was low, while the rate of expansion increased towards the end of exposure duration. It could be due to the capability of accommodating reaction products within the pores of concrete matrix. Once the pores got filled up, the expansion of prisms became measurable.

#### 4.12.5. Mechanism of Sodium Sulphate Attack

The mechanism of sodium sulphate attack on concrete depends on both physical and chemical characteristics of the mix. At the physical level, permeability of the mixes played an important role in defining the extent of sodium sulphate exposure. The sorptivity results of various mixes indicated that the addition of marble waste resulted in reduced permeability. The penetration of aggressive media reduced drastically.

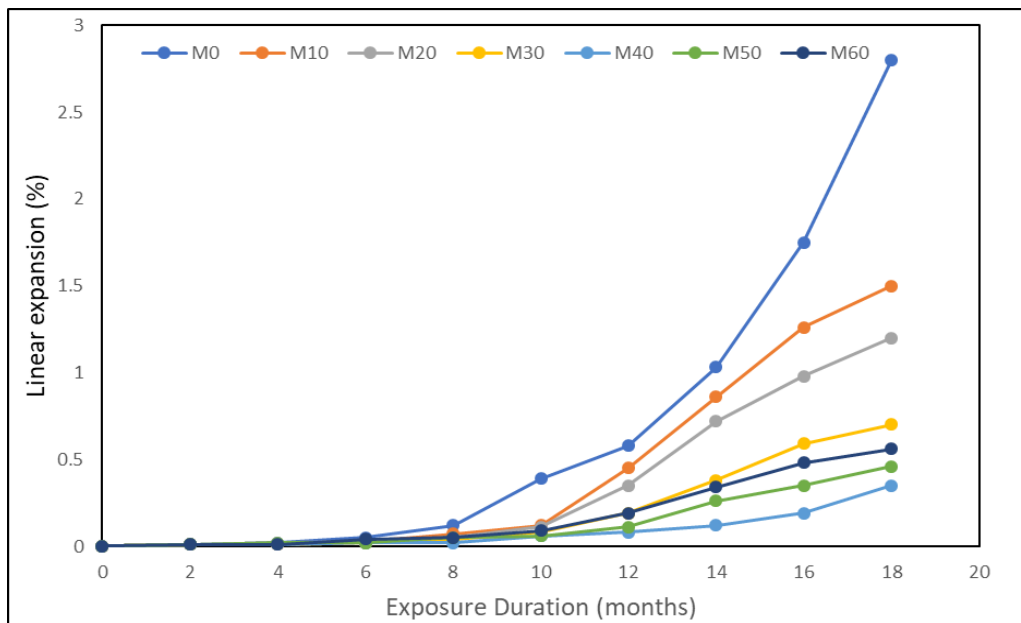


**Fig. 4.41: Linear expansion registered in various concrete mixes under cyclic exposure to 5% sodium sulfate solution**

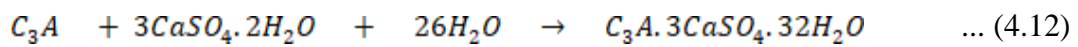
At the chemical level, the ions in the aggressive media interacted with the concrete matrix; leading to chemical reaction between the constituents of cement hydration products and the ions present in the aggressive media. Out of all the cement hydration

products,  $\text{Ca}(\text{OH})_2$  is most vulnerable to sodium sulphate exposure, which results in the formation of gypsum. The resulting chemical reaction is:



*Calcium hydroxide*      *Sodium sulphate*      *Water*      *Gypsum*      *Sodium hydroxide*

Gypsum, so formed, further has a tendency to react with tricalcium aluminate ( $\text{C}_3\text{A}$ ) of cement, resulting in the formation of ettringite. The chemical reaction is represented as:



*Tricalcium aluminate*      *Gypsum*      *Water*      *Ettringite*

The formed ettringite is sometimes referred to as the secondary ettringite, in order to distinguish it from the primary ettringite formed when the concrete is still in the plastic stage.

Gypsum has low solubility with about 0.22 grams of gypsum dissolve in 100 gram of water at  $0^\circ\text{C}$  (Pavlík, 1994; Zivica and Bajza, 2001). Due to low solubility, it occupies the space available in the voids of concrete matrix. The deposition of gypsum leads to initial increase in weight and compressive strength of concrete upon exposure to sodium sulphate solution. However, with the increase in duration of exposure, gypsum gets further converted into ettringite. Both gypsum and ettringite are voluminous in nature, which lead to development of tensile stresses in concrete, thereby leading to softening of outer surface and spalling of concrete concrete (Chatveera and Lertwattanaruk, 2014; Girardi and Maggio, 2011), which negatively affected the properties of concrete. Now when marble waste is used as fine aggregates, the calcium carbonate of marble waste chemically binds  $\text{C}_3\text{A}$  to form calcium carbo-aluminate.



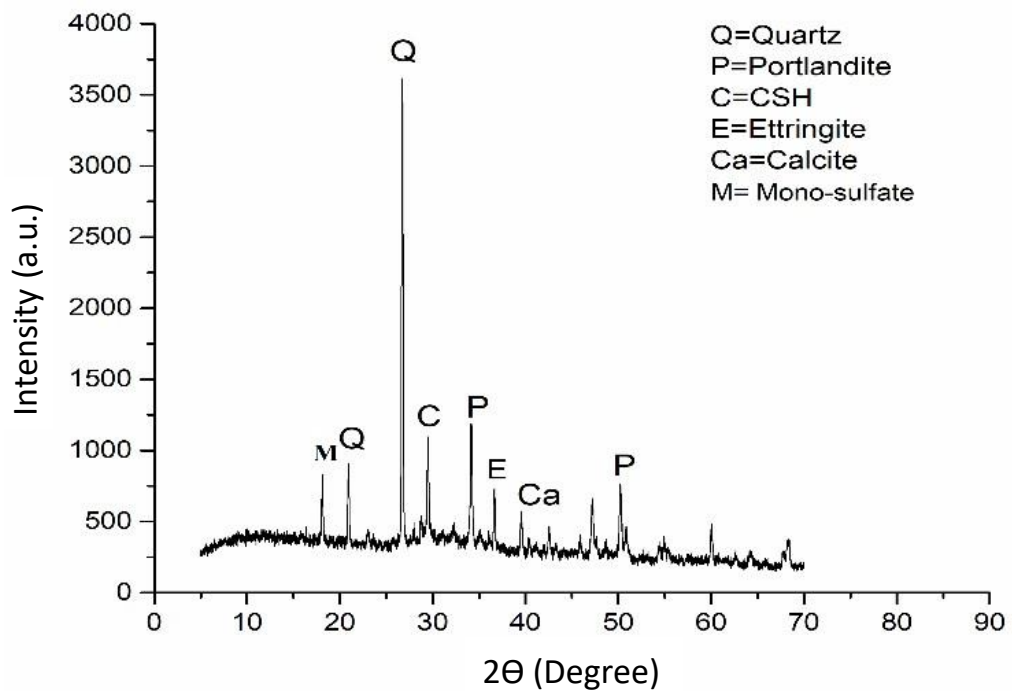
*Tricalcium aluminate*      *Calcium carbonate*      *Calcium carbo-aluminate*

Due to this reaction,  $C_3A$  becomes unavailable for reaction with gypsum. It further lowers the formation of expansive ettringite in the matrix, thereby reducing the tensile stresses in the concrete matrix. Higgins et al. (2003) also reported that the presence of calcium carbonate in concrete improved the resistance to sulphate exposure.

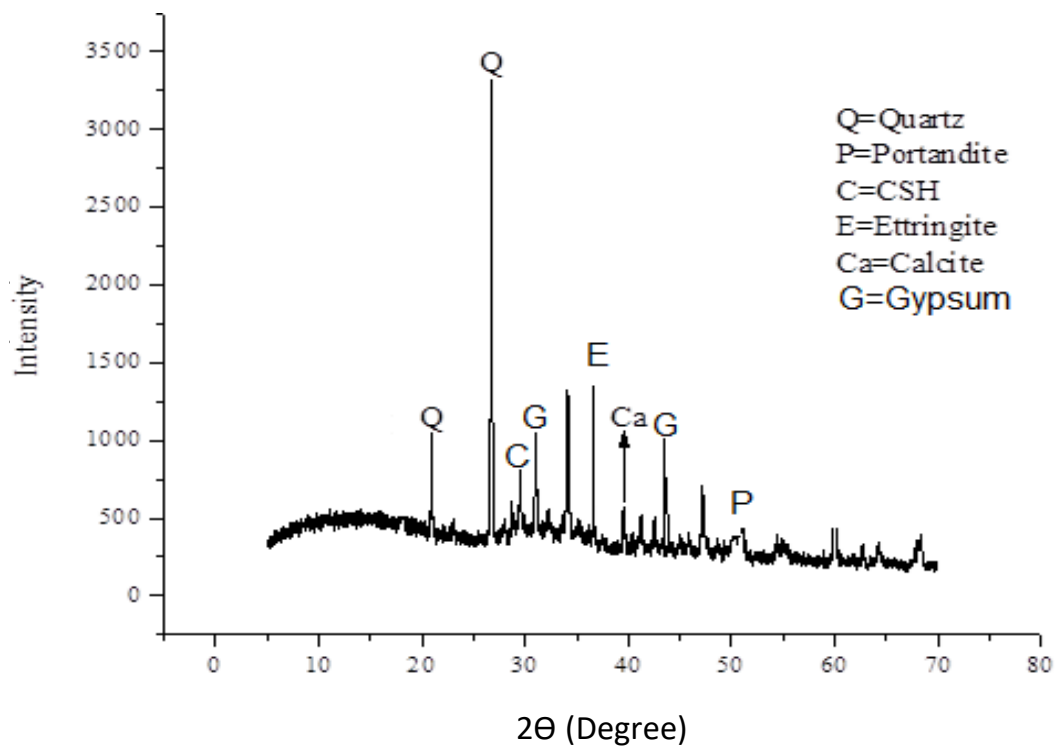
#### **4.12.6. Microstructure Analysis**

The microstructure of the concrete subjected to contamination with sodium sulfate was investigated in terms of XRD and SEM-EDS analysis. In order to clearly understand the changes with progressive exposure, for the control mix both the analysis were carried out I.e. at the initial exposures (4 months of exposure) and at later stages of exposure (18 months). However, it was observed from weight loss and compressive strength loss data (Figs. 4.37 and 4.39 respectively) that the pattern of both weight loss and compressive strength loss was almost same in all mixes irrespective of marble waste incorporation levels at exposure duration of 4 months. Thus, the microscopic investigation was omitted at this duration and done only at the exposure duration of 18 months.

The XRD graph for control mix at the exposure duration of 4 months and 18 months is presented in Fig. 4.42. The figure clearly depicts that at exposure duration of 4 months (Fig. 4.42 (a)), low intensity peaks of mono-sulfate and ettringite were observed. The formation of fine ettringites at the initial exposure duration lead to volume expansion in cement paste matrix, thereby leading to initial weight gain and linear expansion as clearly noticed in Figs. 4.37 and Fig. 4.41 respectively. On further exposure to sodium sulphate till 18 months, XRD graph of the control mix showed disappearance of mono-sulfate peaks and widening of ettringite peaks (Fig. 4.42 b). Along with the widening in ettringites peaks, gypsum peaks became visible at diffraction angle of  $31^\circ$ . The decrease in intensity of portlandite peak indicates consumption of portlandite during gypsum formation.



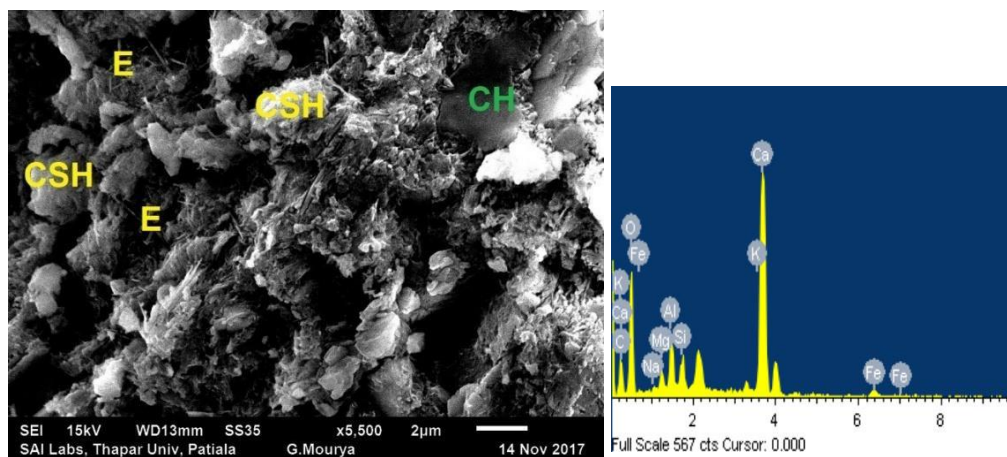
(a) XRD after 4 months of exposure



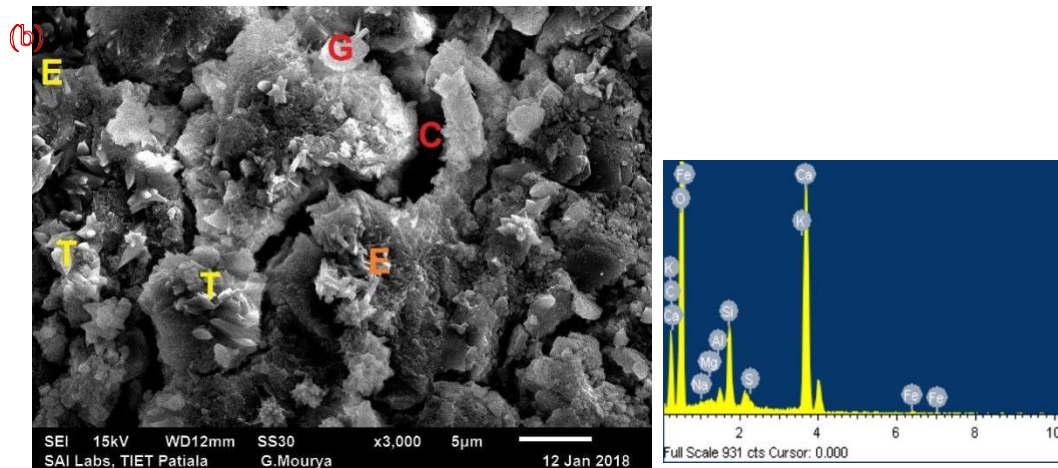
(b) XRD after 18 months of exposure

**Fig. 4.42: XRD of the control mix (M0) at 4 month and 18 months of 5% sodium sulphate exposure**

Fig. 4.43 show the SEM-EDS images for control mix obtained at the exposure duration of 4 months and 18 months. At the exposure duration of 4 months, first stage cement hydration products of portlandite in the form of solid plates along with the second stage hydration product of C-S-H gel were observed. C-S-H gel observed at this duration is fibrous in nature, which is responsible for the gain in compressive strength as indicated in Fig. 4.39. Also, the transformation of C-S-H to fine needle like structures namely ettringites approximately 1-2  $\mu\text{m}$  was observed. It was reported that these fine ettringites while progressing inward the matrix, can destroy the microstructure and lead to cracking in the surface layer. The appearance of these cracks became distinct at exposure duration of 18 months (Fig. 4.43b). At this duration, the initially formed fine ettringites convert into thick bar crystal of ettringites which filled the cracks. Gypsum was formed as white blocky crystals that were sub-parallel to the surface. The reduction in fibrous C-S-H gel indicate the conversion into tobermorite gel and gypsum after reacting with sulphates (Qing et al., 2017). This expansive product, large bar like crystals of ettringites and gypsum are mainly responsible for the crack formation, leading to destruction of concrete.



(a) SEM and EDS of M0 mix at 4 months of exposure



(b) SEM and EDS of M0 mix at 18 months of exposure

**Fig. 4.43: SEM-EDS image for control mix (M0) when exposed to 5% sodium sulphate solution for 18 months**

In figures 4.44 - 4.49 same phase composition was observed with variation in peak intensity. The major peaks observed were corresponding to  $\text{Ca(OH)}_2$ , quartz, ettringite, gypsum and calcium carbonate (calcite). On comparison with the M0 (control) mix, wider peaks of calcium carbonate were found in the diffractogram of M10 to M60 mixes. While the portlandite peak was relatively higher in the control mix as compared to mixes containing marble waste, which is attributed to the consumption of portlandite in secondary pozzolanic reaction of mineral additives. The intensity of ettringite and gypsum peaks became smaller while calcite peaks became wider with the progressive increase in marble waste content. The widened calcite peaks lead to the improvement in resistance of marble enrich mixes towards sulphate exposure.

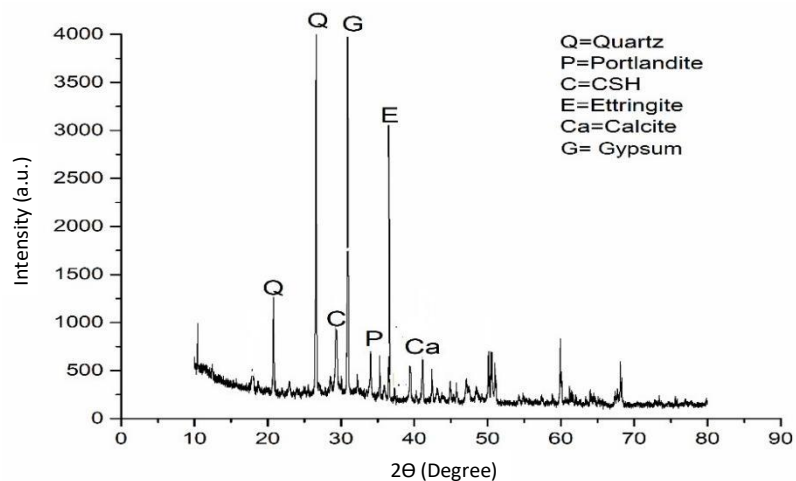


**Fig. 4.44: XRD for M10 mix at exposure duration of 18 months**

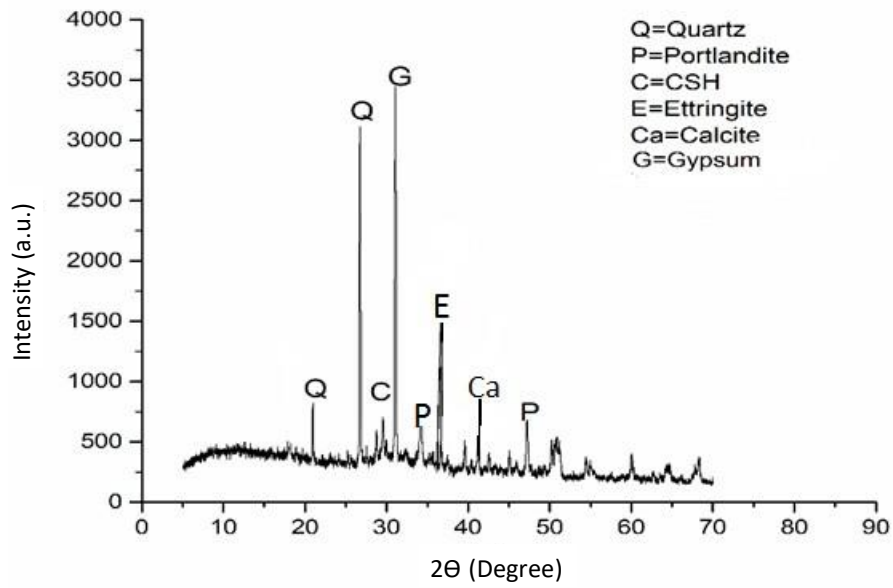


**Fig. 4.45: XRD for M20 mix at exposure duration of 18 months**

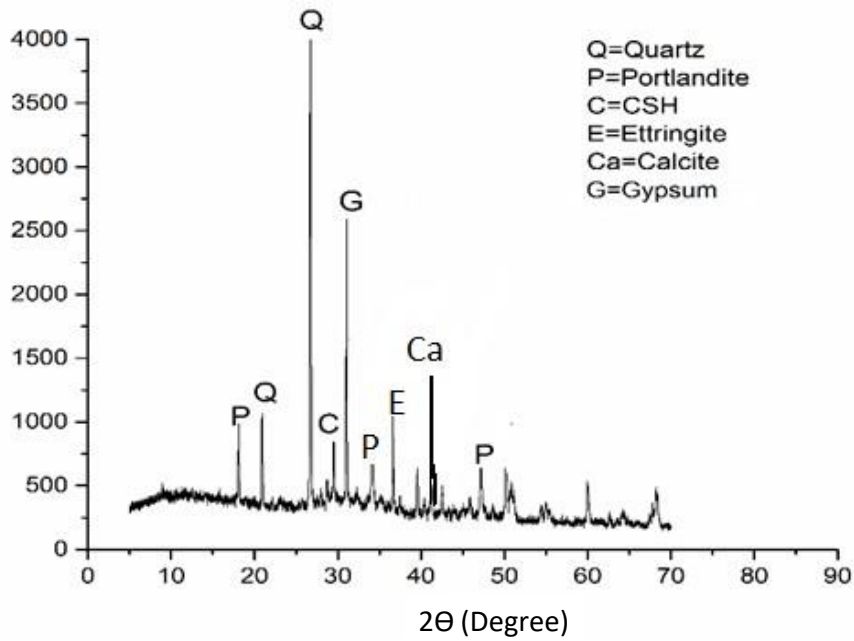


**Fig. 4.46: XRD for M30 mix at exposure duration of 18 months**

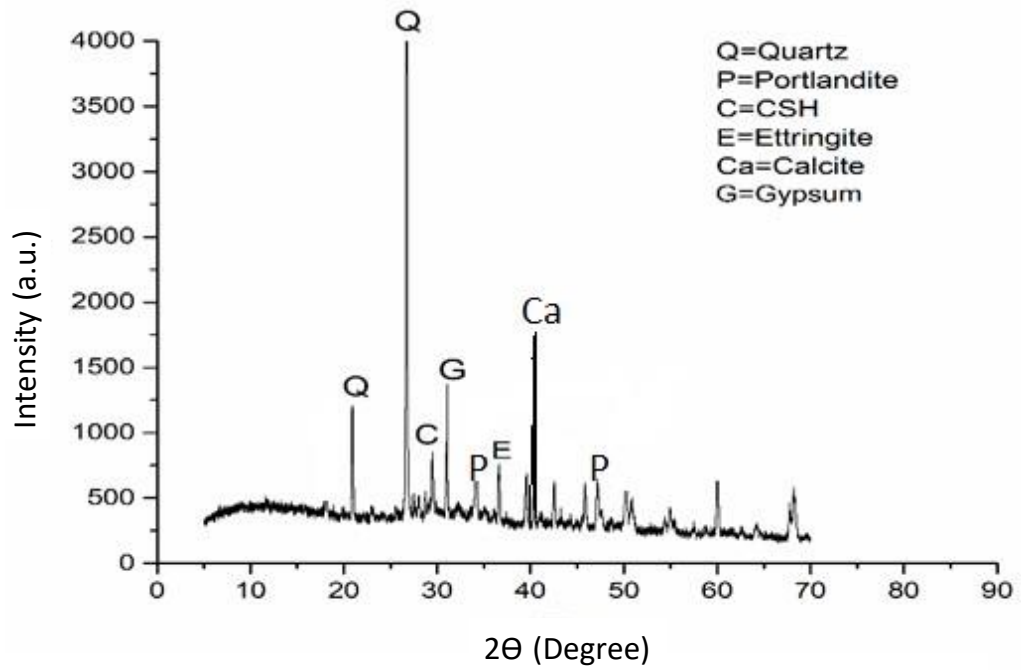


**Fig. 4.47: XRD for M40 mix at exposure duration of 18 months**

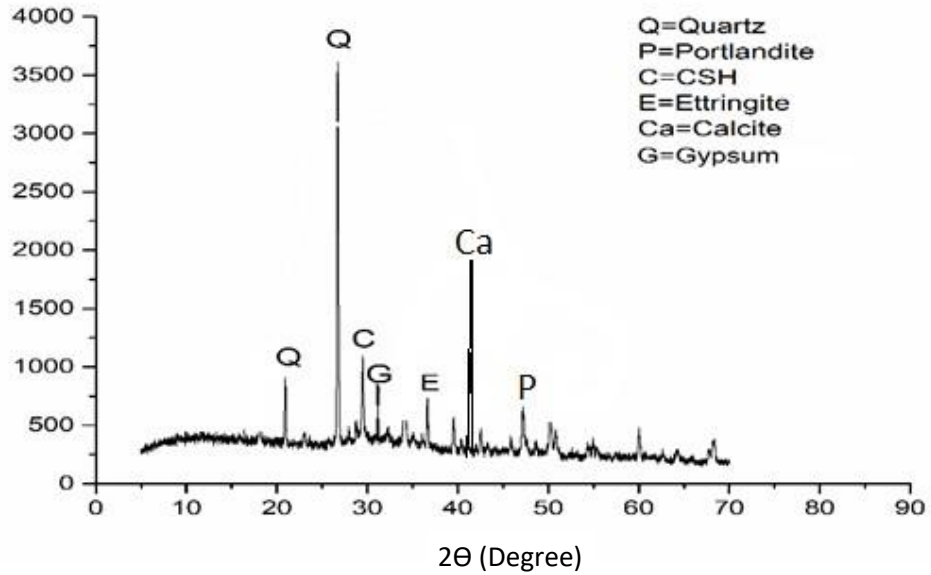


**Fig. 4.48: XRD for M50 mix at exposure duration of 18 months**

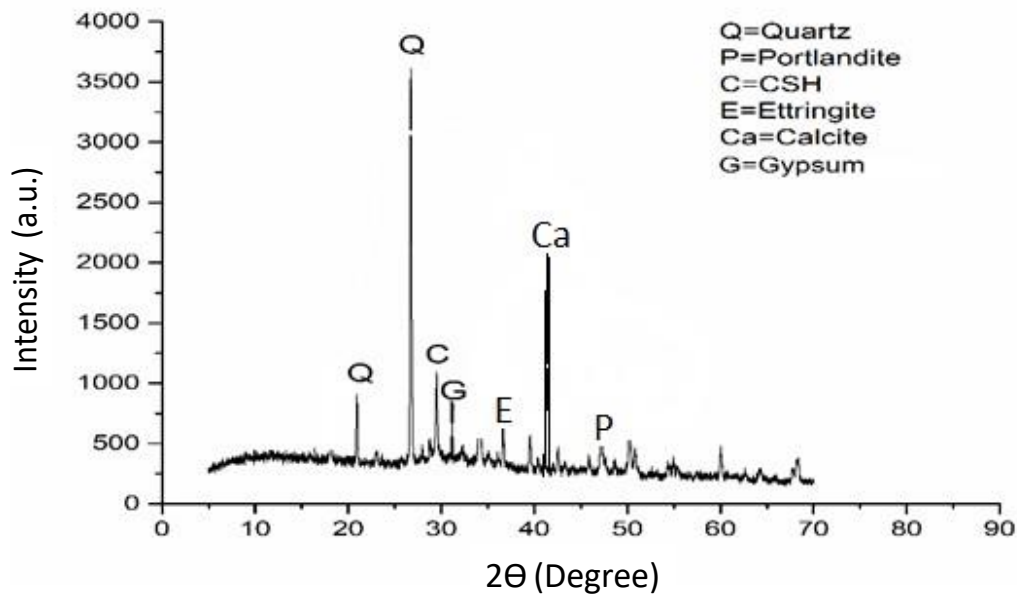


**Fig. 4.49: XRD for M60 mix at exposure duration of 18 months**

Figs. 4.50 to 4.55 shows the SEM-EDS images for mixes incorporating different amount of marble waste after 18 months exposure to sodium sulphate. A compact microstructure enriched with ettringite, gypsum crystals and calcite was seen in mixes containing marble waste on comparison with control mix at this exposure duration. The voids observed are also lower than those observed in control mix (Fig. 4.43b), indicating the higher resistance of incorporated marble waste mixes to sodium sulphate attack. Secondly, the thickness of the micro cracks reduced with the progressive increase in marble waste content.

In EDS spectrum, no qualitative change in phase composition was observed with the marble waste incorporation on comparison with control mix. Only the intensity of the phase peaks was varying with variation in marble waste. The peaks corresponding to calcium, increased with the progressive increase in marble waste addition which lead to the formation of calcite in the mixes. On the other hand, the observed peaks correspond to aluminium were comparatively high in mixes having lower marble waste content such as M10, M20 and M30 on comparison with mixes having higher marble waste content like; M40, M50 and M60. The low intensity peaks of aluminium correspond to lower amount of ettringites formation in mixes containing higher

content of marble waste .As observed in XRD diffractogram, mixes enriched with high amount of marble dust shows the lower formation of gypsum and ettringites.

Figs. 4.50 and 4.51 show the visible cracks along with the fine ettringites and gypsum formation similar to control mix. Fig. 4.52 shows the pore filling of matrix by short fibers of hydrated calcium silicates, cotton shaped calcite and fine ettringites on the entire surface.

A characteristic feature of this phase is transformation of tricalcium aluminate to calcium carbo-aluminate. In M40 (Fig. 4.53) mix the most compact microstructure with sharp needle like crystals of ettringite with white crystals of gypsum was observed. The presence of white crystals corresponds to the formation of gypsum and the fine granular particles are thenardite.

Fig. 4.53 clearly showed that large amount of ettringite so formed deposited in the cracks that originated from the fine ettringites formed at early exposure durations. It was reported that this type of ettringites, only precipitate in the spaces that were originally created by cracking due to expansion and is considered to be non-expansive (Irassar et al., 2003; Liu et al., 2015). Figs. 4.54 and 4.55 shows uniform spread of white crystals of gypsum along with the fine granular particles of thenardite and calcite on the entire surface.

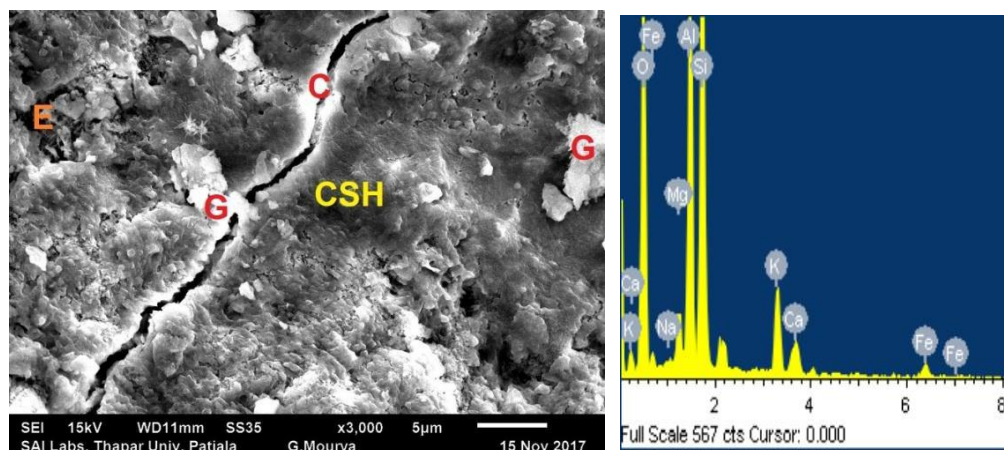


**Fig. 4.50: SEM-EDS image for M10 mix at exposure duration of 18 months to 5% sodium sulphate solution**

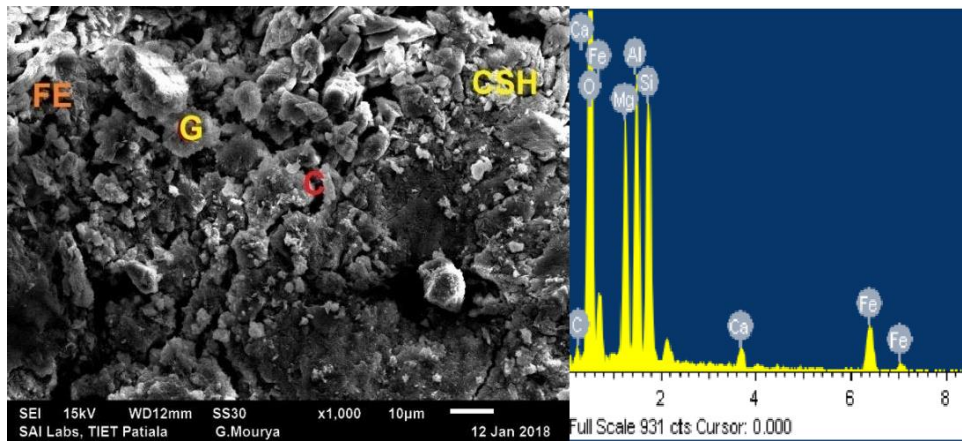


**Fig. 4.51: SEM-EDS image for M20 mix at exposure duration of 18 months to 5% sodium sulphate solution**

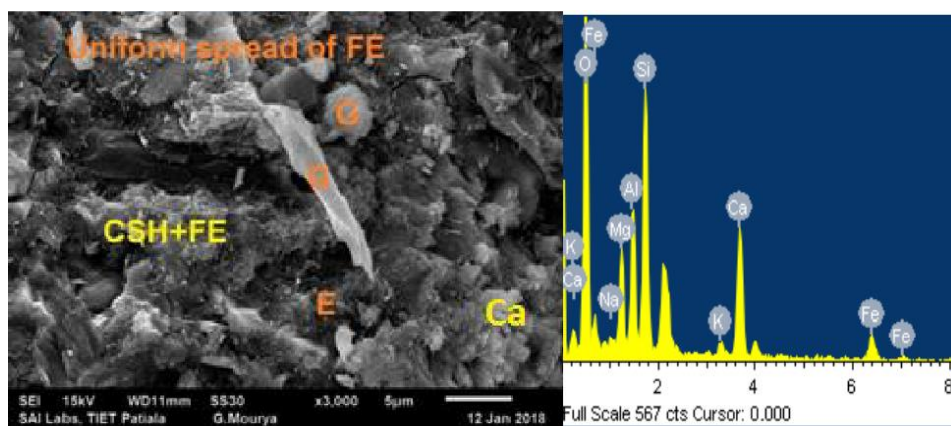


**Fig. 4.52: SEM-EDS image for M30 mix at exposure duration of 18 months to 5% sodium sulphate solution**

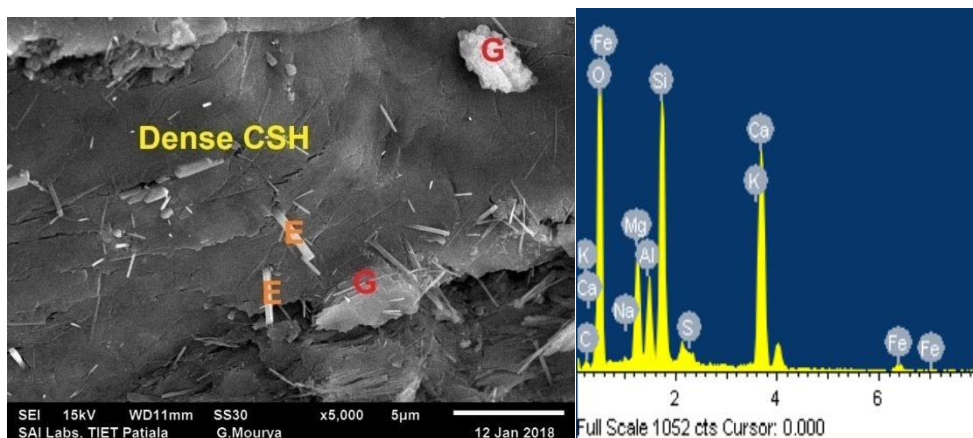


**Fig. 4.53: SEM-EDS image for M40 mix at exposure duration of 18 months to 5% sodium sulphate solution**

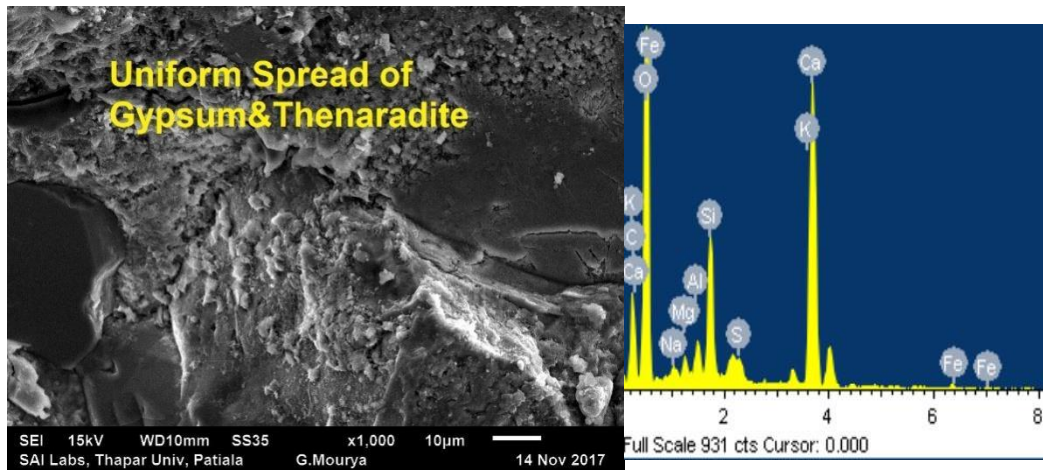


**Fig. 4.54: SEM-EDS image for M50 mix at exposure duration of 18 months to 5% sodium sulphate solution**

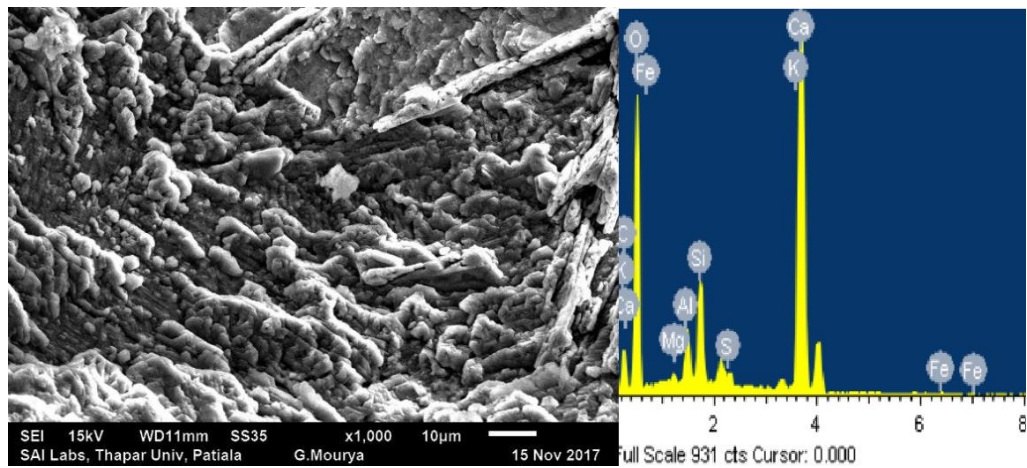


**Fig. 4.55: SEM-EDS image for M60 mix at exposure duration of 18 months to 5% sodium sulphate solution**

## **CHAPTER 5**

### **CONCLUSIONS**

#### **5.1. GENERAL**

The present experimental work was carried out in order to explore the possibility of using marble waste as partial replacement of fine aggregates in concrete mixes. The test results confirm that marble waste has a potential to be used as replacement of fine aggregates, with the most optimum results were obtained by using 40% replacement level. Based on the test results, the conclusions drawn are presented in the following sections:

#### **5.2. FRESH PROPERTIES OF CONCRETE**

Slump test was conducted for determining workability of mix. It was observed that the workability of the mixes decreased with the addition of marble waste as replacement of fine aggregates. The decrease occurred in spite of the fact that the water adsorption of marble was comparatively lower than the water absorption of natural river sand. The loss of workability with the incorporation of marble waste is attributed to the angular shape of marble waste aggregates and an increase in the surface area to be wetted, hence decreasing the workability. Also, the addition of marble waste in a concrete mix makes the mix highly cohesive and less workable, thereby increasing the water demand. The combined effect of increased cohesiveness of the mix and large surface area to be wetted led to loss of workability of the mix containing marble waste as replacement to fine aggregate.

#### **5.3. STRENGTH PROPERTIES OF HARDENED CONCRETE**

Compressive strength and split tensile strength of the mixes was measured. Compressive strength of the mixes was determined as per BIS 516-2004; while split tensile strength of the mixes was tested as per BIS 5816-1999. Both the tests were conducted at 7, 28, 90 and 365 days of casting.

### **5.3.1. Compressive Strength**

Compressive strength of the mixes increased with the increase in marble waste aggregates in the mixes up to 40% replacement level, thereafter it got stabilized with no further change in strength. The increase in compressive strength with the incorporation of marble waste as partial replacement of natural river sand can be attributed to better filler effect provided by marble waste, due to presence of more fines in the particle size range of 1.18 mm-300  $\mu\text{m}$ . Addition of marble waste as fine aggregates can therefore refine the pore structure, thereby improving the micro-structure of concrete matrix. Along with this, the angular sizes of marble waste aggregates helped in better bonding and improvement in interstitial transition zone of the resultant mix. At the chemical level, marble waste improves the binding ability of the concrete mix. The reaction between calcite present in marble with  $\text{C}_3\text{A}$  of cement provides a compact structure and helps in improving binding capability of the concrete matrix.

However, the strength did not improve further after reaching an optimum value at 40% replacement level. It was due to loss of workability of the mix with the addition of marble waste, which could have adversely affected the packing of the constituent materials, hence leading to reduction in strength.

### **5.3.2. Split Tensile Strength**

Similar to the compressive strength results, split tensile strength also increased with the increase in marble waste as partial replacement of natural river sand, with the maximum increase in split tensile strength achieved at 40% replacement level, thereafter split tensile strength registered a small decrease.

On comparing the compressive strength and split tensile strength results of the mixes, it can be seen that the percentage increase in split tensile strength is more than the corresponding increase in compressive strength for all mixes, irrespective of the curing age. The higher improvement in split tensile strength as compared to the compressive strength can be due to better bonding achieved by the shape of marble waste aggregates and formation of carbo-aluminates. The angular marble particles helped in providing better bonding along the crack path developed during split tensile strength test.

### **5.3.3. Relationship between Compressive Strength and Split Tensile Strength**

A multi regression model was developed considering a realistic relationship between compressive strength and split tensile strength that involved the parameters corresponding to age of concrete and percentage of marble waste aggregates. The coefficient of determination for the developed multiple regression model was as high as 0.972.

## **5.4. PERMEATION PROPERTIES**

The permeation characteristics of the mixes were monitored by conducting rapid chloride permeability test (RCPT), sorptivity test and water absorption tests. Rapid chloride permeability test was conducted at 28, 90 and 365 days of casting; while sorptivity test and water absorption test was conducted at 28 and 365 days of casting.

### **5.4.1. Rapid Chloride Permeability Test (RCPT)**

The RCPT values decreased with the increase in marble waste addition. At 28 days of curing, penetration of the control mix was in 'moderate' penetration range; while the penetration of all other mixes having marble waste was in 'low' penetration range; as specified in ASTM C 1202-12. M40 concrete registered least RCPT value among all mixes, irrespective of the curing age. The least RCPT value of M40 mix at all curing ages indicates its best performance.

### **5.4.2. Sorptivity**

The value of primary sorptivity coefficient decreased systematically, as the amount of marble waste is increased in the mix. Initially, the value decreased rapidly up to 40% replacement level; thereafter the values become nearly constant and a small increase in sorptivity was registered. Minimum sorptivity value was obtained for M40 mix at both 28 and 365 days of testing.

### **5.4.3. Water Absorption**

Water absorption decreased with the addition of marble waste. Since water absorption is generally related to the structural pores, especially in the aggregate-interface zone; decrease in water absorption by marble waste addition confirms refinement of aggregate-interface zone, resulting in improvement of overall durability of the mix. Least value of water absorption is observed in M40 mix.

## **5.5. MICROSTRUCTURE ANALYSIS**

The microstructural analysis of the mixes was carried out at 28 days and 365 days of curing. It involved X-ray diffraction (XRD) analysis of the powdered specimens and scanning electron micrographs (SEM) on the concrete pieces obtained after conducting compressive strength studies.

### **5.5.1. XRD Analysis**

The obtained spectra obtained for all the mixes indicate that the major phases formed in all mixes remain same, irrespective of the replacement levels of marble waste with natural river sand as fine aggregates. It further strengthens the fact that marble waste is largely an inert material and has filler effect on the properties of the resultant mix. Major phases identified for all mixes are C-S-H gel, calcium hydroxide, calcium carbonate, dolomite and quartz. The XRD patterns show major presence of dolomite in concrete made with marble waste aggregates. The intensity of dolomite peaks increased rapidly with an increase in percentage of marble waste beyond 40%. This indicates that dolomite was initially involved in reaction with C<sub>3</sub>A. However, with a higher percentage of marble waste, much of the dolomite goes un-reacted and the same has been observed in XRD analysis. The quartz peaks also diminished with the partial replacement of natural river sand with marble waste aggregates.

### **5.5.2. Scanning Electron Micrographs**

Mixes incorporating marble waste aggregates exhibited denser microstructure, indicating the filler effect of marble waste. Also, densification of the mixes was achieved by the improvement in the binding ability due to presence of calcium carboaluminate phase. Major phases, i.e. C-S-H gel and CH remain almost the same in all mixes, indicating that the incorporation of marble waste has not much influence on the hydration of cement. However, there is a better spread of C-S-H with the addition of marble waste. Thus, better mechanical properties of the mix can be explained by filler effect of marble waste aggregates and the densification of concrete matrix.

## **5.6. ABRASION RESISTANCE OF CONCRETE**

Abrasion resistance of concrete is an important durability property of concrete and is particularly important for concrete floors, concrete pavements and concrete dams. The property typically refers to the ability to resist wearing due to frictional movement between the surfaces of different characteristics. In the present study, abrasion resistance was measured in terms of depth of wear.

### **5.6.1. Effect of Addition of Marble Waste**

The addition of marble waste reduced the depth of wear as compared to the control mix at all curing ages. The maximum improvement in depth of wear was observed at 40% replacement level, wherein the depth of wear reduced by 30% as compared to the control mix.

The lower depth of wear achieved by using marble waste was due to the denser pore structure achieved, angular sizes of marble waste aggregates which helped in better bonding and improvement in interstitial transition zone (ITZ) of the resultant mix. Also, at the chemical level, marble waste improved the binding ability of the mix.

### **5.6.2. Relationship between Abrasion Resistance and Compressive Strength**

General trend of variation of compressive strength and depth of wear indicates that the depth of wear is inversely proportional to the compressive strength of the mix. The exponential form of relationship was developed which was found to be best suitable with the maximum regression coefficient ( $R^2$ ) of 0.88.

## **5.7. DRYING SHRINKAGE**

Unrestrained drying shrinkage of hardened concrete was measured as per ASTM C157-17.

### **5.7.1. Effect of Marble Waste Addition**

Incorporation of marble waste as fine aggregates led to reduction in drying shrinkage strain of concrete mixes. During 270 days of drying duration, the ultimate shrinkage strain reduced gradually from  $478 \times 10^{-6}$  mm/mm to  $332 \times 10^{-6}$  mm/mm as the percentage of marble waste is increased from 10 to 60% of fine aggregates. The ultimate shrinkage strain decreased by 7.7, 16.7, 22.0, 25.2, 27.6 and 30.5% respectively for M10, M20, M30, M40, M50 and M60 mixes, as compared to the control mix.

### **5.7.2. Drying Shrinkage Strain Prediction Model**

A shrinkage prediction model incorporating 28-day compressive strength, drying duration and proportion of marble waste used, is proposed. The proposed model had high correlation coefficient ( $R^2$ ) which indicates its effectiveness in predicting drying shrinkage accurately. It further confirms that an additional parameter based on the proportion of marble waste used as fine aggregates can be adopted in the existing models to predict drying shrinkage of such mixes accurately.

### **5.8. RESISTANCE TO ACID ATTACK**

The concrete mixes were subjected to 3% sulphuric acid exposure. It was observed that mixes incorporating marble waste had better performance under severe sulphuric acid exposure. The decrease in compressive strength has been reduced from 32.4% to 7.8%, when the marble waste percentage is increased to 60%. It indicated that marble waste reduced the rate of deterioration of concrete under severe acid exposure. It was because of highly dissolvable carbonates present in marble waste, which not allow the carbonates of cement compounds to dissolve initially and will help in alleviating the cement hydration products from participating in the reaction at the first stage. Due to this, local neutralization of acid takes place and the acid required for attacking binder is decreased. XRD analysis of the mixes also show higher peaks of both gypsum and portlandite in the mixes incorporating marble waste. It clearly indicates that gypsum was formed due to reaction of marble waste with sulphuric acid, thereby allowing portlandite and other cement hydration products to remain intact even after severe acid exposure.

### **5.9. RESISTANCE TO SODIUM SULPHATE EXPOSURE**

All seven concrete mixes were exposed to 5% sodium sulphate salt in order to investigate their performance in the presence of sulphate ions. The test methods employed for judging performance of mixes included visual observations, weight loss measurement, compressive strength loss measurement, length change and microstructural analysis by SEM and XRD.

The mixes incorporating marble waste as partial replacement of river sand as fine aggregates registered lower weight loss. The compressive strength loss also reduced when marble waste was incorporated in mixes. Also the expansion of the mixes reduced drastically. It clearly indicates that the incorporation of marble waste helped

in arresting the sodium sulphate attack. Lesser amount of expansion products, viz. gypsum and ettringites were formed in the mixes incorporating marble waste. The mechanism of sodium sulphate attack on concrete depends on both physical and chemical characteristics of the mixes. At the physical level, lower permeability of the mix with marble powder played an important role in defining lower extent of exposure to sodium sulphate. At the chemical level, the ions in the aggressive media interacts with the concrete matrix; leading to chemical reaction between the constituents of cement hydration products and the ions present in the aggressive media. When marble waste is used as fine aggregates, the calcium carbonate of marble waste chemically binds  $C_3A$  to form calcium carbo-aluminate. Due to this reaction,  $C_3A$  becomes unavailable for reaction with gypsum. It further lowers the formation of expansive ettringite in the matrix, thereby reducing the tensile stresses in the concrete matrix.

#### **5.10: Scope for Future Work:**

Although an extensive work is done in the present study to use waste marble as replacement of fine aggregates. However, the work can be extended so that the material finds usage in actual practice. The topics that have scope for future work are:

1. The main crystalline mineral present in marble waste is dolomite. Previous studies have shown that some phase transformations and subsequent concrete deterioration phenomena during aging may be due to the presence of alkali- carbonate reaction (ACR). The ACR in concrete is described as the dedolomitisation process of the aggregate in concrete by the chemical reaction between dolomite crystals in the aggregates and alkalis present in the pore solution of hydrated cement paste. Since the marble was mainly consists of dolomite, a thorough study of ACR of such mixes is required.
2. A detailed microstructural analysis of the mixes incorporating marble waste will help in understanding that whether filler effect or chemical reactions played a major role in improving the performance of mixes with waste marble.

## REFERENCES

- ACI 224, 2001. ACI 224R-01 Control of Cracking in Concrete Structures, ACI Committee 224R-01.
- ACI Committee 209, 2005. Report on factors affecting Shrinkage and creep of hardened concrete, ACI 209.1R-05. <https://doi.org/10.1038/423132a>
- ACI committee 318, 2011. Building Code Requirements for Structural Concrete and Commentary (ACI 318M-11), American Concrete Institute, Farmington Hills, MI.
- Aldea, C.M., Young, F., Wang, K. and Shah, S.P., 2000. Effects of curing conditions on properties of concrete using slag replacement. *Cem. Concr. Res.* 30, 465–472.
- Aliabdo, A.A., Abd Elmoaty, A.E.M., Auda, E.M., 2014. Re-use of marble waste dust in the production of cement and concrete. *Constr. Build. Mater.* 50, 28–41. <https://doi.org/10.1016/j.conbuildmat.2013.09.005>
- Alyamaç, K.E., Aydin, A.B., 2015. Concrete properties containing fine aggregate marble powder. *KSCE J. Civ. Eng.* 19, 2208–2216. <https://doi.org/10.1007/s12205-015-0327-y>
- Alyamaç, K.E., Ince, R., 2009. A preliminary concrete mix design for SCC with marble powders. *Constr. Build. Mater.* 23, 1201–1210. <https://doi.org/10.1016/j.conbuildmat.2008.08.012>
- André, A., De Brito, J., Rosa, A., Pedro, D., 2014. Durability performance of concrete incorporating coarse aggregates from marble industry waste. *J. Clean. Prod.* 65, 389–396. <https://doi.org/10.1016/j.jclepro.2013.09.037>
- Arel, H.S., 2016. Recyclability of marble waste in concrete production. *J. Clean. Prod.* <https://doi.org/10.1016/j.jclepro.2016.05.052>
- Aruntaş, H.Y., Gürü, M., Dayi, M., Tekin, I., 2010. Utilization of marble waste dust as an additive in cement production. *Mater. Des.* 31, 4039–4042. <https://doi.org/10.1016/j.matdes.2010.03.036>

- Ashish, D.K., 2018. Feasibility of marble waste powder in concrete as partial substitution of cement and sand amalgam for sustainable growth. *J. Build. Eng.* 15, 236–242. <https://doi.org/10.1016/j.jobbe.2017.11.024>
- ASTM C1202, 2012. Standard Test Method for Electrical Indication of Concrete's Ability to Resist Chloride Ion Penetration. ASTM Int. West Conshohocken, PA, 2017 1–8. <https://doi.org/10.1520/C1202-12.2>
- ASTM C150, 2017. Standard Specification for Portland Cement, American Society for Testing and Materials. [https://doi.org/10.1520/C0150\\_C0150M-17](https://doi.org/10.1520/C0150_C0150M-17)
- ASTM C157, 2017. Standard Test Method for Length Change of Hardened Hydraulic-Cement Mortar and Concrete. ASTM Int. West Conshohocken, PA, 2017.
- ASTM C1585-13, 2004. Standard test method for measurement of rate of absorption of water by hydraulic cement concretes. ASTM Int. West Conshohocken, PA, 2017. <https://doi.org/10.1520/C1585-13.2>
- ASTM C33 / C33M, 2013. Standard Specification for Concrete Aggregates. Annu. B. ASTM Stand. <https://doi.org/10.1520/C0033>
- ASTM C33 / C33M, ASTM C33, 2003. Standard Specification for Concrete Aggregates. ASTM Int. West Conshohocken, PA, 2017 i, 11. <https://doi.org/10.1520/C0033>
- ASTM C642-13, 2008. Standard Test Method for Density, Absorption, and Voids in Hardened Concrete. <https://doi.org/10.1520/C0642-13.5>.
- Atiş, C.D., Sevim, U.K., Özcan, F., Bilim, C., Karahan, O., Tanrikulu, A.H., Ekşi, A., 2004. Strength properties of roller compacted concrete containing a non-standard high calcium fly ash. *Mater. Lett.* <https://doi.org/10.1016/j.matlet.2003.10.007>
- Ayber, S., Ulutas, B.H., 2017. Assessing Sustainable Manufacturing Related Problems for Marble Facilities: An Application. *Procedia Manuf.* <https://doi.org/10.1016/j.promfg.2017.02.015>
- Aydin, E., Arel, H.Ş., 2019. High-volume marble substitution in cement-paste:

Towards a better sustainability. *J. Clean. Prod.*  
<https://doi.org/10.1016/j.jclepro.2019.117801>

Bassuoni, M.T., Nehdi, M.L., 2007. Resistance of self-consolidating concrete to sulfuric acid attack with consecutive pH reduction. *Cem. Concr. Res.*  
<https://doi.org/10.1016/j.cemconres.2007.04.014>

Bazant, Z.P., Baweja, S., 1995. Justification and refinement of model B3 for concrete creep and shrinkage. *Mater. Struct.* 28, 488–495.

Beddoe, R.E., Dorner, H.W., 2005. Modelling acid attack on concrete: Part I. The essential mechanisms. *Cem. Concr. Res.*  
<https://doi.org/10.1016/j.cemconres.2005.04.002>

Belaidi, A.S.E., Azzouz, L., Kadri, E., Kenai, S., 2012. Effect of natural pozzolana and marble powder on the properties of self-compacting concrete. *Constr. Build. Mater.* <https://doi.org/10.1016/j.conbuildmat.2011.12.109>

Berra, M., Carassiti, F., Mangialardi, T., Paolini, A.E., Sebastiani, M., 2012. Effects of nanosilica addition on workability and compressive strength of Portland cement pastes. *Constr. Build. Mater.*  
<https://doi.org/10.1016/j.conbuildmat.2012.04.132>

Bilgin, N., Yeprem, H.A., Arslan, S., Bilgin, A., Günay, E., Maroglu, M., 2012. Use of marble waste powder in brick industry. *Constr. Build. Mater.*  
<https://doi.org/10.1016/j.conbuildmat.2011.10.011>

Binici, H., Aksogan, O., 2018. Durability of concrete made with natural granular granite, silica sand and powders of marble waste and basalt as fine aggregate. *J. Build. Eng.* <https://doi.org/10.1016/j.job.2018.04.022>

Binici, H., Kaplan, H., Yilmaz, S., 2007. Influence of marble and limestone dusts as additives on some mechanical properties of concrete. *Sci. Res. Essays.*

Binici, H., Shah, T., Aksogan, O., Kaplan, H., 2008. Durability of concrete made with granite and marble as recycle aggregates. *J. Mater. Process. Technol.* 208, 299–308. <https://doi.org/10.1016/j.jmatprotec.2007.12.120>

- BIS 4031: Part5, 1988. METHODS OF PHYSICAL TESTS FOR HYDRAULIC CEMENT. Bur. Indian Stand. New Delhi.
- BIS 516, 2004. Method of Tests for Strength of Concrete. Bur. Indian Stand. New Delhi.
- BIS 5816, 1999. Method of Test Splitting tensile strength of concrete. Bur. Indian Stand.
- Bonavetti, V.L., Rahhal, V.F., Irassar, E.F., 2001. Studies on the carboaluminate formation in limestone filler-blended cements. *Cem. Concr. Res.* 31, 853–859. [https://doi.org/10.1016/S0008-8846\(01\)00491-4](https://doi.org/10.1016/S0008-8846(01)00491-4)
- Boubekeur, T., Boulekbache, B., Aoudjane, K., Ezziane, K., Kadri, E.H., 2019. Prediction of the durability performance of ternary cement containing limestone powder and ground granulated blast furnace slag. *Constr. Build. Mater.* <https://doi.org/10.1016/j.conbuildmat.2019.03.120>
- Buyuksagis, I.S., Uygunoglu, T., Tatar, E., 2017. Investigation on the usage of marble waste powder in cement-based adhesive mortar. *Constr. Build. Mater.* 154, 734–742. <https://doi.org/10.1016/j.conbuildmat.2017.08.014>
- C267-01, A., 1998. Standard Test Methods for Chemical Resistance of Mortars , Grouts , and Monolithic. *Astm C267-01*. <https://doi.org/10.1520/C0267-01R06.2>
- Careddu, N., Marras, G., 2015. Marble processing for future uses of CaCO<sub>3</sub>-microfine dust: A study on wearing out of tools and consumable materials in stoneworking factories. *Miner. Process. Extr. Metall. Rev.* <https://doi.org/10.1080/08827508.2014.900616>
- Careddu, N., Marras, G., Siotto, G., 2014. Recovery of sawdust resulting from marble processing plants for future uses in high value-added products. *J. Clean. Prod.* <https://doi.org/10.1016/j.jclepro.2013.11.062>
- Central Pollution Control Board, 2010. Disposal Options of Marble Slurry In Rajasthan [WWW Document]. URL <https://www.cpcb.nic.in/>
- Chang, Z.T., Song, X.J., Munn, R., Marosszeky, M., 2005. Using limestone

aggregates and different cements for enhancing resistance of concrete to sulphuric acid attack. *Cem. Concr. Res.* <https://doi.org/10.1016/j.cemconres.2005.03.006>

Chatveera, B., Lertwattanak, P., 2014. Evaluation of nitric and acetic acid resistance of cement mortars containing high-volume black rice husk ash. *J. Environ. Manage.* <https://doi.org/10.1016/j.jenvman.2013.12.010>

Chavhan, P.J., Bhole, S.D., 2014. To study the behaviour of marble powder as supplementary cementitious Material in concrete. *Int. J. Eng. Res. Appl.* 4, 377–381.

Çınar, M., Karpuzcu, M., Çanakcı, H., 2020. The measurement of fresh properties of cement-based grout containing marble waste powder. *Meas. J. Int. Meas. Confed.* <https://doi.org/10.1016/j.measurement.2019.07.061>

Corinaldesi, V., Moriconi, G., Naik, T.R., 2010. Characterization of marble powder for its use in mortar and concrete. *Constr. Build. Mater.* 24, 113–117. <https://doi.org/10.1016/j.conbuildmat.2009.08.013>

De Belie, N., Monteny, J., Beeldens, A., Vincke, E., Van Gemert, D., Verstraete, W., 2004. Experimental research and prediction of the effect of chemical and biogenic sulfuric acid on different types of commercially produced concrete sewer pipes. *Cem. Concr. Res.* <https://doi.org/10.1016/j.cemconres.2004.02.015>

Demirel, B., 2010. The effect of the using marble waste dust as fine sand on the mechanical properties of the concrete. *Int. J. Phys. Sci.* 5, 1372–1380. <https://doi.org/10.1016/j.envint.2006.11.003>

Dodds, L., 2012. Microstructure Characterisation of Ordinary Portland Cement Composites for the Immobilisation of Nuclear Waste. *Characterisation Ordinary Portl. Cem.*

Dyer, T., 2014. Chemical mechanisms of concrete degradation. *Concr. Durab.* 99–182.

EN 196-3+ A1, 2010. Cement Test methods - Section 3 Set up Times and expansion

estimation. Eur. Stand. Inst.

EN 206-1, 2000. Concrete - Part 1: Specification, performance, production and conformity, European Committee for Standardization (CEN).

Ergün, A., 2011. Effects of the usage of diatomite and marble waste powder as partial replacement of cement on the mechanical properties of concrete. *Constr. Build. Mater.* 25, 806–812. <https://doi.org/10.1016/j.conbuildmat.2010.07.002>

Fattuhi, N. I., Hughes, B.P., 1988a. The performance of cement paste and concrete subjected to sulphuric acid attack. *Cem. Concr. Res.* [https://doi.org/10.1016/0008-8846\(88\)90047-6](https://doi.org/10.1016/0008-8846(88)90047-6)

Fattuhi, Nijad I., Hughes, B.P., 1988. Ordinary portland cement mixes with selected admixtures subjected to sulfuric acid attack. *ACI Mater. J.* <https://doi.org/10.14359/2269>

Fattuhi, N. I., Hughes, B.P., 1988b. SRPC and modified concretes subjected to severe sulphuric acid attack. *Mag. Concr. Res.* <https://doi.org/10.1680/mac.1988.40.144.159>

Gameiro, F., De Brito, J., Correia da Silva, D., 2014. Durability performance of structural concrete containing fine aggregates from waste generated by marble quarrying industry. *Eng. Struct.* 59, 654–662. <https://doi.org/10.1016/j.engstruct.2013.11.026>

Gardner, N.J., Lockman, M.J., 2001. Design Provisions for Drying Shrinkage and Creep of Normal Strength Concrete. *ACI Mater. J.* 98, 159–167.

Gesoğlu, M., Güneyisi, E., Kocabağ, M.E., Bayram, V., Mermerdaş, K., 2012. Fresh and hardened characteristics of self compacting concretes made with combined use of marble powder, limestone filler, and fly ash. *Constr. Build. Mater.* 37, 160–170. <https://doi.org/10.1016/j.conbuildmat.2012.07.092>

Ghafoori, N., Sukandar, B.M., 1995. Abrasion resistance of concrete block pavers. *ACI Mater. J.* <https://doi.org/10.14359/1174>

Girardi, F., Maggio, R. Di, 2011. Resistance of concrete mixtures to cyclic sulfuric

- acid exposure and mixed sulfates: Effect of the type of aggregate. *Cem. Concr. Compos.* <https://doi.org/10.1016/j.cemconcomp.2010.10.015>
- Goyal, S., 2008. Strength and durability studies on silica fume concrete. Thapar Institute of Engineering and Technology.
- Goyal, S., Kumar, M., Sidhu, D.S., Bhattacharjee, B., 2009. Resistance of mineral admixture concrete to acid attack. *J. Adv. Concr. Technol.* <https://doi.org/10.3151/jact.7.273>
- Hadigheh, S.A., Gravina, R.J., Smith, S.T., 2017. Effect of acid attack on FRP-to-concrete bonded interfaces. *Constr. Build. Mater.* <https://doi.org/10.1016/j.conbuildmat.2017.06.140>
- Hebhoub, H., Aoun, H., Belachia, M., Houari, H., Ghorbel, E., 2011. Use of marble waste aggregates in concrete. *Constr. Build. Mater.* 25, 1167–1171. <https://doi.org/10.1016/j.conbuildmat.2010.09.037>
- Higgins, D.D., 2003. Increased sulfate resistance of ggbs concrete in the presence of carbonate, in: *Cement and Concrete Composites*. [https://doi.org/10.1016/S0958-9465\(03\)00148-3](https://doi.org/10.1016/S0958-9465(03)00148-3)
- Horszczaruk, E., 2005. Abrasion resistance of high-strength concrete in hydraulic structures, in: *Wear*. <https://doi.org/10.1016/j.wear.2005.02.079>
- Huber, B., Hilbig, H., Mago, M.M., Drewes, J.E., Müller, E., 2016. Comparative analysis of biogenic and chemical sulfuric acid attack on hardened cement paste using laser ablation-ICP-MS. *Cem. Concr. Res.* <https://doi.org/10.1016/j.cemconres.2016.05.003>
- Irassar, E.F., Bonavetti, V.L., González, M., 2003. Microstructural study of sulfate attack on ordinary and limestone Portland cements at ambient temperature. *Cem. Concr. Res.* 33, 31–41. [https://doi.org/10.1016/S0008-8846\(02\)00914-6](https://doi.org/10.1016/S0008-8846(02)00914-6)
- IS:10262-2009, 2009. Concrete mix proportioning- guidelines. Bur. Indian Stand.
- IS.7320, 1974. Specification for concrete slump test apparatus. Bur. Indian Stand.

- IS 1237, 2012. CEMENT CONCRETE FLOORING TILES — SPECIFICATION. Bur. Indian Stand. New Delhi.
- IS 383, 2016. Coarse and Fine Aggregate for Concrete - Specification. Bur. Indian Stand.
- IS 8112, 2013. Ordinary Portland cement, 43 grade-Specification. Bur. Indian Stand. New Delhi.
- Kabeer, K.I.S.A., Vyas, A.K., 2019. Experimental investigation on utilization of dried marble slurry as fine aggregate in lean masonry mortars. *J. Build. Eng.* <https://doi.org/10.1016/j.jobe.2019.01.034>
- Kabeer, K.I.S.A., Vyas, A.K., 2018. Utilization of marble powder as fine aggregate in mortar mixes. *Constr. Build. Mater.* 165, 321–332. <https://doi.org/10.1016/j.conbuildmat.2018.01.061>
- Keleştemur, O., Arici, E., Yildiz, S., Gökçer, B., 2014. Performance evaluation of cement mortars containing marble dust and glass fiber exposed to high temperature by using Taguchi method. *Constr. Build. Mater.* <https://doi.org/10.1016/j.conbuildmat.2014.02.061>
- Khatib, J.M., Herki, B.A., Kenai, S., 2013. Capillarity of concrete incorporating waste foundry sand. *Constr. Build. Mater.* 47, 867–871. <https://doi.org/10.1016/j.conbuildmat.2013.05.013>
- Khatib, J.M., Mangat, P.S., 1995. Absorption characteristics of concrete as a function of location relative to casting position. *Cem. Concr. Res.* [https://doi.org/10.1016/0008-8846\(95\)00095-T](https://doi.org/10.1016/0008-8846(95)00095-T)
- Khay, S.E.E., Neji, J., Loulizi, A., 2010. Shrinkage properties of compacted sand concrete used in pavements. *Constr. Build. Mater.* 24, 1790–1795. <https://doi.org/10.1016/j.conbuildmat.2010.02.008>
- Khodabakhshian, A., Ghalehnovi, M., de Brito, J., Asadi Shamsabadi, E., 2018. Durability performance of structural concrete containing silica fume and marble industry waste powder. *J. Clean. Prod.*

<https://doi.org/10.1016/j.jclepro.2017.09.116>

- Khyaliya, R.K., Kabeer, K.I.S.A., Vyas, A.K., 2017. Evaluation of strength and durability of lean mortar mixes containing marble waste. *Constr. Build. Mater.* 147, 598–607. <https://doi.org/10.1016/j.conbuildmat.2017.04.199>
- Konin, A., Kouadio, D.M., 2012. Mechanical and abrasion resistance of recycled aggregates concrete in relation to the cement content. *Mod. Appl. Sci.* <https://doi.org/10.5539/mas.v6n1p88>
- Kore, S.D., Vyas, A.K., 2016. Impact of marble waste as coarse aggregate on properties of lean cement concrete. *Case Stud. Constr. Mater.* <https://doi.org/10.1016/j.cscm.2016.01.002>
- Kwasny, J., Aiken, T.A., Soutsos, M.N., McIntosh, J.A., Cleland, D.J., 2018. Sulfate and acid resistance of lithomarge-based geopolymer mortars. *Constr. Build. Mater.* <https://doi.org/10.1016/j.conbuildmat.2018.01.129>
- Lavigne, M.P., Bertron, A., Botanch, C., Auer, L., Hernandez-Raquet, G., Cockx, A., Foussard, J.N., Escadeillas, G., Paul, E., 2016. Innovative approach to simulating the biodeterioration of industrial cementitious products in sewer environment. Part II: Validation on CAC and BFSC linings. *Cem. Concr. Res.* <https://doi.org/10.1016/j.cemconres.2015.10.002>
- Li, B., Ke, G., Zhou, M., 2011. Influence of manufactured sand characteristics on strength and abrasion resistance of pavement cement concrete. *Constr. Build. Mater.* <https://doi.org/10.1016/j.conbuildmat.2011.04.004>
- Li, L.G., Huang, Z.H., Tan, Y.P., Kwan, A.K.H., Liu, F., 2018a. Use of marble dust as paste replacement for recycling waste and improving durability and dimensional stability of mortar. *Constr. Build. Mater.* 166, 423–432. <https://doi.org/10.1016/j.conbuildmat.2018.01.154>
- Li, L.G., Wang, Y.M., Tan, Y.P., Kwan, A.K.H., Li, L.J., 2018b. Adding granite dust as paste replacement to improve durability and dimensional stability of mortar. *Powder Technol.* <https://doi.org/10.1016/j.powtec.2018.04.055>

- Liu, K., Deng, M., Mo, L., Tang, J., 2015. Deterioration mechanism of Portland cement paste subjected to sodium sulfate attack. *Adv. Cem. Res.* <https://doi.org/10.1680/adcr.14.00051>
- Mahdikhani, M., Bamshad, O., Fallah Shirvani, M., 2018. Mechanical properties and durability of concrete specimens containing nano silica in sulfuric acid rain condition. *Constr. Build. Mater.* <https://doi.org/10.1016/j.conbuildmat.2018.01.137>
- Marras, G., Bortolussi, A., Peretti, R., Careddu, N., 2017a. Characterization methodology for re-using marble slurry in industrial applications, in: *Energy Procedia*. pp. 656–665. <https://doi.org/10.1016/j.egypro.2017.08.277>
- Marras, G., Careddu, N., Siotto, G., 2017b. Filler calcium carbonate industrial applications: The way for enhancing and reusing marble slurry. *Ital. J. Eng. Geol. Environ.* <https://doi.org/10.4408/IJEGE.2017-02.S-07>
- Mehta, A., Siddique, R., 2017. Sulfuric acid resistance of fly ash based geopolymer concrete. *Constr. Build. Mater.* <https://doi.org/10.1016/j.conbuildmat.2017.04.077>
- Mohamadien, H.A., 2012. The Effect of marble powder and silica fume as partial replacement for cement on mortar. *Int. J. Civ. Struct. Eng.*
- Mokarem, D.W., Weyers, R.E., Lane, D.S., 2005. Development of a shrinkage performance specifications and prediction model analysis for supplemental cementitious material concrete mixtures. *Cem. Concr. Res.* 35, 918–925. <https://doi.org/10.1016/j.cemconres.2004.09.013>
- Molnar, L.M., Manea, D.L., 2016. New Types of Plastering Mortars Based on Marble Powder Slime. *Procedia Technol.* <https://doi.org/10.1016/j.protcy.2016.01.076>
- Munir, M.J., Kazmi, S.M.S., Wu, Y.F., 2017. Efficiency of marble waste powder in controlling alkali–silica reaction of concrete: A sustainable approach. *Constr. Build. Mater.* 154, 590–599. <https://doi.org/10.1016/j.conbuildmat.2017.08.002>
- Naik, T.R., 2008. Sustainability of Concrete Construction. *Pract. Period. Struct. Des.*

- Constr. 13, 98–103. [https://doi.org/10.1061/\(ASCE\)1084-0680\(2008\)13:2\(98\)](https://doi.org/10.1061/(ASCE)1084-0680(2008)13:2(98))
- Naik, T.R., Kraus, R.N., Siddique, R., 2003. Controlled low-strength materials containing mixtures of coal ash and new pozzolanic material. *ACI Mater. J.* 100, 208–215. <https://doi.org/10.14359/12621>
- Neville, A.M., Brooks, J.J., 2010. *Concrete Technology, Building and Environment*. [https://doi.org/10.1016/0360-1323\(76\)90009-3](https://doi.org/10.1016/0360-1323(76)90009-3)
- Nijland, T.G., Larbi, J.A., 2010. Microscopic examination of deteriorated concrete, in: *Non-Destructive Evaluation of Reinforced Concrete Structures: Deterioration Processes and Standard Test Methods*. <https://doi.org/10.1533/9781845699536.2.137>
- Ozcelik, Y., Ozguven, A., 2014. Water absorption and drying features of different natural building stones. *Constr. Build. Mater.* <https://doi.org/10.1016/j.conbuildmat.2014.04.030>
- Pavlík, V., 1994. Corrosion of hardened cement paste by acetic and nitric acids part I: Calculation of corrosion depth. *Cem. Concr. Res.* [https://doi.org/10.1016/0008-8846\(94\)90144-9](https://doi.org/10.1016/0008-8846(94)90144-9)
- Rai, B., Naushad, K.H., Kr, A., Rushad, T.S., Professor, -Assistant, 2011. Influence of Marble powder/granules in Concrete mix. *Int. J. Civ. Struct. Eng.* 1. <https://doi.org/10.6088/ijcser.00202010070>
- Ramesh Kumar, G.B., Sharma, U.K., 2014. Abrasion resistance of concrete containing marginal aggregates. *Constr. Build. Mater.* <https://doi.org/10.1016/j.conbuildmat.2014.05.084>
- Rana, A., Kalla, P., Csetenyi, L.J., 2015. Sustainable use of marble slurry in concrete. *J. Clean. Prod.* <https://doi.org/10.1016/j.jclepro.2015.01.053>
- Rashad, A.M., 2013. A preliminary study on the effect of fine aggregate replacement with metakaolin on strength and abrasion resistance of concrete. *Constr. Build. Mater.* 44, 487–495. <https://doi.org/10.1016/j.conbuildmat.2013.03.038>
- Rizzo, G., D'Agostino, F., Ercoli, L., 2008. Problems of soil and groundwater

- pollution in the disposal of “marble” slurries in NW Sicily. *Environ. Geol.*  
<https://doi.org/10.1007/s00254-007-1043-9>
- Rodrigues, R., De Brito, J., Sardinha, M., 2015. Mechanical properties of structural concrete containing very fine aggregates from marble cutting sludge. *Constr. Build. Mater.* <https://doi.org/10.1016/j.conbuildmat.2014.12.104>
- Saboya, F., Xavier, G.C., Alexandre, J., 2007. The use of the powder marble by-product to enhance the properties of brick ceramic. *Constr. Build. Mater.* <https://doi.org/10.1016/j.conbuildmat.2006.05.029>
- Sadek, D.M., El-Attar, M.M., Ali, A.M., 2017. Physico-mechanical and durability characteristics of concrete paving blocks incorporating cement kiln dust. *Constr. Build. Mater.* 157, 300–312. <https://doi.org/10.1016/j.conbuildmat.2017.09.107>
- Sadek, D.M., El-Attar, M.M., Ali, H.A., 2016. Reusing of marble and granite powders in self-compacting concrete for sustainable development. *J. Clean. Prod.* <https://doi.org/10.1016/j.jclepro.2016.02.044>
- Sakalkale, A.D., Dhawale, G.D., Kedar, R.S., 2014. Experimental Study on Use of Marble waste Dust in concrete. *Int. J. Eng. Res. Appl.* 4, 44–50.
- Samimi, K., Kamali-Bernard, S., Maghsoudi, A.A., 2018. Durability of self-compacting concrete containing pumice and zeolite against acid attack, carbonation and marine environment. *Constr. Build. Mater.* 165, 247–263. <https://doi.org/10.1016/j.conbuildmat.2017.12.235>
- Sankh, A.C., Biradar, P.M., Naghathan, P.S.J., Manjunath, B., 2014. Recent Trends in Replacement of Natural Sand With Different Alternatives. *IOSR J. Mech. Civ. Eng.* 2014, 59–66.
- Sardinha, M., de Brito, J., Rodrigues, R., 2016. Durability properties of structural concrete containing very fine aggregates of marble sludge. *Constr. Build. Mater.* <https://doi.org/10.1016/j.conbuildmat.2016.05.071>
- Scrivener, K., De Belie, N., 2013. Bacteriogenic sulfuric acid attack of cementitious materials in sewage systems. *RILEM State-of-the-Art Reports.*

[https://doi.org/10.1007/978-94-007-5413-3\\_12](https://doi.org/10.1007/978-94-007-5413-3_12)

Shariq, M., Prasad, J., Abbas, H., 2016. Creep and drying shrinkage of concrete containing GGBFS. *Cem. Concr. Compos.* 68, 35–45. <https://doi.org/10.1016/j.cemconcomp.2016.02.004>

Siddique, R., 2013. Compressive strength, water absorption, sorptivity, abrasion resistance and permeability of self-compacting concrete containing coal bottom ash. *Constr. Build. Mater.* <https://doi.org/10.1016/j.conbuildmat.2013.06.081>

Siddique, R., Bennacer, R., 2012. Use of iron and steel industry by-product (GGBS) in cement paste and mortar. *Resour. Conserv. Recycl.* 69, 29–34. <https://doi.org/10.1016/j.resconrec.2012.09.002>

Siddique, R., Kapoor, K., Kadri, E.H., Bennacer, R., 2012. Effect of polyester fibres on the compressive strength and abrasion resistance of HVFA concrete. *Constr. Build. Mater.* <https://doi.org/10.1016/j.conbuildmat.2011.09.011>

Siddique, R., Khatib, J.M., 2010. Abrasion resistance and mechanical properties of high-volume fly ash concrete. *Mater. Struct. Constr.* <https://doi.org/10.1617/s11527-009-9523-x>

Silva, D., Gameiro, F., de Brito, J., Silva, B.D., Gameiro F., B.J.D., 2014. Mechanical properties of structural concrete containing fine aggregates from waste generated by the marble quarrying industry. *J. Mater. Civ. Eng.* 26(6), 1–8. [https://doi.org/10.1061/\(ASCE\)MT.1943-5533.0000948](https://doi.org/10.1061/(ASCE)MT.1943-5533.0000948)

Singh, M., Siddique, R., 2013. Effect of coal bottom ash as partial replacement of sand on properties of concrete. *Resour. Conserv. Recycl.* <https://doi.org/10.1016/j.resconrec.2012.12.006>

Singh, M., Srivastava, A., Bhunia, D., 2017. An investigation on effect of partial replacement of cement by marble waste slurry. *Constr. Build. Mater.* 134, 471–488. <https://doi.org/10.1016/j.conbuildmat.2016.12.155>

Sotiriadis, K., Nikolopoulou, E., Tsivilis, S., 2012. Sulfate resistance of limestone cement concrete exposed to combined chloride and sulfate environment at low

temperature. Cem. Concr. Compos.  
<https://doi.org/10.1016/j.cemconcomp.2012.05.006>

Specifier, M., For, G., 2017. Michigan Specifier ' S Guide for Pervious Concrete 1–22.

Talah, A., Kharchi, F., Chaid, R., 2015. Influence of Marble Powder on High Performance Concrete Behavior, in: Procedia Engineering.  
<https://doi.org/10.1016/j.proeng.2015.08.010>

Tennich, M., Ben Ouezdou, M., Kallel, A., 2017. Behavior of self-compacting concrete made with marble and tile wastes exposed to external sulfate attack. Constr. Build. Mater. <https://doi.org/10.1016/j.conbuildmat.2016.12.193>

Thomas, B.S., Gupta, R.C., Kalla, P., Cseteneyi, L., 2014. Strength, abrasion and permeation characteristics of cement concrete containing discarded rubber fine aggregates. Constr. Build. Mater. 59, 204–212.  
<https://doi.org/10.1016/j.conbuildmat.2014.01.074>

Topçu, I.B., Bilir, T., Uygunoğlu, T., 2009. Effect of marble waste dust content as filler on properties of self-compacting concrete. Constr. Build. Mater. <https://doi.org/10.1016/j.conbuildmat.2008.09.007>

Topçu, I.B., Uygunoğlu, T., 2010. Effect of aggregate type on properties of hardened self-consolidating lightweight concrete (SCLC). Constr. Build. Mater. <https://doi.org/10.1016/j.conbuildmat.2009.12.007>

Torii, K., Kawamura, M., 1994. Effects of fly ash and silica fume on the resistance of mortar to sulfuric acid and sulfate attack. Cem. Concr. Res. [https://doi.org/10.1016/0008-8846\(94\)90063-9](https://doi.org/10.1016/0008-8846(94)90063-9)

Ulubeyli, G.C., Bilir, T., Artir, R., 2016. Durability Properties of Concrete Produced by Marble Waste as Aggregate or Mineral Additives, in: Procedia Engineering.  
<https://doi.org/10.1016/j.proeng.2016.08.689>

Vaidevi, C., Felix Kala, T., Kalaiyarrasi, A.R.R., 2020. Mechanical and durability properties of self-compacting concrete with marble fine aggregate, in: Materials

Today: Proceedings. <https://doi.org/10.1016/j.matpr.2019.11.019>

Varadharajan, S., Jaiswal, A., Verma, S., 2020. Assessment of mechanical properties and environmental benefits of using rice husk ash and marble dust in concrete. Structures. <https://doi.org/10.1016/j.istruc.2020.09.005>

Vardhan, K., Goyal, S., Siddique, R., Singh, M., 2015. Mechanical properties and microstructural analysis of cement mortar incorporating marble powder as partial replacement of cement. Constr. Build. Mater. 96, 615–621. <https://doi.org/10.1016/j.conbuildmat.2015.08.071>

Vardhan, K., Siddique, R., Goyal, S., 2019. Strength, permeation and micro-structural characteristics of concrete incorporating marble waste. Constr. Build. Mater. <https://doi.org/10.1016/j.conbuildmat.2019.01.079>

Xie, S., Qi, L., Zhou, D., 2004. Investigation of the effects of acid rain on the deterioration of cement concrete using accelerated tests established in laboratory. Atmos. Environ. <https://doi.org/10.1016/j.atmosenv.2004.05.017>

Zain, M.F.M., Mahmud, H.B., Ilham, A., Faizal, M., 2002. Prediction of splitting tensile strength of high-performance concrete. Cem. Concr. Res. [https://doi.org/10.1016/S0008-8846\(02\)00768-8](https://doi.org/10.1016/S0008-8846(02)00768-8)

Zhang, S., Cao, K., Wang, C., Wang, X., Wang, J., Sun, B., 2020. Effect of silica fume and marble waste powder on the mechanical and durability properties of cellular concrete. Constr. Build. Mater. <https://doi.org/10.1016/j.conbuildmat.2019.117980>

Zhuang, X.Y., Chen, L., Komarneni, S., Zhou, C.H., Tong, D.S., Yang, H.M., Yu, W.H., Wang, H., 2016. Fly ash-based geopolymers: Clean production, properties and applications. J. Clean. Prod. <https://doi.org/10.1016/j.jclepro.2016.03.019>

Zivica, V., Bajza, A., 2001. Acidic attack of cement based materials - A review. Part 1. Principle of acidic attack. Constr. Build. Mater. [https://doi.org/10.1016/S0950-0618\(01\)00012-5](https://doi.org/10.1016/S0950-0618(01)00012-5)